Bilaga B.3.A

Ran
Offshore Wind Farm

Underwater Noise Prognosis

Construction and operation

NIRAS A/S

Date: 29 February 2024

Rev.no.	Date	Description	Prepared by	Verified by	Approved by
1	29-02-2024	Final Version	MAM	MAWI	MAM

Executive Summary

Ran Vindpark AB is planning the construction of Ran Offshore Wind Farm (OWF) in the Baltic Sea, 12 km east of Gotland. NIRAS has been tasked with preparation of an underwater noise prognosis for the construction and operational phase of the OWF, as input for an environmental impact assessment for marine mammals and fish.

Underwater noise during construction

Underwater noise during the construction phase was estimated using sound propagation modelling of pile driving, in 3 representative worst case positions within the Ran OWF area. The prognosis included underwater sound propagation modelling for the following foundation types:

- 14 m diameter monopile foundation
- Jacket foundation with 4x 5 m diameter pin piles

A 3D acoustic environmental model, based on available online data sources, as well as client input, for bathymetry, sediment, salinity, temperature and sound speed, was created in QGIS and NIRAS TRANSMIT (NIRAS proprietary MATLAB toolbox). Worst case hydrographic conditions, represented by historical data for the month of March, was used. Underwater sound propagation modelling was carried out in dBSea 2.3.4, using the 3D acoustic environmental model, as well as a source model derived from available literature and NIRAS experience. Sound propagation was calculated in a 25 x 0.5 m range-depth grid in 45-90 directions from each source (4 - 8° resolution). Source positions near land masses utilized 90 directions, whereas positions further from land utilized 45 directions. Resulting sound propagation losses were processed in NIRAS SILENCE (NIRAS proprietary MATLAB toolbox) to determine impact ranges to relevant marine mammal and fish threshold criteria. All results represent the installation of a single foundation within a 24 hour duration. For installation of multiple piles, either concurrently or sequentially within a 24 hour duration, a discussion is provided in Appendix 1, however no calculations of cumulative impact are provided in this report. The installation of all foundations in the wind farm area does not affect the prognosis, as it considers each pile individually.

For the project area, underwater sound propagation losses of 13.3 – 14.5 dB/decade were found for the unmitigated pile driving. This corresponds to a sound level decrease of 13.3 – 14.5 dB for each 10 fold increase of the distance between source and receiver. This indicates a marine environment with a strong sound propagation, and thereby a high potential for long-reaching impacts from underwater noise, with regards to relevant marine mammal and fish threshold criteria.

For marine mammals, threshold criteria include hearing loss (threshold shift), resulting from cumulative underwater noise exposure, as well as instantaneous behavioural reaction resulting from a sudden change in the experienced noise level. A noise induced threshold shift is a temporary (TTS) or permanent (PTS) reduction in hearing sensitivity, following exposure to a high cumulative noise dose. The level of injury depends on both the intensity and duration of noise exposure. Small levels of TTS will disappear in a matter of minutes or hours, whereas more severe levels of TTS can last for days. At higher levels of noise exposure, the hearing threshold does not recover fully, but leaves a smaller or larger amount of PTS. An initial TTS of 40 dB or higher is generally considered to constitute a significantly increased risk of developing PTS (NOAA, 2018). Behavioural reaction on the other hand is linked to the instantaneous change in sound level, causing a reaction, such as avoidance or change in behaviour.

Marine mammals included in the prognosis are harbour porpoise (*Phocoena phocoena*) and earless seals (harbour seal and grey seal). For marine mammals, PTS and TTS threshold criteria are used, and for harbour porpoise the behaviour criterion is also included.

For fish, TTS threshold criteria and physical injury threshold criteria are used. For larvae and eggs, only the injury criteria are considered. Fish species included in the prognosis are cod and herring, as well as larvae and eggs. Stationary fish, in the context of this report, refers to fish that are not expected to flee as a result of exposure to sound.

Impact range for PTS, TTS and injury describe the minimum distance from the source a marine mammal or fish must at least be, prior to onset of pile driving, in order to avoid the respective impact. It therefore does not represent a specific measurable sound level, but rather a safe starting distance. For marine mammals, fleeing behaviour is included. For fish both fleeing behaviour and stationary behaviour is included. Larvae and eggs are considered stationary only.

Impact range for behaviour, describes a specific distance, up to which, the behavioural response is likely to occur, when maximum hammer energy is applied to a pile strike. For pile strikes at less than 100% hammer energy, such as during soft start and ramp up, the distance is shorter.

To investigate likely installation scenarios, noise emission mitigation measures were also included in the model. For monopiles, noise mitigation equivalent to documented noise reduction of HSD+DBBC was applied. For jacket foundations, noise mitigation equivalent to documented noise reduction of DBBC was applied. It should be noted, that application of noise mitigation systems in the modelling, does not set a requirement for using the specific mitigation systems in the future installation process. It should be regarded as a limitation of the emitted noise. During final foundation design, specific mitigation systems must be considered such that the impact ranges in this report are not exceeded.

With mitigation applied, the impact ranges for each of the relevant threshold criteria, are listed in Table 1.1 for marine mammals, and in Table 1.2.

Table 1.1: Impact ranges for marine mammal threshold criteria, with mitigation measures

Position	**Impact range for marine mammal threshold criteria**				
	PTS		TTS		Behaviour
	Porpoise (VHF)	Seal (PCW)	Porpoise (VHF)	Seal (PCW)	Porpoise (VHF)
14 m monopile; HSD+DBBC equivalent mitigation effect; March					
1	< 200 m	< 200 m	325 m	< 200 m	5.9 km
3	< 200 m	< 200 m	325 m	< 200 m	6.0 km
4 x 5 m pin pile (jacket foundation); DBBC equivalent mitigation effect; March					
1	< 200 m	< 200 m	700 m	< 200 m	8.3 km
2	< 200 m	< 200 m	975 m	< 200 m	9.4 km
3	< 200 m	< 200 m	700 m	< 200 m	7.6 km

For the worst case position, the PTS and TTS impact ranges for seals are up to 200 m, regardless of foundation type. For harbour porpoise, PTS impact range is up to 200 m, whereas TTS can occur up to 325 m away from the installation site for the monopile foundation type, and up to 975 m away from the installation site for the jacket foundation type. Behaviour threshold criterion for harbour porpoise is up to 6 km for the monopile and up to 9.4 km for jacket foundations.

Table 1.2: Impact range for fish threshold criteria, with mitigation measures.

Position	**Impact range for fish threshold criteria**								
	Injury (r_{injury})					TTS (r_{TTS})			
	Stationary	Juvenile Cod	Adult Cod	Herring	Larvae and eggs	Stationary	Juvenile Cod	Adult Cod	Herring
14 m monopile; HSD+DBBC equivalent mitigation effect; March									
1	1.35 km	< 200 m	< 200 m	< 200 m	850 m	9.8 km	5.1 km	2.4 km	2.0 km
3	1.35 km	< 200 m	< 200 m	< 200 m	875 m	8.9 km	4.85 km	2.2 km	1.85 km
4 x 5 m pin pile (jacket foundation); DBBC equivalent mitigation effect; March									
1	500 m	< 200 m	< 200 m	< 200 m	275 m	5.5 km	< 200 m	< 200 m	< 200 m
2	450 m	< 200 m	< 200 m	< 200 m	275 m	5.8 km	< 200 m	< 200 m	< 200 m
3	500 m	< 200 m	< 200 m	< 200 m	275 m	5.6 km	< 200 m	< 200 m	< 200 m

For fish, TTS impact ranges extend to 9.8 km for monopile foundation, and up to 5.8 km for jacket foundation. The impact range is largest for the slowest moving fish (stationary fish being the slowest), whereas faster moving fish have significantly shorter impact range. For herring, TTS impact ranges are therefore 2.0 km for monopile, and less than 200 m for jacket foundations. Injury ranges for fish follow the same pattern, with up to 1.35 km for the slowest fish for monopile foundations and up to 200 m for herring. For jacket foundations, the corresponding distances are 500 m and up to 200 m. For larvae and eggs, injury ranges up to 875 m, and 275 m are calculated for monopile, and jacket foundations, respectively.

Underwater noise during operation

Underwater noise during operation was estimated, based on available existing measurements and modelling results. The latest scientific review by (Bellmann, et al., 2023) includes all latest measurements from OWFs ranging in size from 2.3 MW up to 8 MW turbines. Based on the latest data a trend for underwater noise emission as a function of wind turbine size was provided and used to estimate impact ranges on marine mammals and fish from Ran OWF in operation. For both marine mammals and fish, auditory injures are considered unlikely to occur as a result of underwater noise from a single turbine as well as from the entire offshore wind farm in operation. Furthermore based on the very limited behavioural impact ranges it is unlikely that harbour porpoises will react to the noise from one operating turbine as well as from the entire offshore wind farm in operation.

Contents

List of abbreviations

Full name	Abbreviation	Symbol
Sound Exposure Level	SEL	$L_{E,p}$
Cumulative Sound Exposure Level	$SEL_{cum,t}$	$L_{E,cum,t}$
Sound Exposure Level - single pile strike	SEL_{SS}	L_{E100}
Sound Pressure Level	SPL	L_p
Source Level at 1 m	SL	L_S
Sound exposure source level at 1 m	ESL	$L_{S,E}$
Permanent Threshold Shift	PTS	
Temporary Threshold Shift	TTS	
National Oceanographic and Atmospheric Administration	NOAA	
Offshore Wind farm	OWF	
Low frequency	LF	
High frequency	HF	
Very High frequency	VHF	
Phocid Pinniped	PCW	
Big Bubble Curtain	BBC	
Double Big Bubble Curtain	DBBC	
Hydro Sound Damper	HSD	
IHC Noise Mitigation Screen	IHC-NMS	
World Ocean Atlas 2023	WOA23	
Sound Exposure Propagation loss	EPL	
National Marine Fisheries Service	NMFS	
Wind Turbine Generators	WTG	
Maximum-over-depth	MOD	

1. Introduction and objectives

Ran Vindpark AB is planning the construction of Ran Offshore Wind Farm (OWF) in the Baltic Sea, 17 km east of Gotland. NIRAS has been tasked with preparation of an underwater noise prognosis for the construction and operational phase of the OWF, as input for an environmental impact assessment for marine mammals and fish. The report also includes a description of the ambient underwater noise based on available literature.

The report is structured as outlined below.

Chapter	Content
2	Project description
3	Definitions: A brief introduction to terms and metrics used throughout the report
4	Marine mammal and fish threshold criteria for auditory impact
5	Ambient underwater noise study
6	Underwater noise prognosis for construction phase
7	Evaluation of underwater noise during operational phase

2. Project description

Ran Vindpark AB is planning to establish an offshore wind farm, Ran, in the Baltic Sea east of Gotland. The Ran wind farm is located in Swedish territorial waters, approximately 12 kilometers east of the east coast of Gotland. The water depth in the area varies between approximately 40 and 85 meters, see Figure 2.1.

The area for the wind farm is approximately 327 km^2 and when fully developed, the park will include 90-121 wind turbines with a maximum total height of 310 meters. The wind farm is expected to have an installed capacity of approximately 1.8 GW and is expected to generate around 8 TWh of renewable electricity per year.

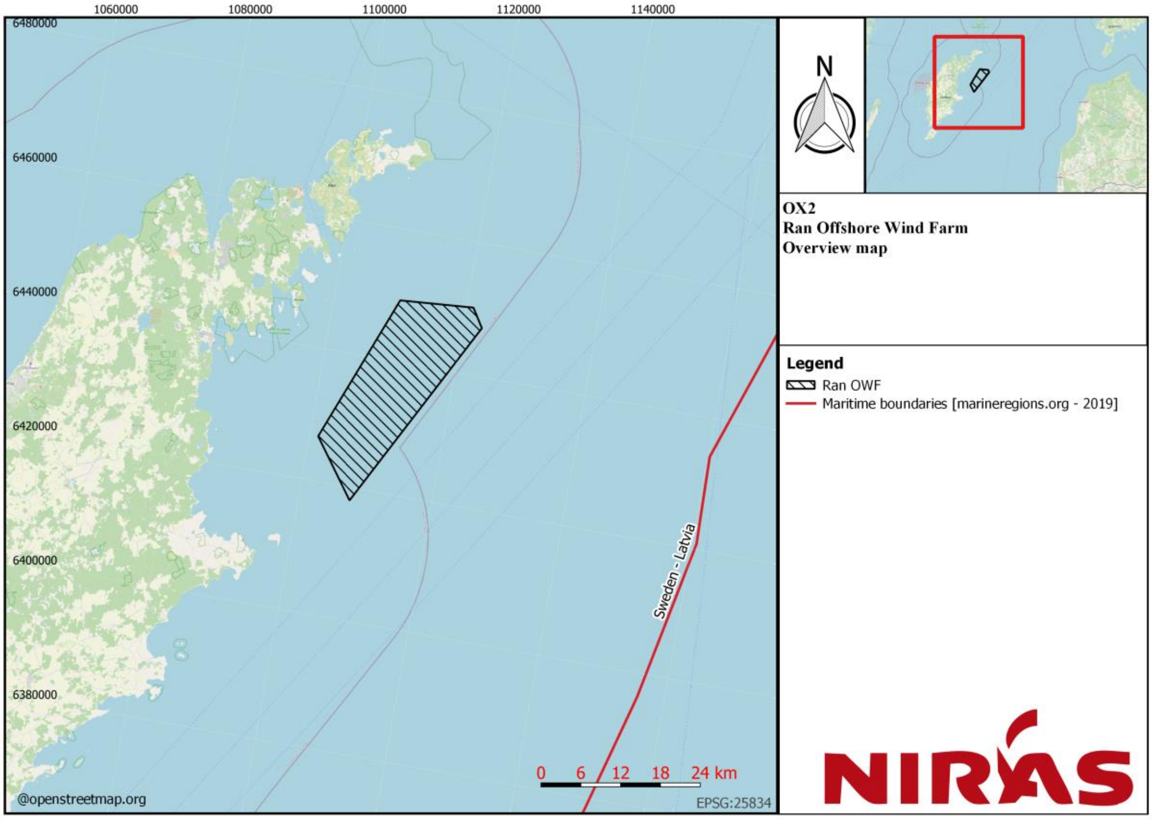

Figure 2.1: Overview of the planned Ran OWF project area.

2.1. Description of Activities

The project includes up to 90 (20 MW) – 121 (15 MW) wind turbine generators (WTG) and up to 4 offshore platforms (sub stations) within the project area shown in Figure 2.1.

2.1.1. Construction of wind farm

Activities during construction of the wind farm, includes installation and support vessels, and foundation installation.

The most common foundation types used for WTGs and substations include monopiles and jacket foundations. Floating foundations are still an emerging technology under rapid development. In Figure 2.2, the different foundation types are illustrated along with their suitability for different depths. Other foundation types, such as gravity based foundations (GBF) and suction bucket are less common, however the underwater noise emission from these foundation types is considered limited. From a worst-case underwater noise emission perspective, monopile, jacket and floating foundations are considered relevant. A brief description of these foundation types is provided below.

Steel monopile foundations are hollow cylindrical steel structures that are driven into the seabed using an impact pile driving hammer. Jacket foundations, on the other hand, are installed by impact pile driving of a number of pin piles securing each leg of the jacket steel structure. Of the two, the monopiles have significantly larger pile diameter, however more pin piles are required per jacket foundation; one or more piles per leg of the jacket structure, typically with 3 or 4 legs.

Installation of monopile foundations therefore typically requires a larger hammer and more force, and as a result, causes higher underwater noise emission than a smaller pin pile for a jacket foundation. Due to the complex steel structure of the jacket foundation, the emitted noise from pin pile installation is likely to be more high-frequent in nature.

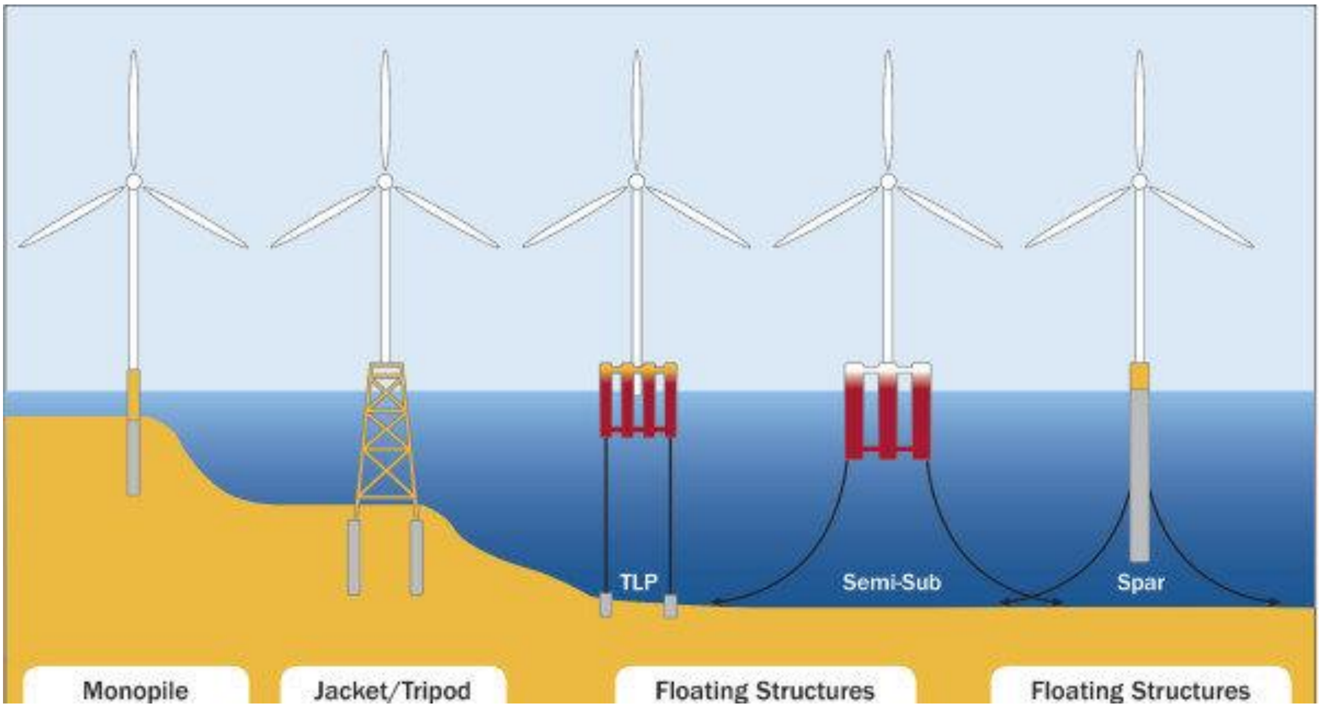

Figure 2.2: Illustration of foundation types and suitability in different water depths (Bailey, et al., 2014).

Additionally, the same mitigation measures used for monopiles might not be suitable for jacket structures. It is therefore not a guarantee that the larger pile diameter results in the largest impact. Jacket foundations also have a larger number of piles per foundation and therefore has a longer installation time.

Gravitation and suction bucket foundations are the foundation types with the lowest underwater noise emissions, and are seldomly used for various technical and economical reasons. These options are not considered further in this prognosis.

Floating foundation is an emerging foundation type, typically suited for projects where the water depth prevents the use of conventional methods. As an emerging foundation type, different concepts are still being tested. The general concept is that the turbine is mounted on a floating steel frame, which is anchored to the seabed through a number of anchor lines. Each anchor line would then be securely fastened in the seabed using one or more anchor piles, or gravitation anchors. Since floating foundation types are still largely untested, little data is available on pile sizes and the number of piles to be used per anchor line, however it is expected that pile size and number of piles is inversely proportional. So the more anchor piles used per anchor line, the smaller each pile would be. It is not expected that the anchor pile diameter in any case would exceed that of a corresponding monopile. Installation in deeper waters would also typically imply that the pile does not cover the entire water column, and both pile and hammer is submerged. Mitigation system effectiveness is also unknown, as traditional methods such as bubble curtains have not been tested at depths beyond several tens of meters.

Foundation handling/positioning is typically considered a low-noise activity compared to the installation of the foundation, especially if impact pile driving is required. Noise from installation and service vessels is also expected to occur.

2.1.2. Operation of wind farm

During the operation of an OWF, underwater noise emission occurs as a result of various sources, most notably vibrations when blades pass the tower, noise from gearboxes, as well as the movement of support and maintenance vessels.

3. Definitions

Acoustic metrics and relevant terms used in the report are defined in this chapter. Terminology generally follows ISO standard 18405 (DS/ISO 18405, 2017).

3.1. Sound Pressure Level

The Sound Pressure Level (SPL), L_p, is used to describe the noise level. The definition for SPL is shown in Equation 1 (Erbe, 2011):

$$L_{p,rms} = 20 * \log_{10}\left(\sqrt{\left(\frac{1}{T}\right)\int_0^T p(t)^2}\right) \quad [\text{dB re. } 1\mu\text{Pa}]$$ Equation 1

Where p is the acoustic pressure of the noise signal during the time of interest, and T is the total time. L_p is the average unweighted SPL over a measured period of time.

For ambient underwater noise and for operational underwater noise, L_p is the preferred metric.

In order to evaluate the behavioural response of the marine mammal a time window is needed. Often, a fixed time window of 125 ms. is used due to the integration time of the ear of mammals (Tougaard & Beedholm, 2018). The metric is then referred to as $L_{p,125ms}$ and the definition is shown in Equation *2* (Tougaard, 2021).

$$L_{p,125ms} = L_{E,p} - 10 * \log_{10}(0.125) = L_{E,p} + 9 \text{ dB} \quad [\text{dB re. } 1\mu\text{Pa}]$$ Equation 2

Where $L_{E,p}$is the sound exposure level, which are explained in the next section.

3.2. Sound Exposure Level

The Sound Exposure Level (SEL), $L_{E,p}$, describes the total energy of a noise event (Jacobsen & Juhl, 2013). A noise event can for instance be the installation of a monopile by impact pile driving, from start to end, or it can be a single noise event like an explosion. The SEL is normalized to 1 second and is defined in (Martin, et al., 2019) through Equation *3*.

$$L_{E,p} = 10 * \log_{10}\left(\frac{1}{T_0 p_0^2}\int_0^T p^2(t)\right) \quad [\text{dB re. } 1\mu\text{Pa}^2\text{s}]$$ Equation 3

Where T_0 is 1 second, 0 is the starting time and T is end time of the noise event, p is the pressure, and p_0 is the reference sound pressure which is $1\ \mu$Pa.

The relationship between SPL, Equation *1*, and SEL, Equation *3*, is given by Equation *4* (Erbe, 2011).

$$L_{E,p} = L_p + 10 * \log_{10}(T)$$ Equation 4

When SEL is used to describe the sum of noise from more than a single event/pulse, the term Cumulative SEL, $(SEL_{cum,t})$, $L_{E,cum,t}$, is used, while the SEL for a single event/pulse, is the single-strike SEL (SEL_{SS}), L_{E100}. The SEL_{SS} is calculated on the base of 100% pulse energy over the pulse duration.

Marine animals can incur hearing loss, either temporarily or permanently as a result of exposure to high noise levels. The level of injury depends on both the intensity and duration of noise exposure. SEL is therefore a commonly used metric to assess the risk of hearing impairment as a result of noisy activities (Martin, et al., 2019).

3.3. Cumulative Sound Exposure level

In the assessment of auditory impact on marine mammals, Temporary Threshold Shift (TTS), and Permanent Threshold Shift (PTS) criteria are based on received cumulative SEL ($L_{E,cum,t}$) as a result of an underwater noise emitting activity. For fish, TTS and injury criteria are used, also based on $L_{E,cum,t}$.

For a stationary source, such as installation of a foundation, the installation procedure, as well as the swim speed for marine mammals and fish, must be included. A method for implementing such conditions in the calculation of $SEL_{cum,t}$ has been proposed by (Energistyrelsen, 2023), for the Danish guidelines for pile driving activities, as given by Equation 5. The duration is fixed to 24 hours to represent the daily cumulative SEL, $L_{E,cum,24h}$. If multiple foundations are installed in the same 24 hour window, all must be included in the calculation.

$$L_{E,cum,24h} = 10 * \log_{10}\left(\sum_{i=1}^{N} \frac{S_i}{100\%} * 10^{\left(\frac{L_{S,E} - X*\log_{10}(r_0+v_f*t_i) - A*(r_0+v_f*t_i)}{10}\right)}\right) \quad \text{Equation 5}$$

Where:

- S_i is the percentage of full hammer energy of the i'th strike.
- N is the total number of strikes for the pile installation.
- $L_{S,E}$ is the sound exposure source level at 1 m distance at 100% hammer energy.
- X and A describe the sound exposure propagation losses (EPL) for the specific project site.
- r_0 is the marine mammal or fish distance to source at the onset of piling.
- v_f is the swim speed of the marine mammal or fish, swimming directly away from the noise source.
- t_i is the time difference between onset of piling, and the i^{th} strike.

The pile driving parameters related to the source level, hammer energy, number of strikes and time interval between each strike should be based on realistic worst-case assumptions. For projects in the final design phase, pile-specific drivability analyses are preferred. The relationship between hammer energy level and pile strike number is referred to as the hammer curve.

The sound propagation parameters (X and A) must be determined through advanced sound propagation modelling, in which all relevant site-specific environmental parameters are considered.

3.4. Source level

Two representations for the acoustic output of pile driving are used in this report, namely Source Level (SL), L_S, and the sound exposure source level (ESL), $L_{S,E}$.

SL is defined for a continuous source as the SPL_{rms} at a distance of 1 m from the source with a reference value of $1\ \mu Pa \cdot m$. The metric is used primarily for non-impulsive source types, such as vessels and operational noise from turbines.

ESL is used to describe a transient sound source and is defined as the SEL at a distance of 1 m from the source with a reference value of $1\ \mu Pa^2\ m^2\ s$. This is the standard metric used to describe the source level of impact pile driving activities.

3.5. Frequency weighting functions

In underwater noise assessments, frequency weighting is often used to more accurately reflect the underwater noise impact on specific marine mammals.

Humans are most sensitive to frequencies in the range of 2 kHz - 5 kHz and for frequencies outside this range, the sensitivity decreases. This frequency-dependent sensitivity correlates to a weighting function, for the human auditory system it is called A-weighting. For marine mammals, the same principle applies through the weighting function, W(f), defined through Equation *6* (NOAA, 2018).

$$W(f) = C + 10 * \log_{10}\left(\frac{\left(\frac{f}{f_1}\right)^{2*a}}{\left[1+\left(\frac{f}{f_1}\right)^2\right]^a * \left[1+\left(\frac{f}{f_2}\right)^2\right]^b}\right)\ [dB]$$

Equation 6

Where:

- $\mathbf{a}$ is describing how much the weighting function amplitude is decreasing for the lower frequencies.
- $\mathbf{b}$ is describing how much the weighting function amplitude is decreasing for the higher frequencies.
- $\mathbf{f_1}$ is the frequency at which the weighting function amplitude begins to decrease at the lower frequencies [kHz]
- $\mathbf{f_2}$ is the frequency at which the weighting function amplitude begins to decrease at the higher frequencies [kHz]
- $\mathbf{C}$ is the function gain [dB].

For an illustration of the parameters see Figure 3.1.

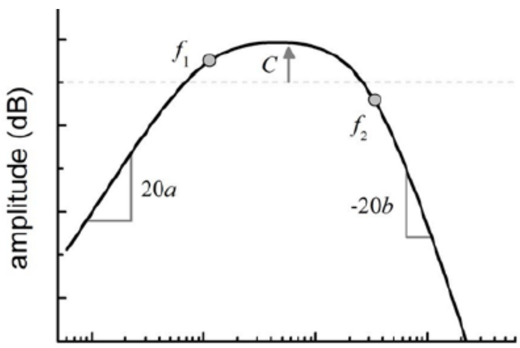

Figure 3.1: Illustration of the 5 parameters in the weighting function (NOAA, 2018).

Marine mammals are divided into four hearing groups, in regard to their frequency specific hearing sensitivities: 1) Low-frequency (**LF**) cetaceans, 2) High-frequency (**HF**) cetaceans, 3) Very High-frequency (**VHF**) cetaceans, 4) and Phocid Carnivores in Water (**PCW**) (NOAA, 2018; Southall, et al., 2019). The parameters in Equation *6* are defined for the hearing groups and the values are presented in Table 3.1.

Table 3.1: Parameters for the weighting function for the relevant hearing groups (NOAA, 2018).

Hearing Group	a	b	f_1 [kHz]	f_2 [kHz]	C [dB]
Low frequency (LF) Cetaceans	1.0	2	0.2	19	0.13
High frequency (HF) Cetaceans	1.6	2	8.8	110	1.20
Very high frequency (VHF) Cetaceans	1.8	2	12	140	1.36
Phocid Carnivores in Water (PCW)	1.0	2	1.9	30	0.75

The weighting function amplitude for the four hearing groups is achieved by inserting the values from Table 3.1 into Equation 6. The resulting spectra for the four hearing groups are shown in Figure 3.2.

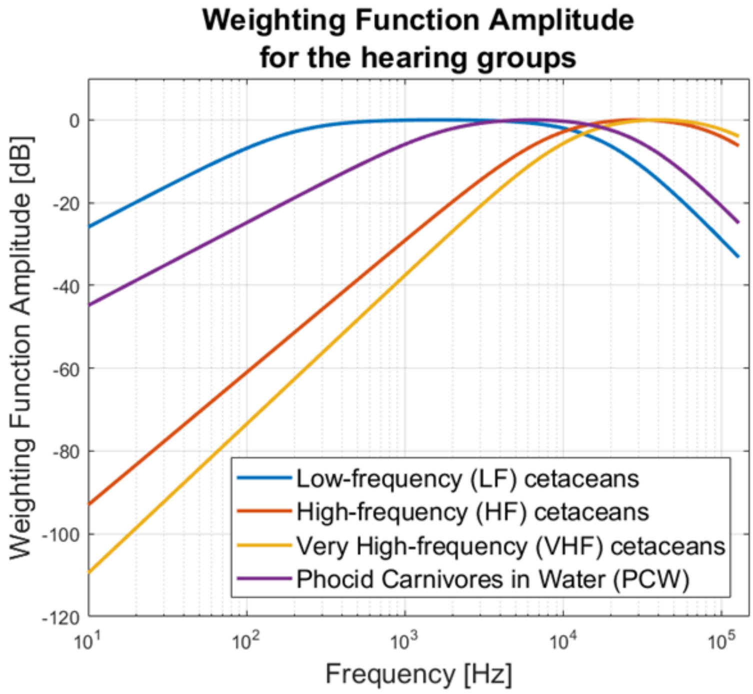

Figure 3.2: The weighting functions for the different hearing groups.

For this project, relevant species include seal (classified as a Phocid Carnivores in Water (PCW)), and harbour porpoise (classified as a Very High Frequency Cetacean (VHF)). Frequency weighting functions are not used for fish.

4. Underwater Noise Threshold Criteria

In Sweden, no guidelines are available for the emission of underwater noise, which is instead handled by the authorities on a project-by-project basis. In order to provide a prognosis of impact, best available scientific knowledge from (NOAA, 2018), (Tougaard, 2021), (Energistyrelsen, 2023) is instead used.

Two sets of threshold criteria are typically considered in evaluating the impact of underwater noise, based on the impulsiveness of the noise source. Following the definition of impulsive vs. non-impulsive noise sources in (NOAA, 2018), the terms are considered as follows:

- Impulsive: Sounds that are typically transient, brief (duration < 1 s), broadband, and consist of high peak sound pressure with rapid rise time and rapid decay.

- Non-impulsive: Sounds that are broadband, narrowband or tonal, brief or prolonged, continuous or intermittent, and typically do not have a high peak sound pressure with rapid rise nor decay time.

Impact pile driving is characterized as an impulsive source type, although the characteristics of the pulse are expected to transition into non-impulsive over distance. It is however not scientifically established, when such a change would occur. Impact pile driving is therefore considered impulsive at all distances in this prognosis, as this provides a stricter, and thereby more conservative, measure of the impact of underwater noise.

Vibration installation however is considered non-impulsive. Vessel noise and operational noise from turbines are also considered non-impulsive sources.

4.1. Threshold criteria for fish

Threshold criteria for fish, larvae and eggs (Table 4.1) are all based on unweighted cumulative SEL ($L_{E,cum,24h}$), as defined in section 3.3. The criteria and swim speed for the different fish species are adopted from (Andersson, et al., 2016) and (Popper, et al., 2014). Modelling also includes calculations assuming stationary, non-fleeing fish.

Table 4.1: Threshold criteria for fish. TTS and injury criteria are unweighted (Andersson, et al., 2016), (Popper, et al., 2014).

Species	Swim speed [m/s]	Threshold criteria, $L_{E,cum,24h}$ $[dB\ re. 1\ \mu Pa^2 s]$	
		TTS [dB]	Injury [dB]
Stationary (Non-fleeing fish)	0.00	186	204
Juvenile Cod	0.38	186	204
Adult Cod	0.90	186	204
Herring	1.04	186	204
Larvae and eggs	-	-	207

4.2. Threshold criteria for marine mammals

Based on the newest scientific literature, species specific frequency weighted $L_{E,cum,24h}$ threshold values (NOAA, 2018), (Southall, et al., 2019) for TTS and PTS are used, Table 4.2. For avoidance behaviour, $L_{p,125ms,VHF} = 103\ dB\ re. 1\ \mu Pa$ (Tougaard, 2021) is used for harbour porpoise.

There is a general lack of quantitative information about avoidance behaviour and impact ranges of seals exposed to pile driving noise and the few studies that have been carried out, point in different directions. During construction of OWF in the Wash, south-east England in 2012, harbour seals abundance was significantly reduced up to 25 km from the pile driving site during unmitigated pile driving (Russell, et al., 2016). Based on the results, Russell et al. (2016) suggested that the reaction distance for seals to unmitigated pile driving was comparable to that of harbour porpoises. On the other hand, Blackwell et al. (2004) studied the reaction of ringed seals to pile driving in connection with establishment of an artificial island in the arctic and saw limited reactions to the noise. As a precautionary approach, it is conservatively assumed that seals react to underwater noise from pile driving at the same distances as harbour porpoise.

The definition of impulsive vs. non-impulsive above, does not apply for the behaviour criterion, only for PTS and TTS. The behaviour criterion is only valid for impulsive noise sources, while there are no scientifically established threshold criteria for behaviour in neither seals nor harbour porpoise for non-impulsive noise sources.

Table 4.2: Threshold criteria for marine mammals. PTS and TTS criteria (NOAA, 2018), behaviour criterion (Tougaard, 2021) for hearing group classifications in (Southall, et al., 2019). "xx" notation refers to species specific weighted levels.

Species	Swim speed [m/s]	Threshold criteria $L_{E,cum,24h,xx}$ $[dB\ re.1\ \mu Pa^2 s]$				Threshold criterion $L_{p,125ms,xx}$ $[dB\ re.1\ \mu Pa]$
		PTS		TTS		Behaviour
		Non-impulsive	impulsive	Non-impulsive	Impulsive	
Porpoise (VHF)	1.5	173 dB	155 dB	153 dB	140 dB	103 dB
Seal (PCW)	1.5	201 dB	185 dB	181 dB	170 dB	-

5. Ambient Underwater Noise Study

In this chapter, the ambient noise levels in the region are examined, based on available information, and the implications are discussed.

No site specific measurements of ambient noise for the Ran OWF area were carried out. For the Baltic Sea however, the ICES continuous underwater noise dataset (ICES, 2018), presents the underwater noise levels in the Baltic Sea as an average of each quarter of 2018 (Q1 – Q4). The noise maps represent a simplified modelled ambient noise level consisting of underwater noise from wind speed and vessel noise (based on AIS data). Noise levels are presented for individual 1/3 octave frequency bands as the median ambient noise level (SPL_{rms}) over all water depths for the quarter.

The available noise levels are limited to three frequency bands of 63, 125 and 500 Hz. The two one-third octave band acoustic measurements centred at 63 and 125 Hz are used as international (European Union Marine Strategy Framework Directive) indicators for underwater ambient noise levels driven by shipping activity (EC Decision 2017/848, 2017). Noise maps for the project area and surroundings are shown in Figure 5.1 - Figure 5.3, for the frequency bands 63 Hz, 125 Hz and 500 Hz respectively. In addition to the 2018 ICES data set, the data portal also features a 2014 data set (ICES, 2014) including a modelled noise map for the frequency band 2 kHz, see Figure 5.4.

The ICES maps show that the ambient noise levels vary significantly with season, and with frequency. The levels at 63 Hz and 125 Hz are higher than those at 500 Hz and 2 kHz. Noise levels also vary by season, with a tendency of higher levels in the colder months/seasons. The latter is attributed to the hydrography, whereby the sound propagation in the Baltic Sea during the warmer months has higher sound attenuation properties.

What is also visible from the maps, is that variations spatially tend to correlate with shipping traffic, illustrated in Figure 5.5. Here, the EMODnet vessel density map (EMODnet, CLS, 2022), is shown for the project area and surroundings for the months of February, May, August and November (as representative months for Q1 – Q4).

It is clear that underwater noise from vessels in the nearby shipping lanes greatly influence the overall ambient noise level inside and outside the project area.

It should be noted that the ambient noise level is only modelled for four frequency bands, making it difficult to compare the impacts on marine life, especially for species with a high frequency hearing like harbour porpoise.

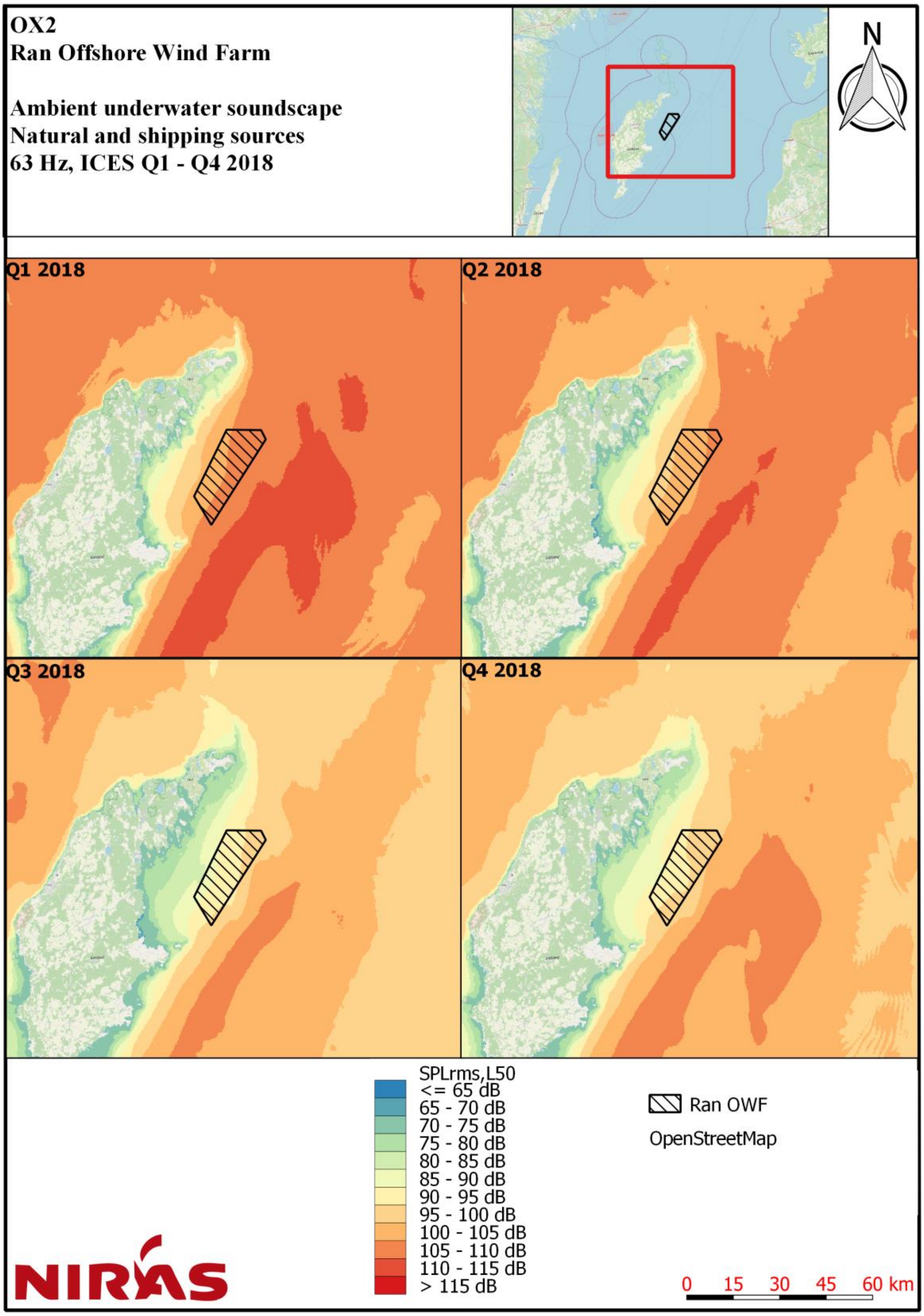

Figure 5.1: ICES soundscape map for 63 Hz, Q1-Q4 2018, 50th percentile $SPL_{rms,63Hz}$ $[dB\ re.1\mu Pa^2]$.

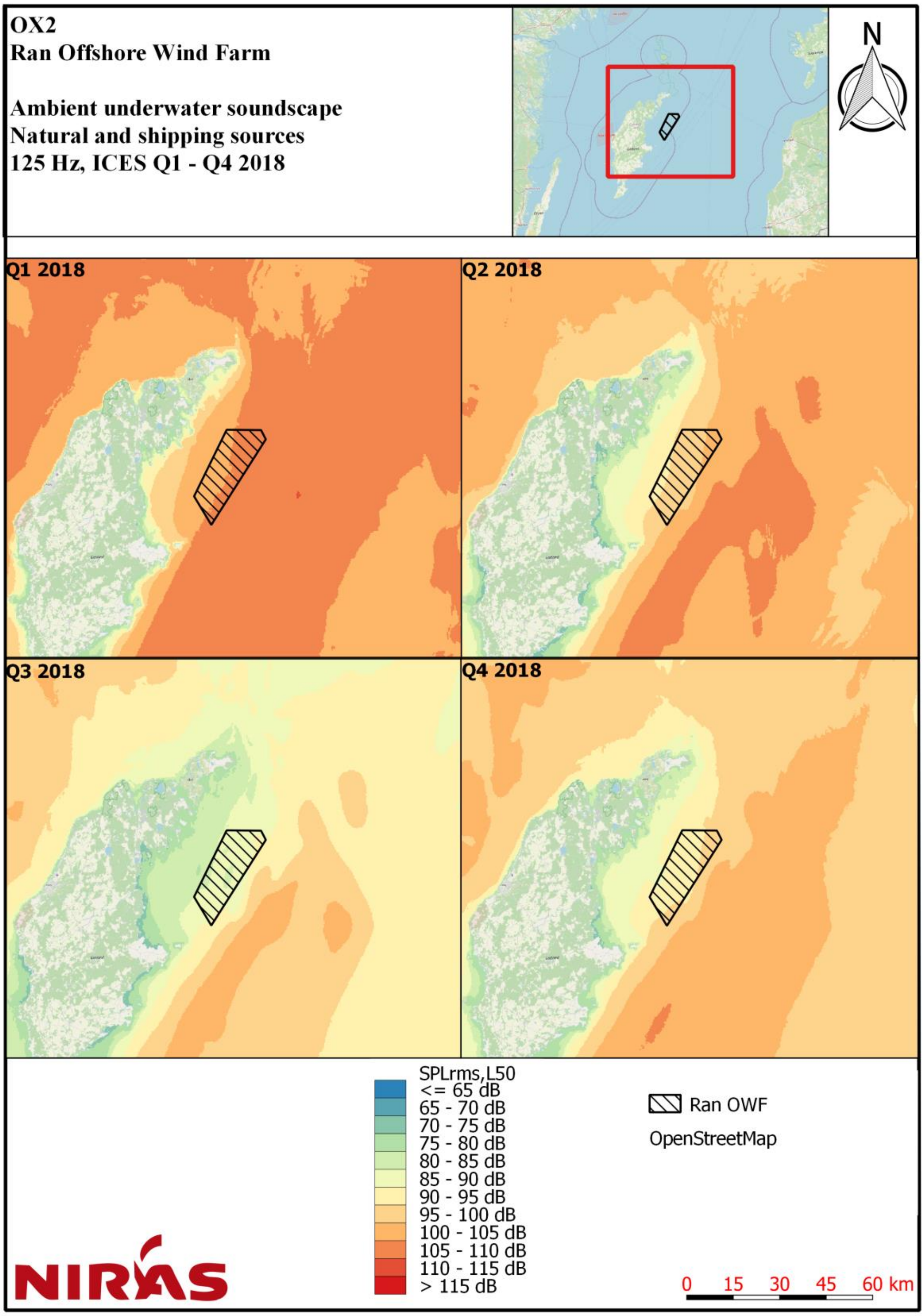

Figure 5.2: ICES soundscape map for 125 Hz, Q1-Q4 2018, 50th percentile $SPL_{rms,125Hz}$ $[dB\ re.1\mu Pa^2]$.

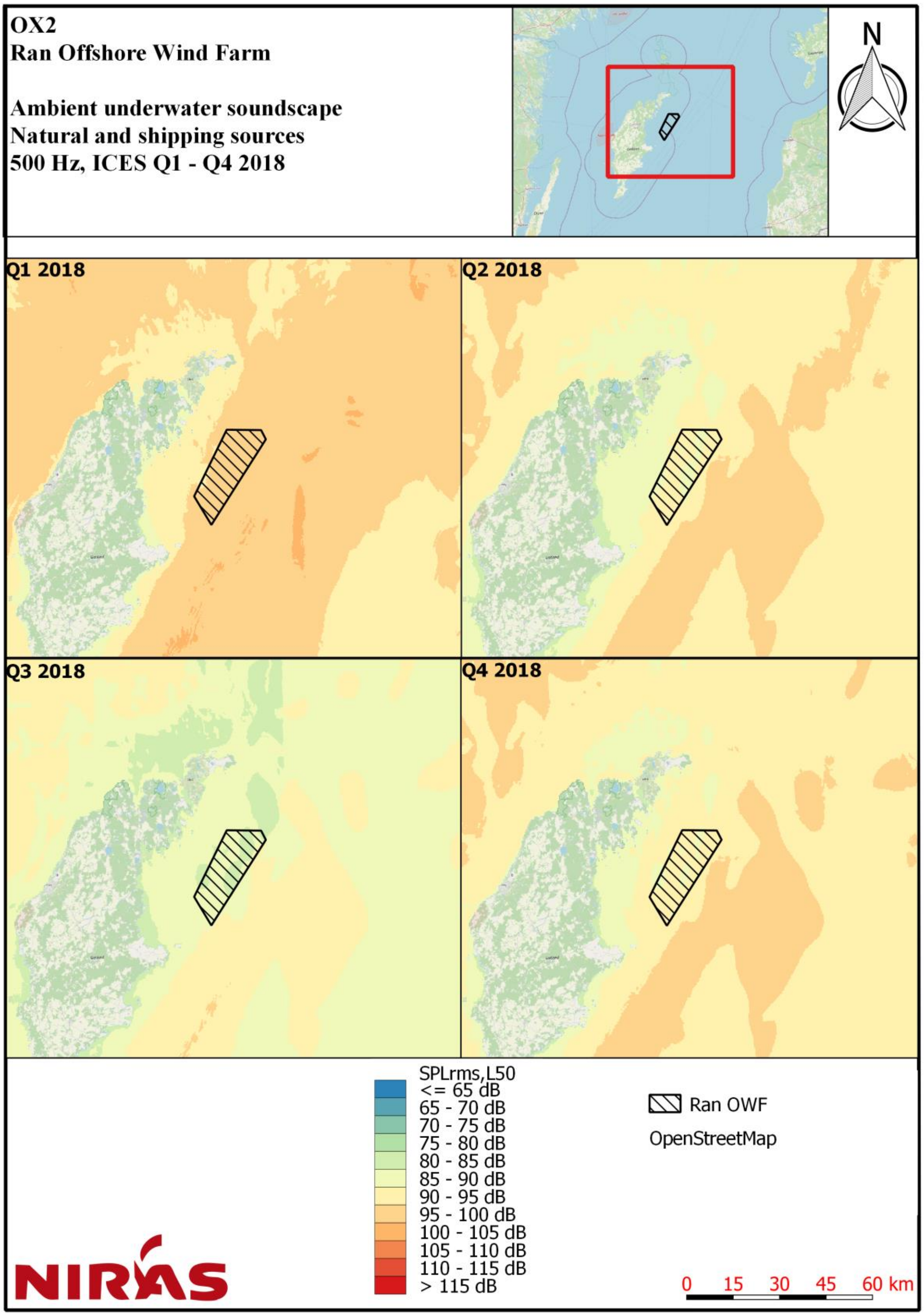

Figure 5.3: ICES soundscape map for 500 Hz, Q1-Q4 2018, 50th percentile $SPL_{rms,500Hz}$ $[dB\ re.1\mu Pa^2]$.

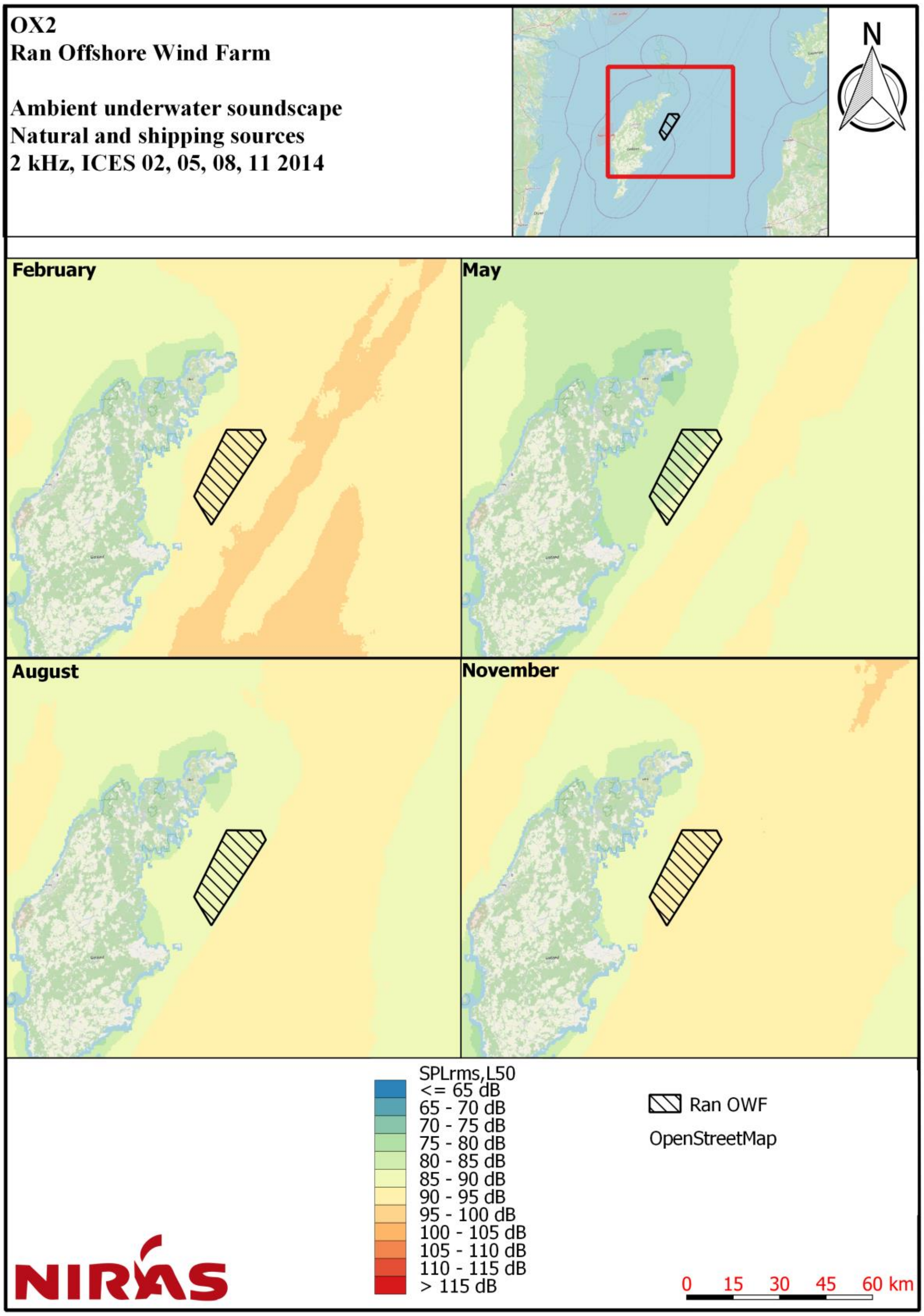

Figure 5.4: ICES soundscape map for 2 kHz, Feb, May, Aug, Nov 2014, 50th percentile $SPL_{rms,2kHz}$ $[dB\ re.1\mu Pa^2]$.

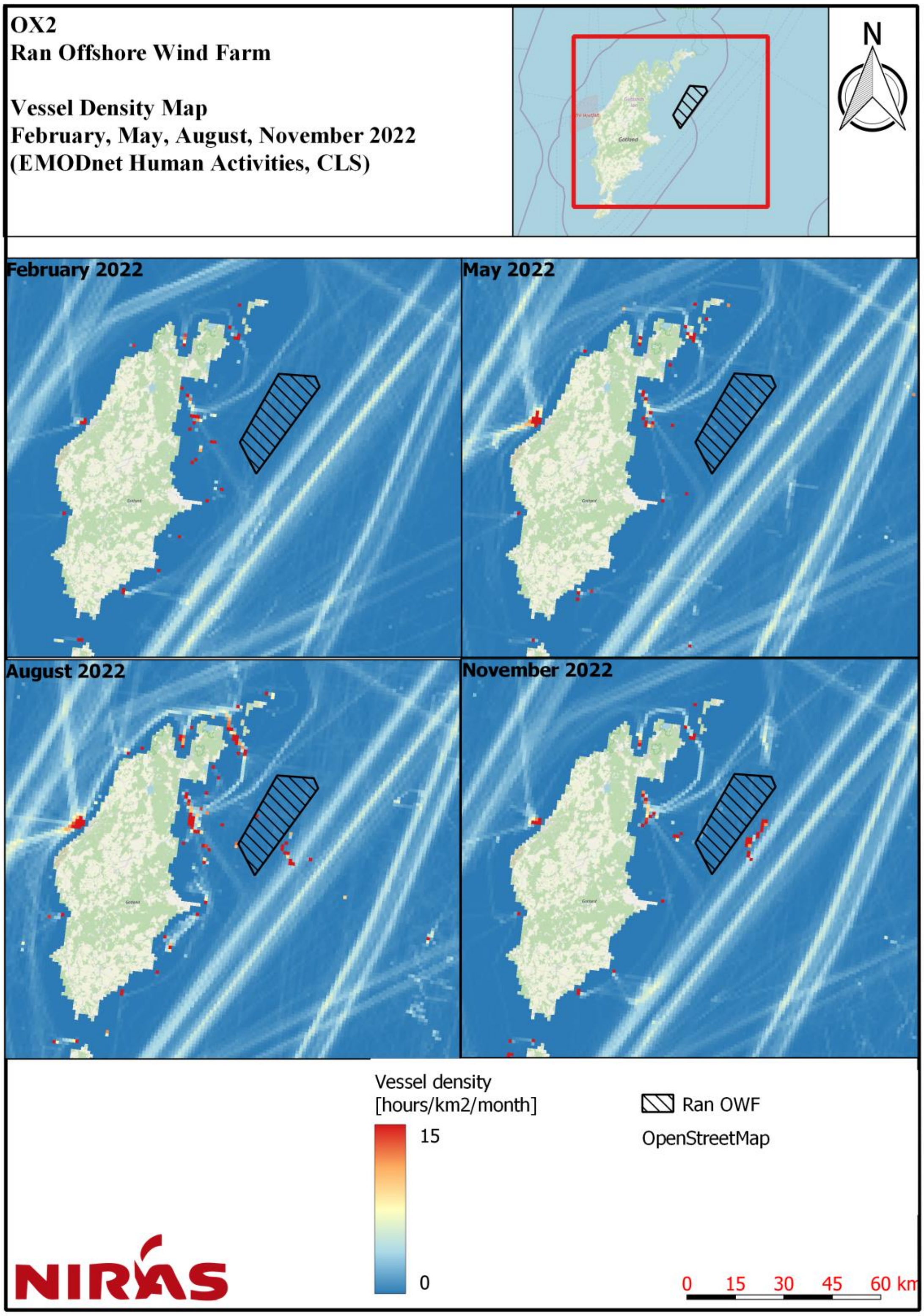

Figure 5.5: Vessel density map from 2022, from EMODnet (EMODnet, CLS, 2022) based on AIS data from CLS.

6. Underwater noise prognosis for construction phase

Ran OWF consists of up to 121 turbine foundations, and up to 4 offshore platforms. Sound propagation modelling is undertaken for individual foundations and does not include the cumulative impact for installation of all turbines. For a discussion on installation of multiple piles, either concurrently or sequentially within a 24 hour duration, see Appendix 1. The cumulative impact from the installation of all foundations within the wind farm, is typically handled in the impact assessment for the relevant species.

Underwater sound propagation modelling consists of three parts:

- A source model, charactering the noise source (pile driving), and the emission of noise into the water column (section 6.2).
- An environmental model, charactering the marine environment and its acoustic properties (section 6.3).
- A sound propagation model, through which the source and environmental model is used to determine the sound propagation loss over distance (section 6.4).

6.1. Project specific inputs

Ran Vindpark AB has informed NIRAS, that the most likely foundation types include:

- Steel monopile foundations up to 14 m diameter.
- Jacket foundation with 3-4 pin piles up to 5 m diameter.

The sound propagation modelling assumes a single pile installation within any 24 hour period for the monopile foundation type, and up to 4 pin piles per 24 hours for jacket foundations. For a discussion on possible implications of multiple foundations installed per day, see Appendix 1.

Furthermore, Ran Vindpark AB has informed NIRAS about which types of foundations that can be installed at different water depths:

- Monopile foundation: 0 m – 60 m
- Jacket foundation: 0 m – 90 m

The technical specifications for the pile installation are provided in Table 6.1 for the monopile foundation, and in Table 6.2 for the jacket foundation.

Parameters for pile installation procedure, including number of pile strikes, intervals and hammer energy levels were chosen in cooperation with Ran Vindpark AB, as realistic worst-case values. It must be recognized that these parameters are not resembling any real-world empirical pile driving data, nor a pile specific drivability analysis, as the final design is still unknown.

Soft start and ramp-up procedures are employed during pile driving, as the upper sediment layers are typically softer and require less energy to penetrate. Instead of starting at full power immediately, the pile driving equipment begins with reduced energy and then gradually ramps up to full power. This allows marine mammals and fish to increase their distance to the pile installation location before full power is applied. While beneficial to the marine fauna, soft start and ramp-up are considered part of the installation technical procedure.

Table 6.1: Technical specifications and pile driving procedure for 14 m monopile foundation. Technical parameters are based on worst-case assumptions.

Technical specification for 14 m monopile foundation			
Foundation type		Monopile	
Impact hammer energy		7000 kJ	
Pile diameter		14 m	
Total number of strikes pr. pile		12850	
Number of piles per foundation		1	
Pile driving procedure			
Name	Number of strikes	% of maximum hammer energy	Time interval between strikes [s]
Soft start	100	10	2
Ramp-up	550 500 1200 1500 1500 1500 1500	30 40 60 70 80 90 100	2 2 2 2 2 2 1.7
Full power	4500	100	1.2

Table 6.2: Technical specifications and pile driving procedure for jacket foundation with 4x 5 m pin piles. Technical parameters are based on worst-case assumptions.

Technical specification for jacket foundation			
Foundation type		Jacket	
Impact hammer energy		7000 kJ	
Pile diameter		5 m	
Total number of strikes pr. pile		12850	
Number of piles per foundation		4	
Time delay between the installation of each pile		0 minutes	
Pile driving procedure			
Name	Number of strikes	% of maximum hammer energy	Time interval between strikes [s]
Soft start	100	10	2
Ramp-up	550 500 1200 1500 1500 1500 1500	30 40 60 70 80 90 100	2 2 2 2 2 2 1.7
Full power	4500	100	1.2

6.2. Source Model

The source model represents the underwater noise emission from the pile driving activity as accurately as possible at the current project stage. NIRAS uses a source model based on best-available empirical data to determine source level and frequency content. It is a simplified model, meaning it approximates the real world data, with certain limitations.

The most comprehensive review of empirical data on underwater noise emission from pile driving, is based on measured sound levels from 21 OWF construction projects involving pile driving activities in the German EEZ of the North Sea and Baltic Sea between 2012 - 2019 (Bellmann, et al., 2020). The review describes and discusses the different factors affecting the pile driving source level and frequency content. In the following, the relevant parameters and uncertainties are discussed, as pertains to the implementation in the NIRAS source model.

6.2.1. Influence of pile dimensions

The emitted underwater noise from pile driving depends primarily on the dimensions of the pile. An increased pile diameter will lead to a larger noise emission not only due to the larger surface area of the pile in contact with water, but also due to the increased hammer energy required to install it.

Bellmann and co-authors (2020), measured sound levels at a distance of 750 m from pile installations of different pile diameters. The results are shown in Figure 6.1, with measured sound levels as a function of pile diameter. The measurements are all normalized to 750 m distance from the pile.

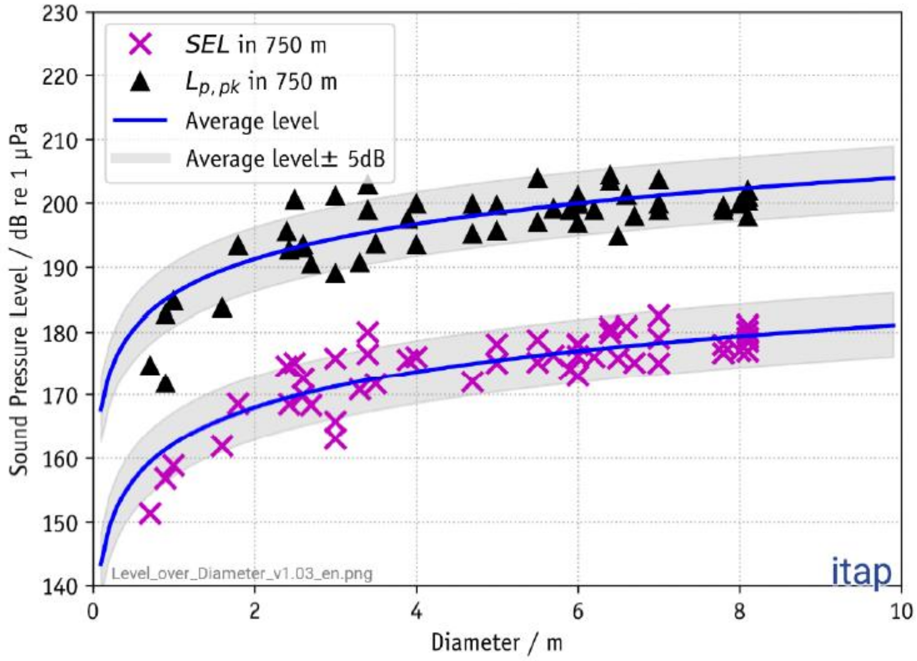

Figure 6.1: Relationship between peak and SEL, measured at 750 m distance, and pile size (Bellmann, et al., 2020).

The blue curves in Figure 6.1 indicate the best fit of the measurement results. For the SEL results (lower curve and crosses in Figure 6.1), the relationship between pile size and measured level is approximately $\Delta \mathrm{SEL} = 20 * \log 10\left(\frac{\mathrm{D2}}{\mathrm{D1}}\right)$ [dB], where D1 and D2 are the diameter of 2 piles, and ΔSEL is the dB difference in sound level between the two. This relationship indicates an increase of 6 dB when doubling the pile diameter.

It should be noted that variations in measured sound levels for a specific pile size do occur, as indicated by the spread of datapoints, around the fitted (blue) lines in Figure 6.1. This spread gives a 95%-confidence interval of ±5 dB which is indicated by the grey shaded areas. The spread is primarily due to site specific conditions, with a key factor being the applied hammer type and energy used.

In the NIRAS source model, the average trend line in Figure 6.1 is generally used to dictate the source level.

6.2.2. Influence of hammer type

Modern impact pile drivers typically consist of a large mass, or weight, suspended inside a hydraulic chamber, where the pressurized hydraulic fluid is used to push up the weight to the desired height, after which it is dropped. The impact is then transferred through an inner construction of shock absorbers and an anvil connected to the pile top. This motion transfers a large part of the applied energy to drive the pile downwards (Adegbulugbe, et al., 2019).

Using a large impact hammer with a heavy falling mass at 50-60% of its full capacity will lead to lower noise output compared to that from a smaller impact hammer using 100% capacity to achieve the same blow energy (Bellmann, et al., 2020). While the two hammers will deliver the same energy to the pile, the maximum amplitude will be lower for the large impact hammer due to extended contact duration between hammer and pile-head. Different impact hammers can give up to several dB difference for the same applied energy (Bellmann, et al., 2020). However, the current level of knowledge does not provide a clear overview of hammer model specific additions/deductions with regards to average underwater noise emission, and is therefore not used as a parameter influencing the NIRAS source model.

6.2.3. Influence of hammer energy

The hammer energy describes the energy (measured in kJ) applied for each pile strike. The hammer energy required to install the pile varies over the installation of a pile, and primarily depends on the soil resistance of the different sediment layers the pile has to penetrate. An increase in hammer energy, will transfer more energy into the pile and therefore also typically results in a higher noise emission. Figure 6.2 shows the SEL versus penetration depth and blow energy. During the first half of the piling sequence, an increase in blow energy leads to an increase in measured SEL (Figure 6.2). This relationship is approximated by 2-3 dB increase in measured SEL every time the blow energy is doubled (Bellmann, et al., 2020). In the second half of the piling sequence, the blow energy is still increasing, however the measured SEL does not increase. One possible explanation for this is that a larger part of the applied energy is converted into downward motion of the pile, rather than radiated to the water column as excess.

In the NIRAS source model, hammer energy is included in the calculation of cumulative SEL, based on the piling procedure agreed with the client. The model does not include penetration depth dependent deductions, and could therefore be considered conservative for the last stage of the pile installation.

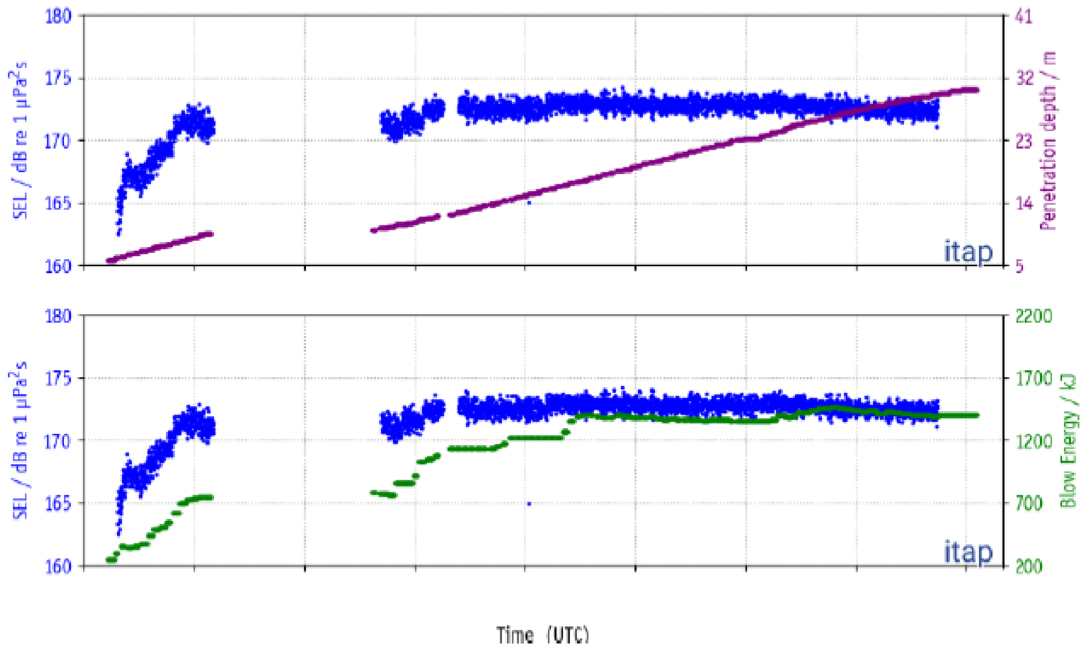

Figure 6.2: Relationship between SEL versus penetration depths and blow energy (Bellmann, et al., 2020).

6.2.4. Influence of pile submersion

A pile installation can be carried out through either above sea level piling, where the pile head is located above water level, or through below sea level piling, where the pile head is located below the water line. The former is typically the case for monopiles, while the latter is often the case for jacket piles (Bellmann, et al., 2020). A combination of the two is also possible, where the pile head is above water at the beginning of the pile installation and is fully submerged in the late stages of the piling. The influence of submersion is illustrated in Figure 6.3, where the top plot illustrates a fully above water piling scenario. Here, the energy is increased over time and the underwater noise level measured also increases over time. In the bottom plot (above water piling initially, then below water piling), after the point of submersion, the measured noise level decreases even though the hammer energy level is kept constant. In the NIRAS source model, pile submersion is not included as a factor due to the limited knowledge of the detailed pile installation procedure. The model is therefore considered conservative for the case of submerged pile driving.

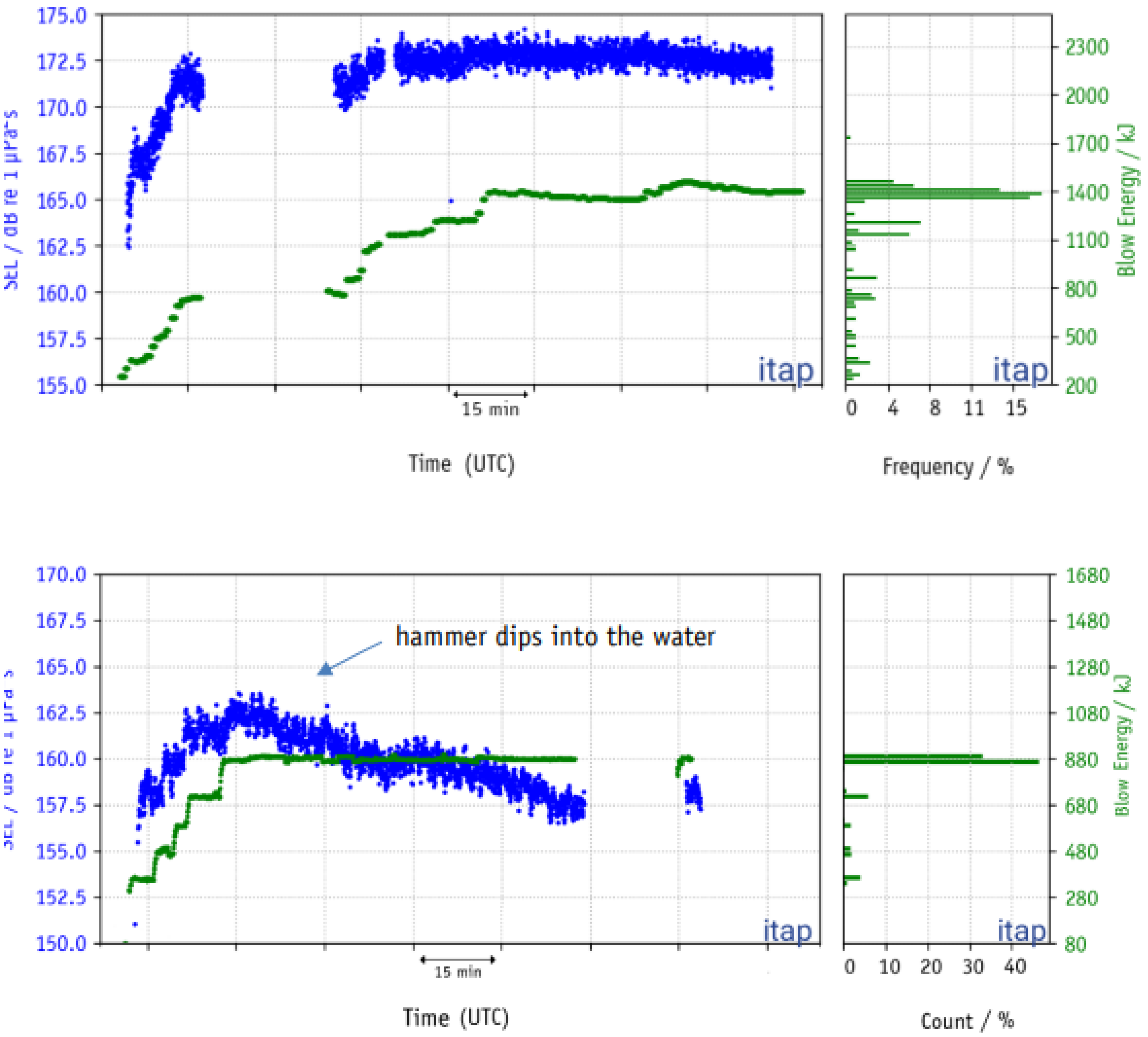

Figure 6.3: Illustration of pile submersion and its effect on measured underwater noise levels. In the top plot (fully above water piling scenario), the energy is increased over time and the underwater noise level measured increases over time. In the bottom plot (above water piling initially, then below water piling), after the point of submersion, the measured noise level decreases even though the hammer energy level is constant. From (Bellmann, et al., 2020). Note that the two plots are for two different installations, pile types and hammers. Levels should therefore not be compared.

6.2.5. Influence of water depth

The water depth, in shallow water, can limit the propagation of low frequency noise. In Figure 6.4, the cut-off frequency as a function of water depth is shown. Frequency content of the noise source, below the cut-off frequency, has difficulty propagating through the water column, and will be attenuated at an increased rate, compared to frequency content above the cut-off (Bellmann, et al., 2020). As an example from Figure 6.4, frequencies below 200 Hz cannot propagate properly in water depths less than ~4 m with a sandy sediment. The influence of water depth is handled through the propagation software (dBSea).

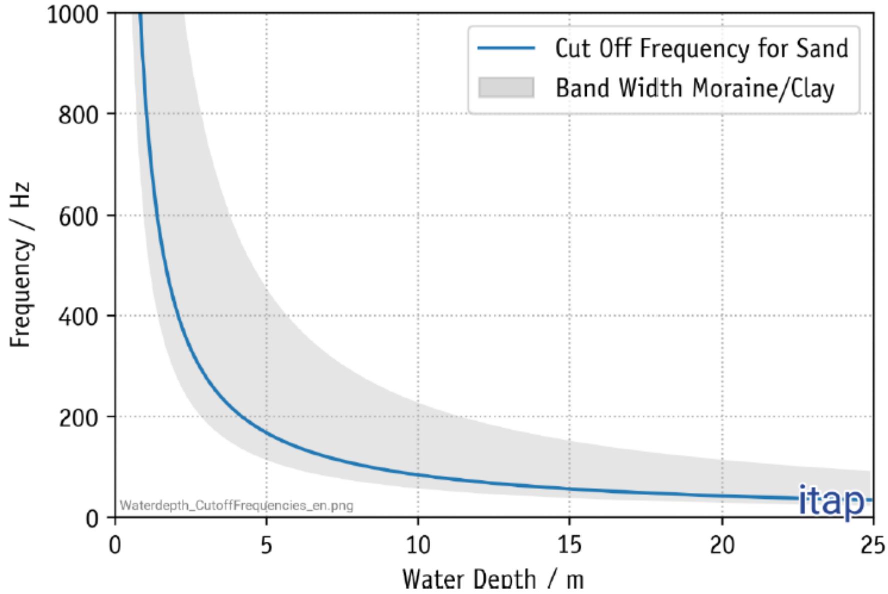

Figure 6.4: Cut off frequency and its dependency on sediment type (in this example: sand) and water depth (Bellmann, et al., 2020).

6.2.6. Frequency spectrum and influence of foundation type

Due to the natural variations of measured frequency content, between sites, piles, water depths, hammer energy levels and other factors, it is almost guaranteed that the frequency response measured for one pile will differ from that of any other pile, even within the same project area (see grey lines in Figure 6.5). Since it is practically impossible to predict the exact frequency spectrum for any specific pile installation, an averaged spectrum (red line), is proposed in (Bellmann, et al., 2020).

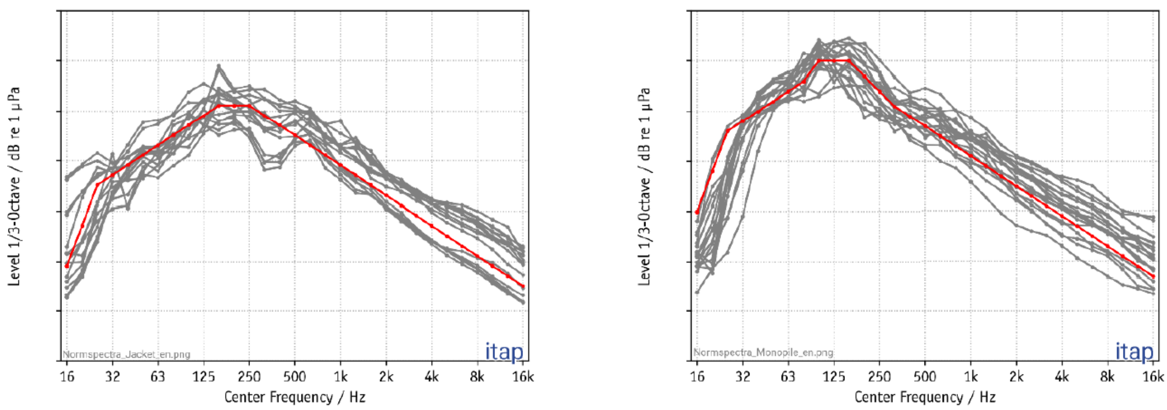

Figure 6.5: Measured pile driving frequency spectrum (grey lines) at 750 m, with the averaged spectrum shown as the red line (Bellmann, et al., 2020). The spectrum ranges from 110-180 dB. Left: jacket foundations; Right: monopile foundations.

The spectrum shown to the left in Figure 6.5 is the pile driving frequency spectrum (grey lines) measured at 750 m for pin piles with diameters up to 3.5 m. The red line indicates the averaged spectrum and is proposed to be used as a theoretical model spectrum for sound propagation modelling of pin piles.

The right side of Figure 6.5 shows the pile driving frequency spectrum (grey lines) measured at 750 m for monopiles with diameter of 5 - 8 m. The red line indicates the averaged spectrum and is proposed to be used as a theoretical model spectrum for sound propagation modelling of monopiles.

The frequency spectrum of the pile depends on its length, diameter and wall thickness as well as other physical properties. To complicate the matter further, piles will not necessarily have the same dimensions in top and bottom. In early stage prognosis, the pile specific parameters are typically based on worst case preliminary designs and are not considered on a pile-by-pile basis. In general, the larger the pile, the lower the resonance frequency, and thereby the lower the "plateau" where the most energy is located in the frequency domain. In Figure 6.5, it is visible that for 6 – 8 m diameter monopiles, the peak is located at 100 – 160 Hz, while for pin piles with a diameter up to 3.5 m diameter, the peak is located at 160 – 250 Hz. A frequency shift from the idealized spectrum could therefore be argued as relevant, when considered piles with diameters outside this range, however a suitable relationship between pile diameter and peak frequencies is not yet established by science. From the perspective of a worst-case prognosis, an unshifted frequency spectrum for larger piles, is considered conservative in a shallow water scenario, where low frequencies need a certain water depth to propagate, as discussed in section 6.2.5. A downward shift in frequency, would therefore risk increased attenuation, compared to an unshifted scenario.

The frequency spectrum of the emitted noise can also be affected by the properties of the surrounding water and seabed. For example, softer seabed materials can absorb more of the acoustic energy, resulting in a frequency spectrum with less high-frequency noise emitted. Detailed site specific knowledge of the seabed is however required to include any such influence in the prognosis.

In the NIRAS source model, the frequency content is not shifted as a function of pile diameter, the applied frequency spectrum is therefore conservative.

6.2.7. Source model implementation

NIRAS' empirical source model is based primarily on the relationship between pile diameter and measured sound levels derived from (Bellmann, et al., 2020), as well as from empirical data available through own and other measurements. The source model is represented by the ESL at 1 m distance from the pile. It is a back-calculated approximation using an equivalent point source that in 750 m distance follows the empirical data presented by the blue curve in Figure 6.1, and at ranges beyond this, will provide a conservative approximation. At ranges closer to the source, uncertainty of prognosis results is however increased, as the equivalent point source model cannot accurately reflect the positive and destructive interference patterns that occur.

Soft-start and ramp up is included in the source model as these are regarded as part of the installation process.

Similarly, the averaged frequency spectrum at 750 m is used to derive the equivalent 1 m source level in each 1/3 octave band. Since different frequencies attenuate differently with distance, the frequency spectrum used as a model input does not directly match that of Figure 6.5, however is chosen so that it, conservatively, approximates it in 750 m.

Based on the project specific pile installation parameters supplied by the client, see section 6.1, source models were derived for each foundation type in the following.

6.2.7.1. Monopile foundation

Following the methodology in section 6.2.7 for setting source level and frequency spectrum, the source model parameters for the 14 m monopile foundation are presented in Table 6.3, with detailed 1/3-octave band source level shown in Figure 6.6.

Table 6.3: Broadband source model parameters for impact pile driving of 14 m monopile.

Parameter	**Value**	**Reference**
Unmitigated reference level @750m distance, $L_{E,p,750m}$ (unweighted)	184.5 dB	Relationship between pile diameter and sound level, Figure 6.1 (Bellmann, et al., 2020).
Unmitigated source level @ 1m distance, $L_{S,E}$ (Unweighted / PCW / VHF)	227.7 dB (-) 206.0 dB (PCW) 182.3 dB (VHF)	Back calculated using NIRAS empirical model, section 6.2.7.

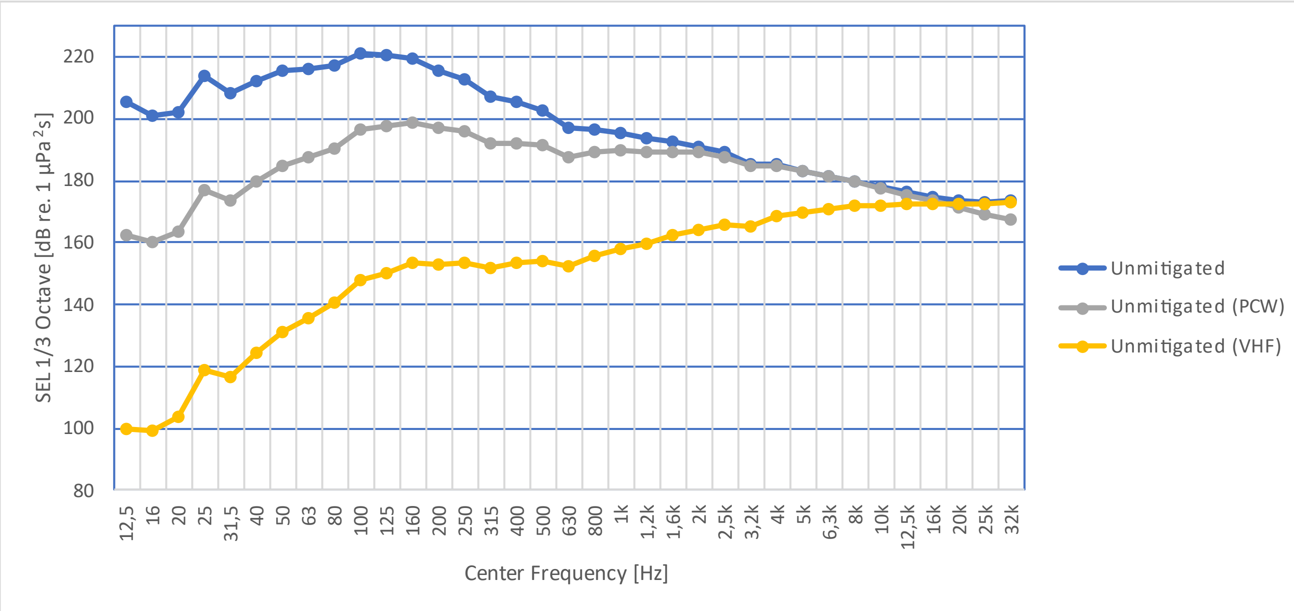

Figure 6.6: Source spectrum at 1 m distance, unmitigated, for pile driving of 14 m monopile.

6.2.7.2. Jacket foundation

Following the methodology in section 6.2.7 for setting source level and frequency spectrum, the source model parameters for the jacket foundation are presented in Table 6.4, with detailed 1/3-octave band source level shown in Figure 6.7.

Table 6.4: Broadband source model parameters for impact pile driving of 5 m pin piles for jacket foundation.

Parameter	**Value**	**Reference**
Unmitigated reference level @750m distance, $L_{E,p,750m}$ (unweighted)	176.4 dB	Relationship between pile diameter and sound level, Figure 6.1 (Bellmann, et al., 2020).
Unmitigated source level @ 1m distance, $L_{S,E}$ (Unweighted / PCW / VHF)	218.4 dB (-) 200.8 dB (PCW) 180.1 dB (VHF)	Back calculated using NIRAS empirical model, section 6.2.7.

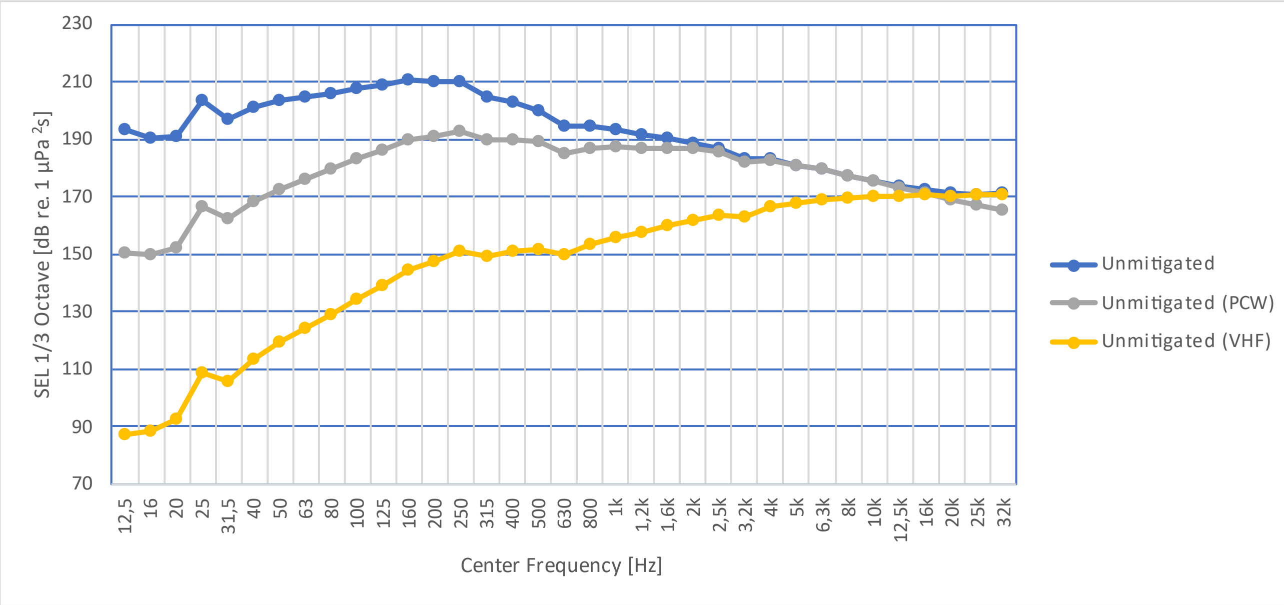

Figure 6.7: Source spectrum at 1 m distance, unmitigated, for pile driving of 5 m pin pile in jacket foundation.

6.2.8. Source positions

In order to ensure a worst-case prognosis with regards to local sound propagation conditions, it was agreed with Ran Vindpark AB to select a number of representative positions throughout the OWF area, such that different sound propagation scenarios within the site are covered. Areas where sound propagation most likely results in the longest impact ranges are identified, taking into account nearby marine mammal and/or fish protection areas if relevant. The chosen source positions are listed in Table 6.5, along with coordinates, and distances to nearby areas of interest. The positions are also shown in Figure 6.8, and the foundation types considered for each position are listed in Table 6.6.

Table 6.5: Source positions used for sound propagation modelling of underwater noise during construction phase.

Position ID	Easting	Northing	EPSG	Water depth	Nearby areas of interest
1	398492	6402915	25834	48 m	Nat2000 area "Gotska Sandön-Salvorev", ~23 km distance Coast of Gotland, ~15 km distance City of Herrvik, ~44 km distance
2	401769	6391340	25834	74 m	Nat2000 area "Gotska Sandön-Salvorev", ~34 km distance Coast of Gotland, ~33 km distance City of Herrvik, ~37 km distance
3	388503	6379078	25834	47 m	Nat2000 area "Gotska Sandön-Salvorev", ~49 km distance Coast of Gotland, ~20 km distance City of Herrvik, ~19 km distance

Table 6.6: Foundation types investigated for the different source positions.

Position ID	Water depth	Monopile	Jacket
1	48 m	X	X
2	74 m		X
3	47 m	X	X

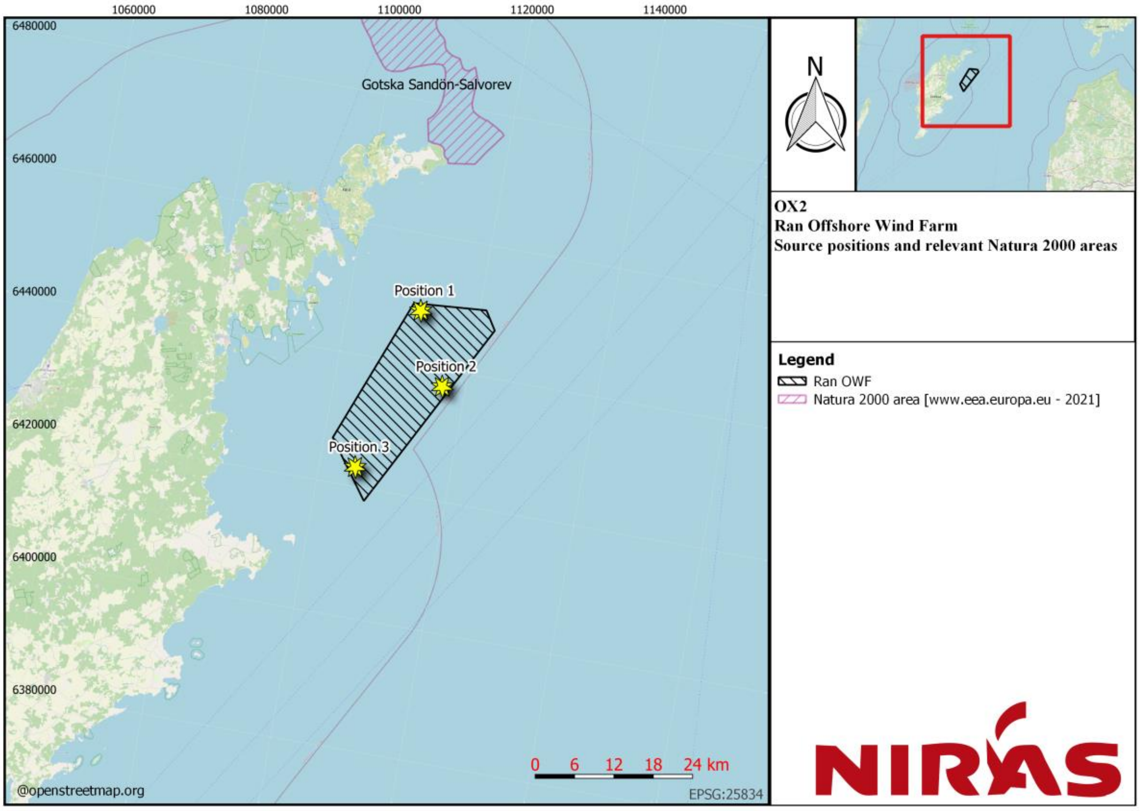

Figure 6.8: Source positions chosen for sound propagation modelling as well as nearby relevant Natura 2000 area.

6.3. Environmental model

The basic principles of underwater sound propagation, as a function of the environmental factors are described in this chapter, and the project specific environmental parameters used for sound propagation modelling are presented. The environmental model is implemented in the underwater sound propagation software tool dBSea. Environmental input parameters for salinity, temperature and their derivative, sound speed depend on the specific source model positions, and are considered individually for the source positions.

Sound travels faster and farther in water than in air because water is denser and more efficient at transmitting sound waves. However, the aquatic environment is complex and heterogeneous, and sound propagation is influenced by a number of environmental parameters:

- Bathymetry,
- seabed sediments,
- temperature, salinity and sound speed,
- sea surface roughness, and
- volume attenuation.

These factors can cause sound to refract, reflect, scatter, and attenuate as the sound waves propagate through water, making it challenging to predict its behavior. These factors, and their implementation for sound propagation modelling, are described in the following sections.

6.3.1. Bathymetry

The shape and composition of the seafloor plays a critical role in the propagation of sound waves through the water. The seafloor can act as a barrier or a reflector for sound waves, depending on its composition and shape.

A smooth, flat seafloor can reflect sound waves back towards the surface, whereas a rough, irregular seafloor can scatter sound waves in different directions, causing them to lose intensity and become weaker over distance.

Additionally, underwater ridges, canyons, and other geological features can act as waveguides, trapping and focusing sound waves in specific depths or regions.

Overall, bathymetry affects underwater sound propagation by influencing the speed, direction, and intensity of sound waves as they travel through the water. A detailed understanding of the bathymetry is critical for predicting and modelling the nature of underwater sound propagation in a real world scenario.

If project specific high resolution bathymetry is available, this is typically preferred over publicly available databases, which tend to be of lower resolution. Project specific bathymetry however seldomly extend beyond the project boundary. To calculate impact ranges for marine mammals and fish, it is necessary for the sound propagation model to extend 10 – 20 km beyond the project boundary. Project specific bathymetry can therefore seldomly be used alone.

For projects where no high resolution bathymetry is available, or where it is limited to the project boundary, publicly available databases, such as (EMODnet, 2021), can be used. A map of the bathymetry for Europe is shown in Figure 6.9, where darker colours indicate deeper areas, and lighter colours indicate more shallow water (EMODnet, 2021).

Figure 6.9: Bathymetry map over European waters from EMODnet, where light blue indicates shallow waters and dark blue indicates deeper waters (EMODnet, 2021).

The bathymetry for the project area and surroundings consists of information from the sources listed in Table 6.7. A visualisation of the bathymetry model for the project area and surroundings is shown in Figure 6.10.

Table 6.7: Bathymetry model data sources.

Data source	Reference
Bathymetry	(EMODnet, 2022)

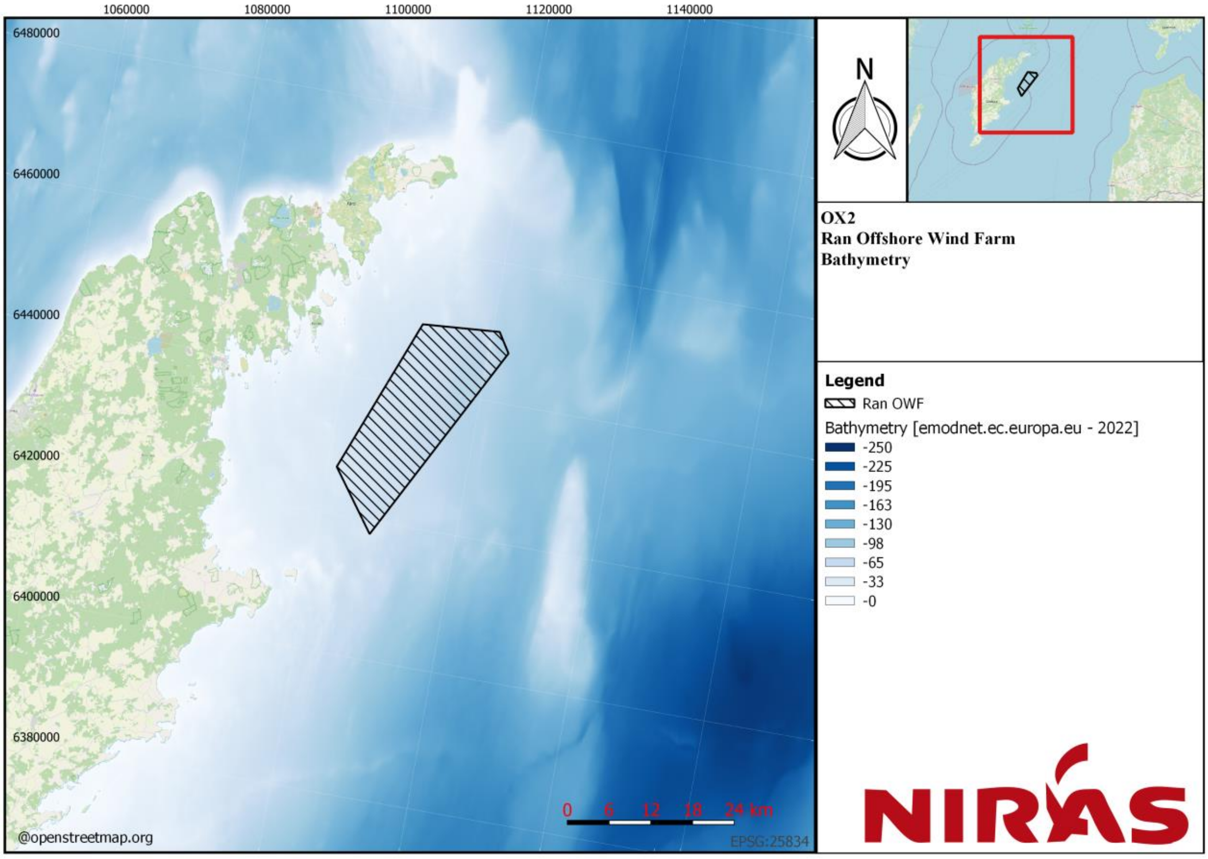

Figure 6.10: Bathymetry for the project area and surroundings, sources as listed in Table 6.7.

6.3.2. Seabed sediment

Seabed sediment layers can have a significant effect on the propagation of sound waves through the water. The acoustic properties of sediment layers are influenced by several factors, including the composition, density, porosity, and grain size distribution of the sediments. Generally, sediments with larger grain sizes and lower porosity have higher acoustic velocities and can transmit sound waves more efficiently than finer grained and more porous sediments.

The properties of sediment layers can also affect the reflection, refraction, and attenuation of sound waves. For example, a layer of fine-grained, soft sediment can absorb and scatter sound waves, causing them to lose intensity and become weaker over distance. Conversely, a layer of hard, compacted sediment can reflect sound waves, resulting in increased sound intensity in certain areas.

The thickness of sediment layers can also play a role in underwater sound propagation. Thicker sediment layers can absorb and scatter sound waves more effectively, while shallower sediment layers can reflect and refract sound waves more strongly.

The thickness and acoustic properties of each seabed layer, from seabed to bedrock, is generally obtained through site specific literature research in combination with available site-specific survey findings.

Where site specific surveys do not reveal the top layer conditions, or where the site specific information is limited to the project boundary, publicly available databases, such as the seabed substrate map from (EMODnet, 2021) (Figure 6.11) is generally used.

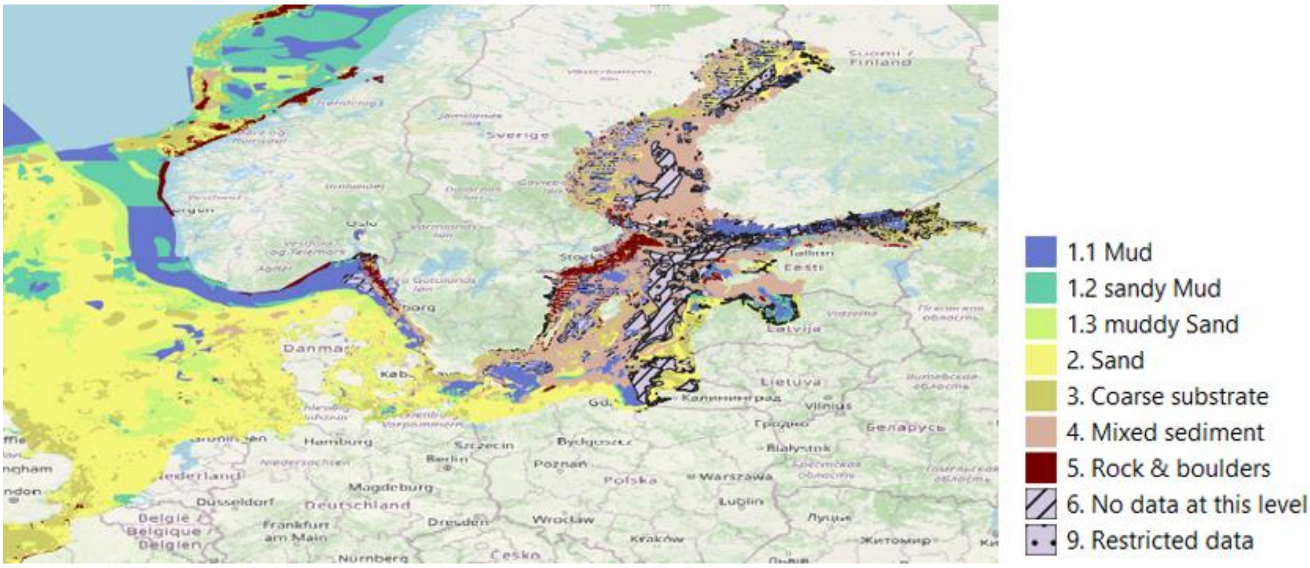

Figure 6.11: A section of the seabed substrate map, (Folk 7) (EMODnet, 2021).

From the available sediment data sources, a discretized and simplified version is created, whereby the layer thicknesses and sediment types are defined in a number of points. A high number of sediment points is necessary, when the variation in sediment types and thicknesses within the project area and surroundings increases.

For each point in the model, the sediment layer types are translated into geoacoustic parameters, in accordance with Table 6.8, utilizing information from (Jensen, et al., 2011; Hamilton, 1980).

Table 6.8: Geoacoustic properties of sediment layers used in the environmental model. Sources: (Jensen, et al., 2011; Hamilton, 1980). Note, mixed sediment is based on a mix of sand, silt and gravel. Moraine boulders is similarly a mix of primarily moraine with boulders.

Sediment	Sound Speed [m/s]	Density [kg/m³]	Attenuation factor [dB/λ]
Clay	1500	1500	0.2
Silt	1575	1700	1.0
Mud (clay-silt)	1550	1500	1.0
Sandy mud	1600	1550	1.0
Sand	1650	1900	0.8
Muddy sand	1600	1850	0.8
Coarse substrate	1800	2000	0.6
Gravel	1800	2000	0.6
Mixed sediment	1700	1900	0.7
Moraine	1950	2100	0.4
Moraine Boulders	2200	2200	0.3
Rock and boulders	5000	2700	0.1
Chalk	2400	2000	0.2

The sediment model is constructed using available sources, see Table 6.9, and resulted in a 480 point sediment model, with topsoil types shown in Figure 6.12. Primary seabed surface layers in the project area are muddy sand, mixed sediment and coarse substrate with occurrences of rock and boulders and sand. For Ran OWF and the surroundings the layer thickness of the upper sediment is not well defined in the available sources and a conservative thickness of 5 m is used throughout. Acoustic parameters for each layer are shown in Table 6.8. As it is not feasible to create an infinitely detailed sediment model, conservative layer thickness, and sediment types are used to provide a worst-case sediment model.

Acoustic parameters for each layer are shown in Table 6.8. As it is not feasible to create an infinitely detailed sediment model, conservative layer thickness, and sediment types are used to provide a worst-case sediment model. The data sources used to inform the sediment model implementation, are shown in Figure 6.13 - Figure 6.16.

Table 6.9: Sediment model data sources.

Data source	Reference
Seabed substrate map	(EMODnet, 2021)
Sediment profile map	(Schäfer, 2020), (Sopher, et al., 2016)
Acoustic parameter model for sediment types	Table 6.8

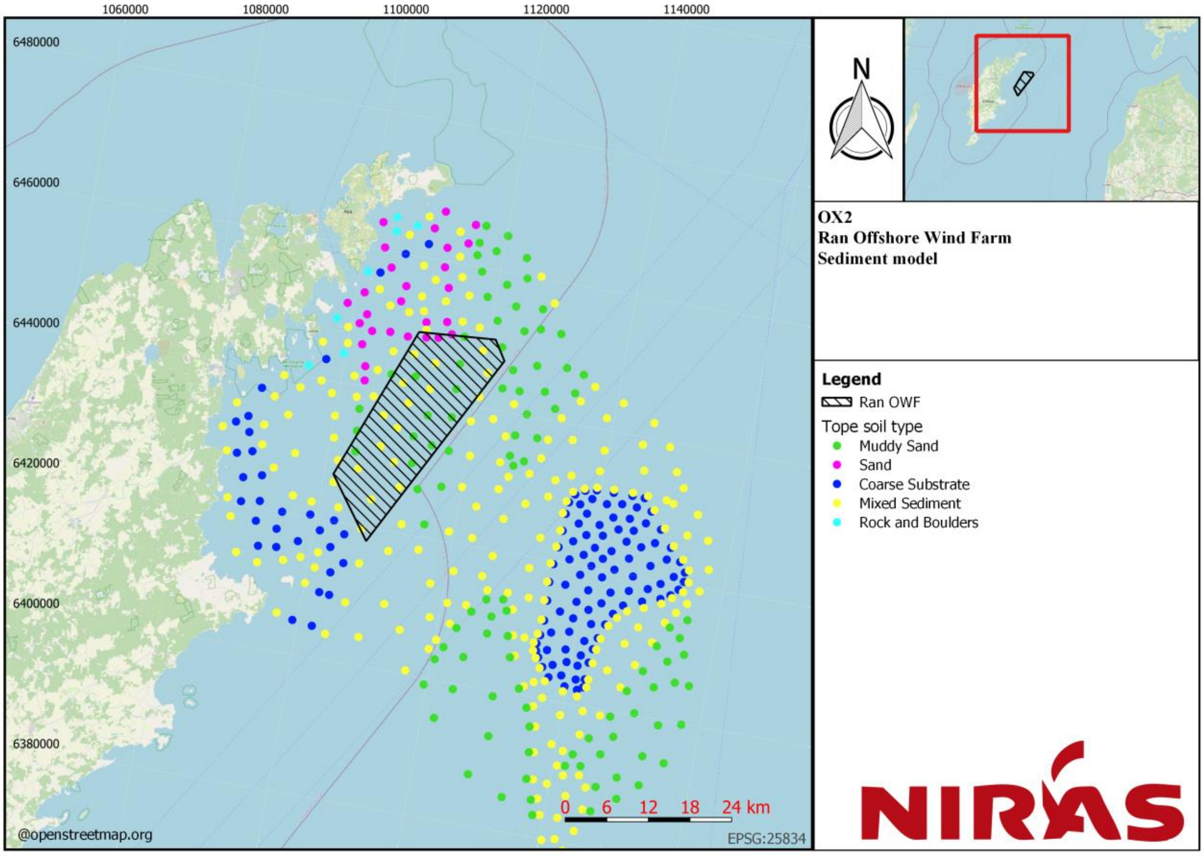

Figure 6.12: Sediment model points and topsoil layer type.

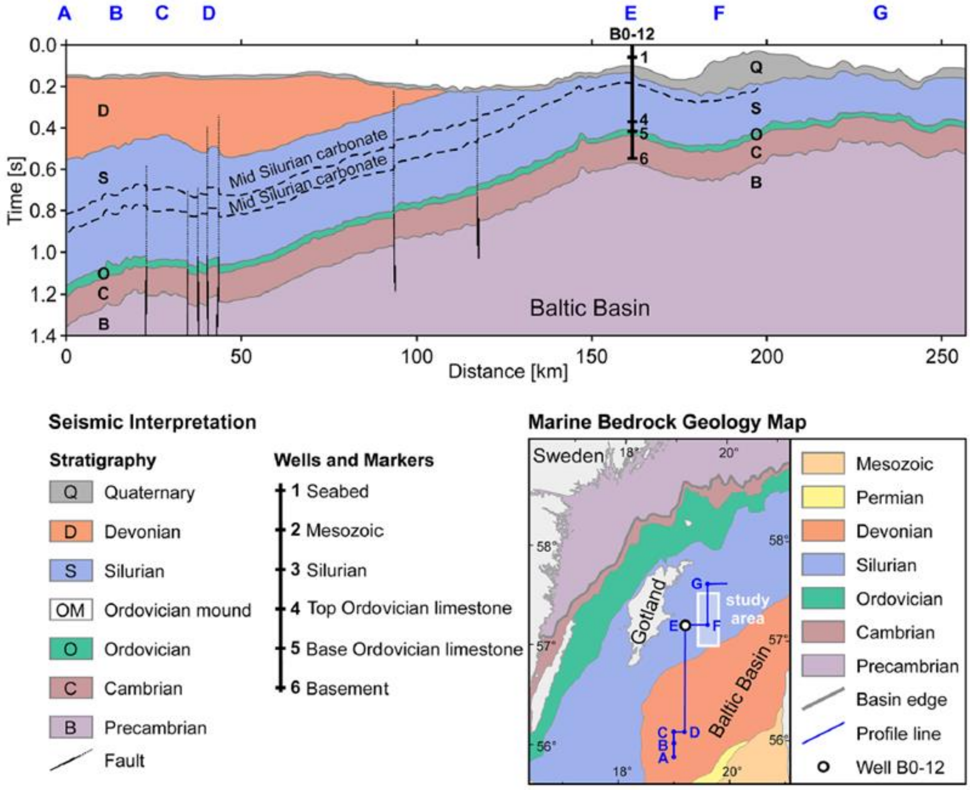

Figure 6.13: Sediment model data source (Schäfer, 2020).

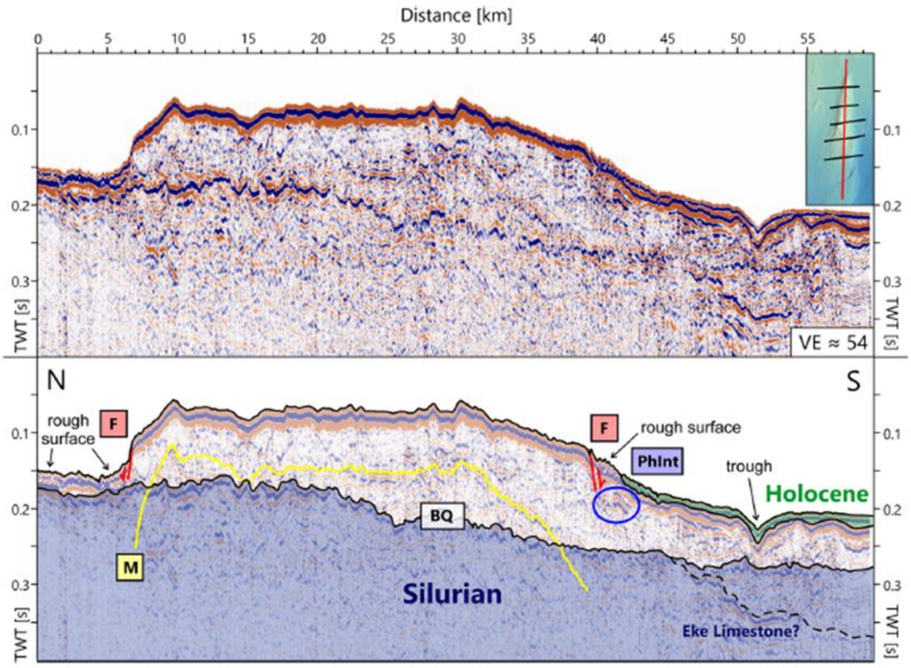

Figure 6.14: Sediment model data source (Schäfer, 2020).

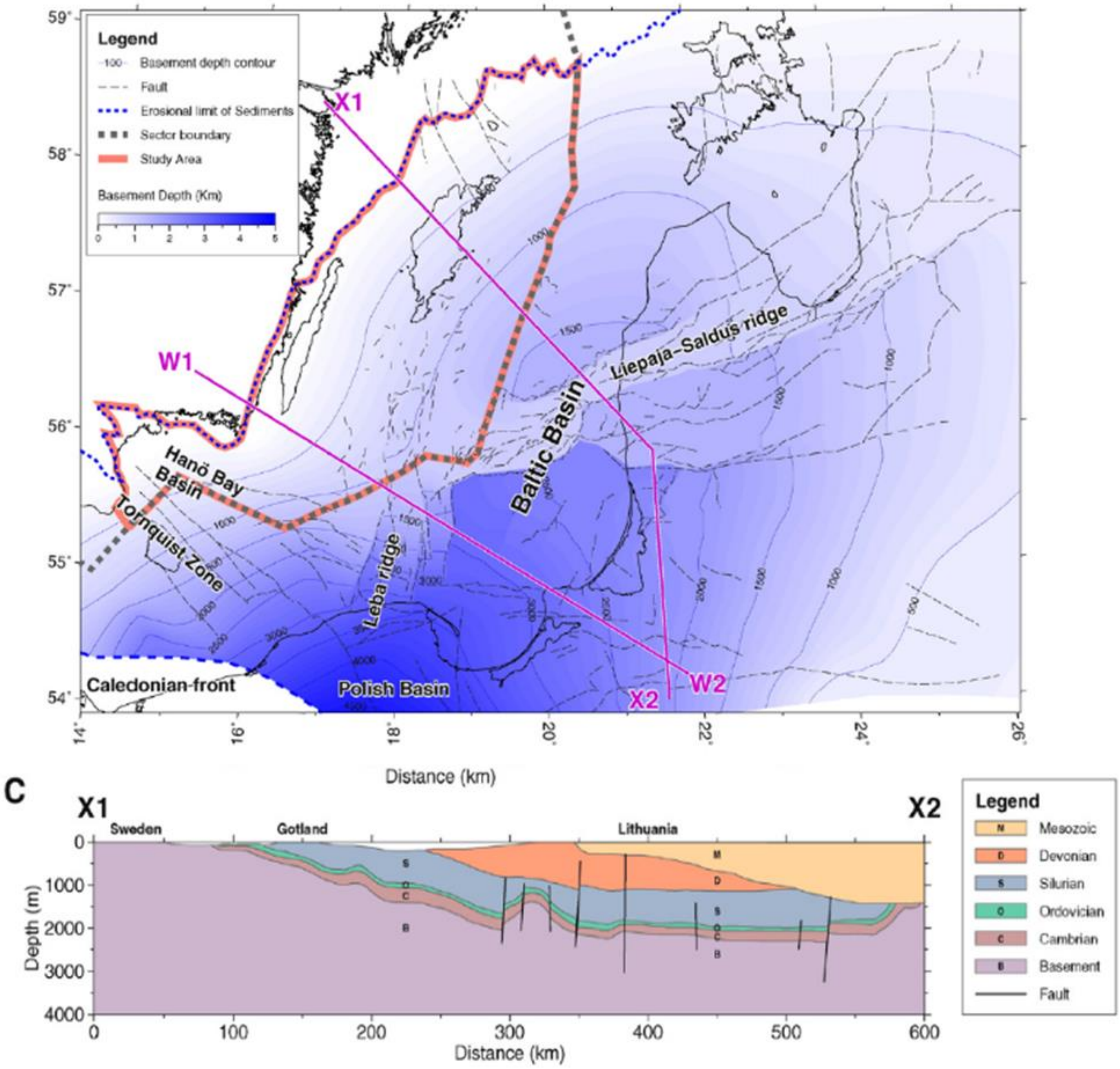

Figure 6.15: Sediment model data source (Sopher, et al., 2016).

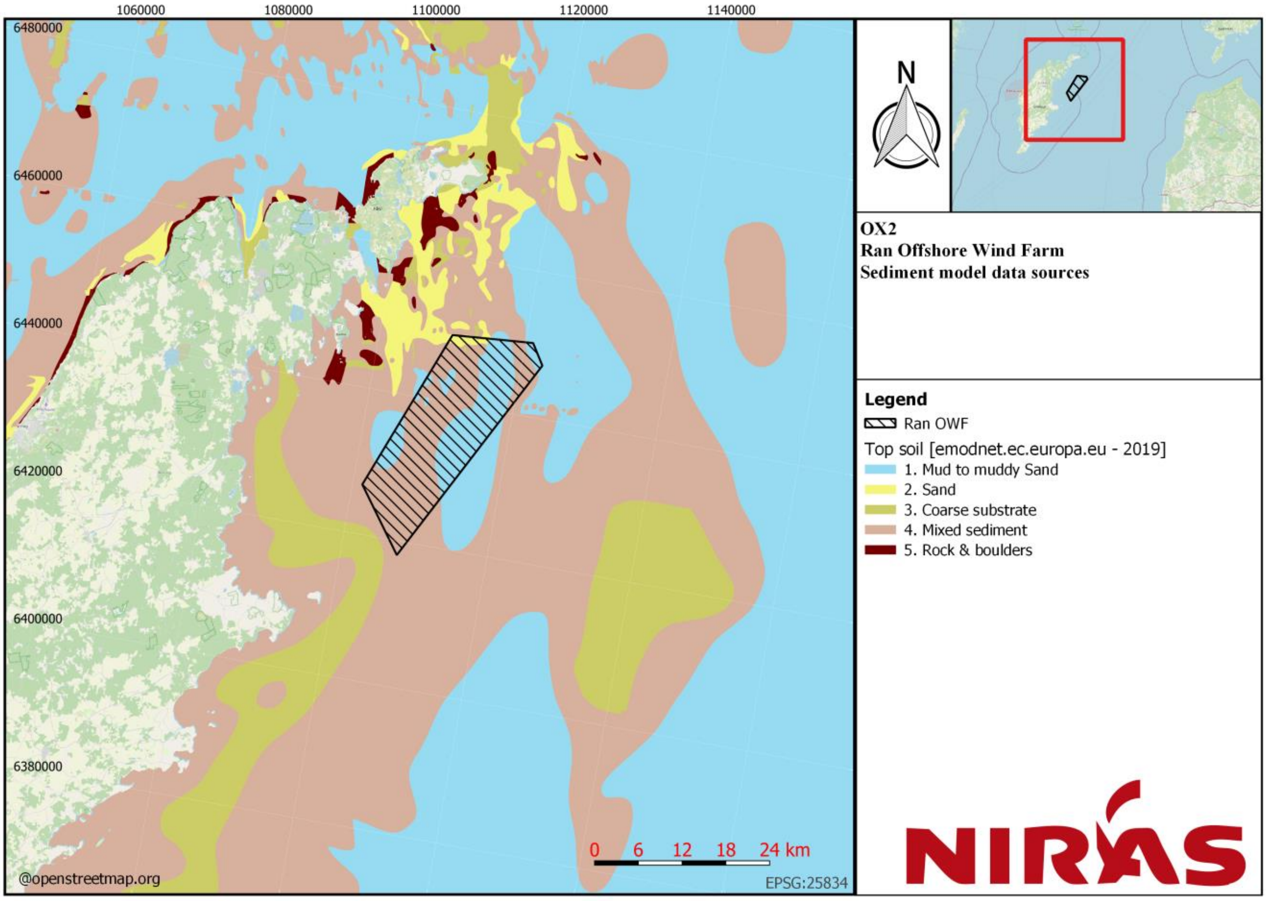

Figure 6.16: Sediment model data source (EMODnet, 2021).

6.3.3. Temperature, salinity and sound speed profile

The combined effects of temperature and salinity on seawater density can create complex sound speed profiles in the sea, particularly in areas with strong vertical stratification or gradients in temperature and salinity. These variations in sound speed can have important implications for underwater sound propagation.

As stated by Snell's law, Equation 7, sound waves bend toward regions of low sound speed (Jensen, et al., 2011). The implications for sound in sea water are, that sound, entering a low velocity layer in the water column, can get trapped there. This results in sound travelling far with very low propagation loss.

$$\frac{\cos(\theta)}{c} = \text{constant} \qquad \text{Equation 7}$$

Where θ is the ray angle [°] and *c* is the speed of sound $\left[\frac{m}{s}\right]$.

There are three main types of sound speed profiles for seawater:

1. **Uniform sound speed profile**: In a uniform sound speed profile, the speed of sound is the same at all depths. This can occur in regions of the sea where temperature and salinity are relatively constant with depth.
2. **Upward refracting sound speed profile**: When the sound speed increases with depth, it is called an upward refracting sound speed profile. Sound waves in this type of environment can be refracted

upward and away from the seabed, potentially travelling over longer distances with lower absorption losses from seabed interaction.

3. **Downward refracting sound speed profile**: When the sound speed decreases with depth, it is called a downward refracting sound speed profile. Sound waves will, in this environment, be refracted downward to a higher degree and toward the seabed, potentially causing them to lose energy and travel shorter distances.

Special cases, where a low speed region is present at a depth in between sea surface and seabed can create channels where specific ranges of frequencies can get trapped and propagate without ever reaching neither seabed nor sea surface. The potential transmission range in such a channel is significantly longer than in any of the typical three sound speed profile types listed above.

In the Baltic Sea, underwater sound propagation varies with season, with upward refracting sound speed profiles in the coldest winter months, downward refracting sound speed profiles in spring – autumn, with the strongest effects during summer. Subsea channels with sound speed minimum within the water column can occur.

The sound speed profiles for a certain project area are calculated using Coppens equation (Coppens, 1981), based on available temperature and salinity data for the area. Data sources for the temperature and salinity profiles can be either based on empirical data, or predictive models. It is important to note, that while empirical data and predictive models can provide a historically likely scenario, they can not accurately predict the weather conditions when the project activities will occur.

For each of the sediment model points, described in section 6.3.2, the nearest available sound speed profile, as well as average temperature and salinity are extracted for the desired months. Temperature and salinity profiles for this project, were extracted from the data sources in Table 6.10, and through the NIRAS proprietary software tool “TRANSMIT”, turned into sound speed profiles.

Table 6.10: Temperature, salinity and sound speed data sources.

Data source	Reference
Temperature	2x2 km grid, monthly averages based on physical forecast (Copernicus, 2023)
Salinity	2x2 km grid, monthly averages based on physical forecast (Copernicus, 2023)
Sound speed profile	Coppens equation (Coppens, 1981) implemented in NIRAS “TRANSMIT”

The temperature and salinity change both temporally (over the year), as well as spatially. Both the timeframe and position of the activities included in sound propagation modelling must therefore be taken into account, when evaluating which sound speed profiles should be used for any given model.

A realistic worst case approach was agreed with Ran Vindpark AB. The temperature, salinity and sound speed profiles for the area are therefore examined for all 12 months, to determine which month has conditions most likely to result in the furthest sound propagation.

Temperature, salinity and sound speed profiles were extracted for a radius of 20 km around each source position mentioned in section 6.2.8. From these profiles, it was assessed, that profiles with the potential for the strongest sound propagation, are those of March. Graphical representations of all profiles for position 1 are given in Figure 6.17 (temperature), Figure 6.18 (salinity), and in Figure 6.19 (sound speed). Profiles for the remaining positions are attached in Appendix 2. The figures each show the nearest 9 data points from the temperature and salinity databases, relative to the source location. These are shown in a gridded x-y format, with the centre plot representing the data point closest to the source location. Empty plots can occur where land masses are present. The coordinates for each data point are provided above the individual plots in EPSG: 4326.

To ensure a realistic worst case approach for the prognosis, sound propagation modelling implements the profiles for March.

For each sediment model position, the spatially closest data point for average temperature and salinity, as well as sound speed profiles, were assigned to the sediment model through NIRAS TRANSMIT, which combines sediment, temperature, salinity and sound speed data, into dBSea import files.

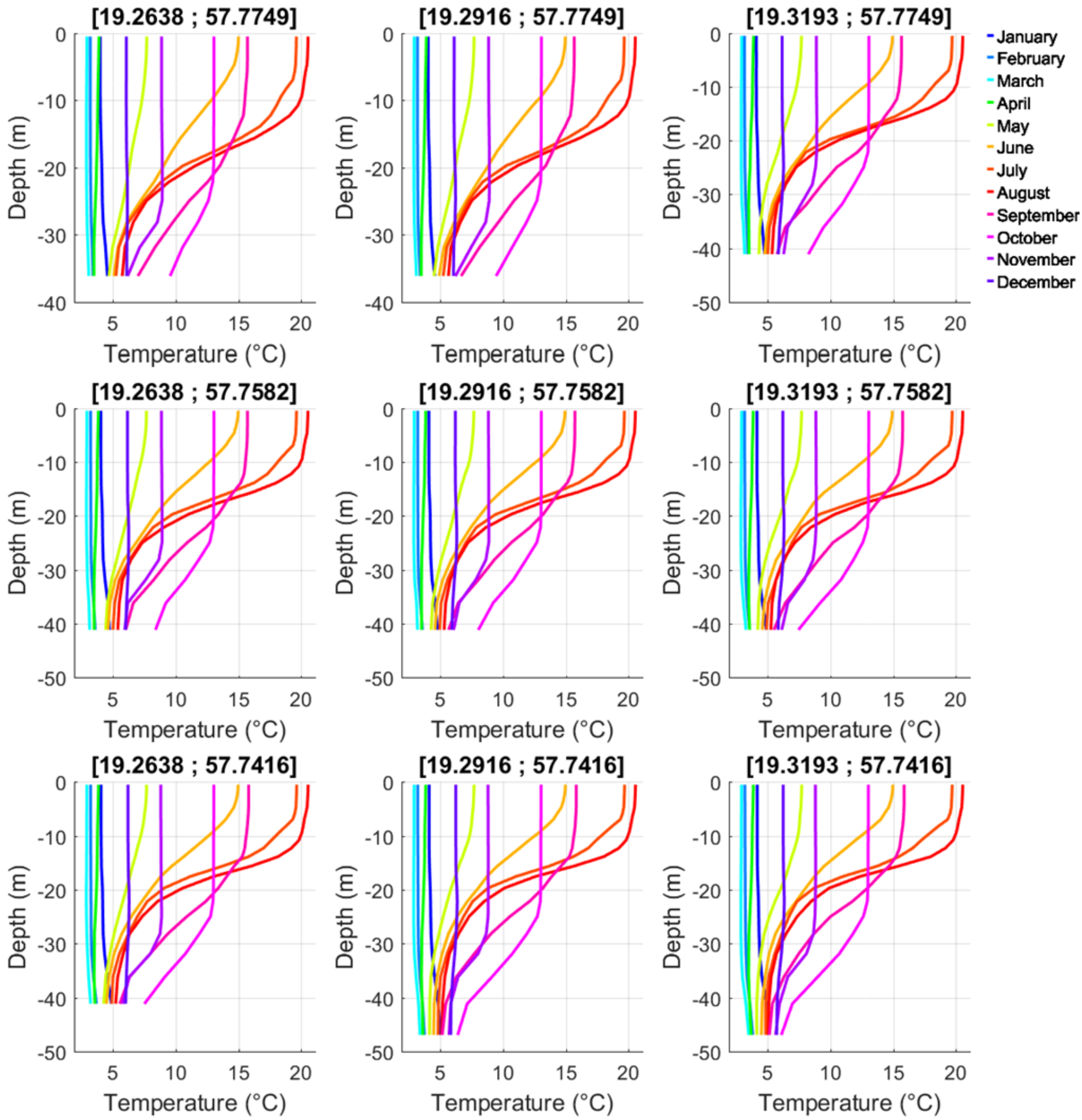

Figure 6.17: Temperature profiles for the area around source position 1 for all months. Gridded layout reflects geographical location.

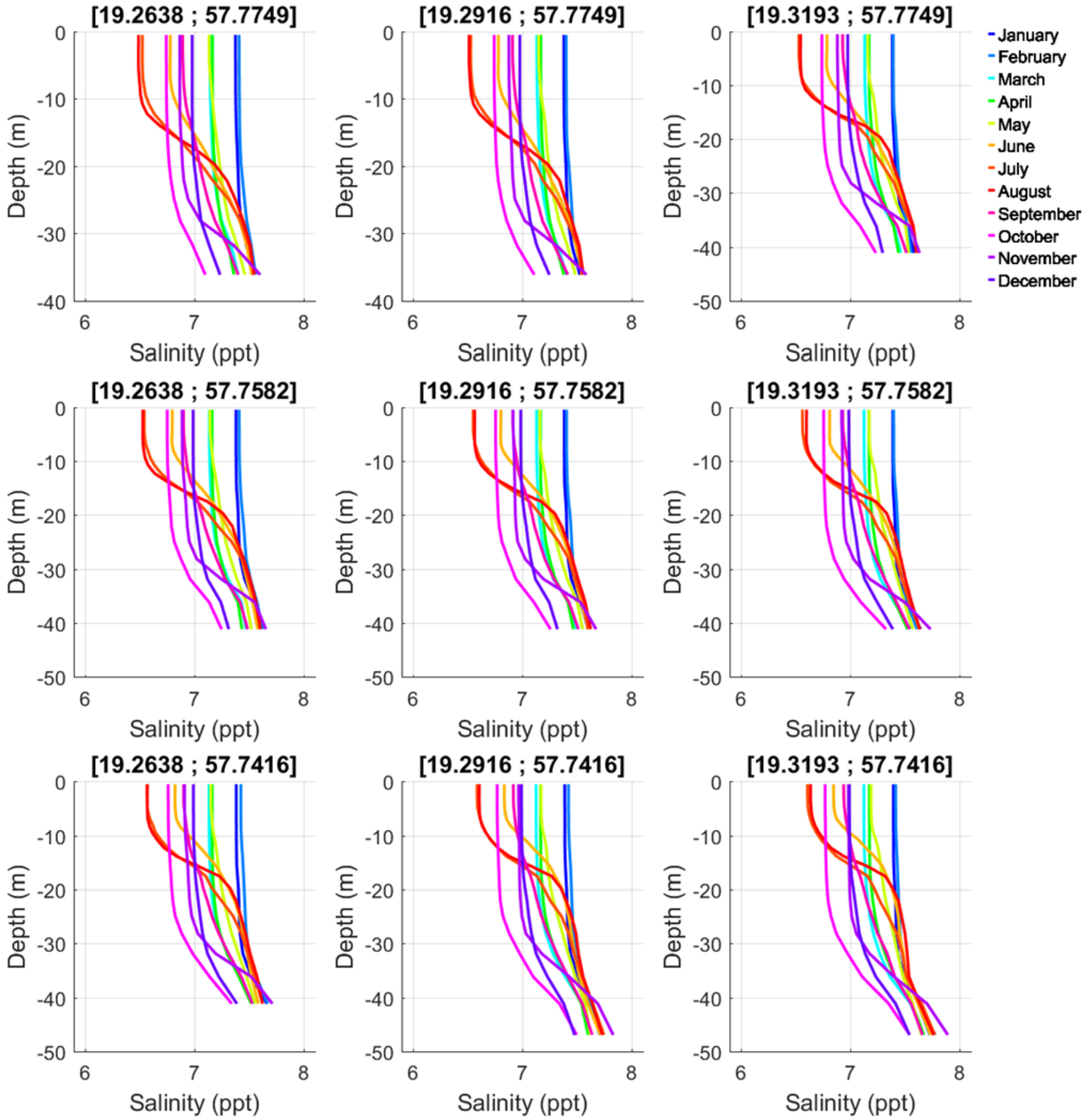

Figure 6.18: Salinity profiles for the area around source position 1 for all months. Gridded layout reflects geographical location.

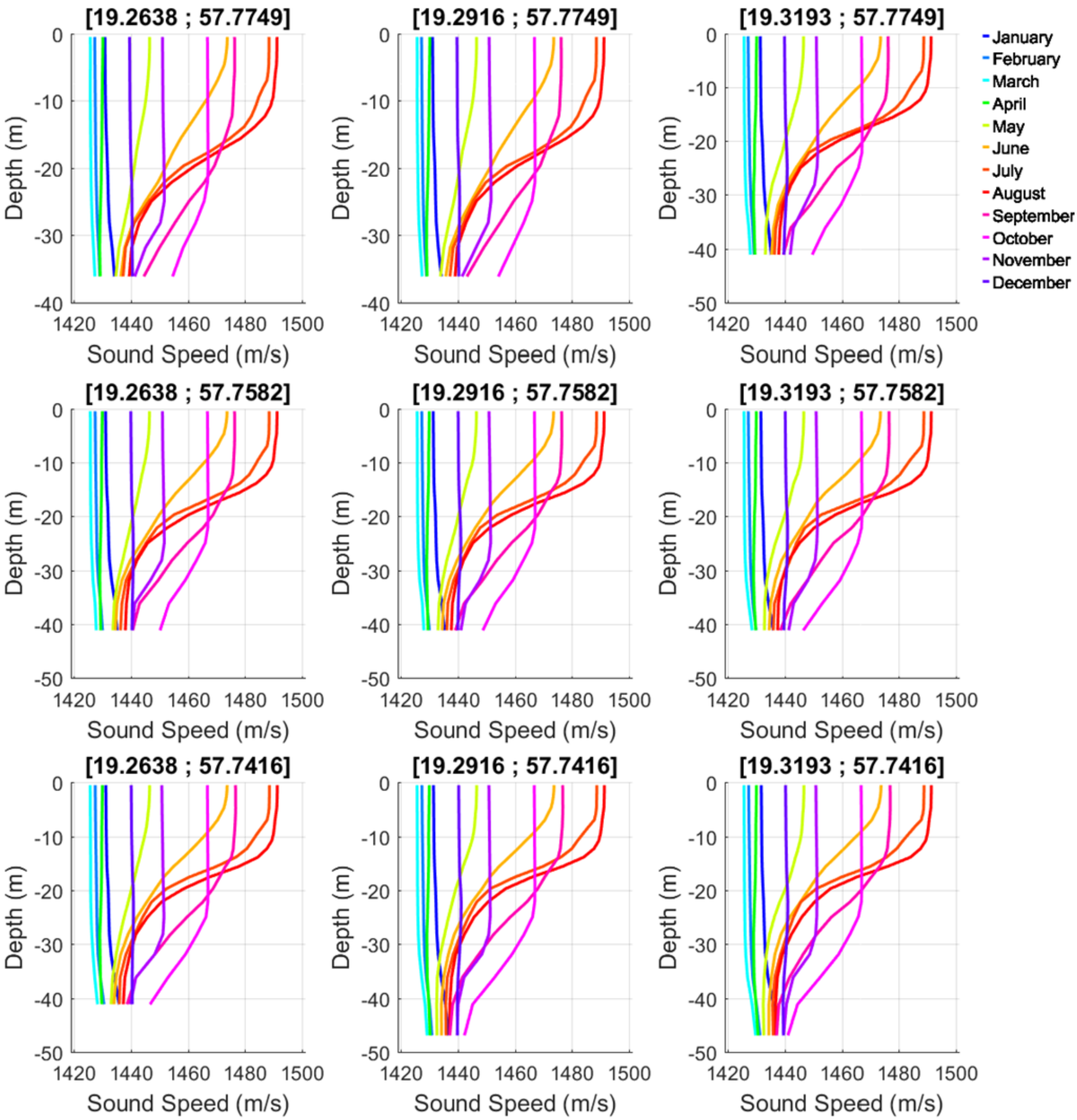

Figure 6.19: Sound speed profiles for the area around source position 1 for all months. Gridded layout reflects geographical location.

6.3.4. Sea surface roughness

Sea surface roughness, either from waves or ice cover can cause sound waves to scatter in many different directions, making it more difficult to propagate through the water. This can result in increased attenuation, backscattering and reduced range of underwater sound propagation, particularly at high frequencies.

As a precautionary approach, sound propagation modelling typically regards the sea surface as a perfect mirror (calm water), as this is also the conditions under which pile installation would be preferred. The model is therefore likely to overestimate sound propagation for any conditions where calm water is not the case.

6.3.5. Volume attenuation

Another parameter that has influence on especially the high frequency propagation loss over distance is the volume attenuation, defined as an absorption coefficient dependent on chemical conditions of the water column. This parameter has been approximated using Equation 8, from which is inferred that increasing frequency leads to increased absorption (Jensen, et al., 2011).

$$\alpha' \cong 3.3 \times 10^{-3} + \frac{0.11f^2}{1+f^2} + \frac{44f^2}{4100+f^2} + 3.0 \times 10^{-4}f^2 \quad \left[\frac{dB}{km}\right]$$ Equation 8

Where f is the frequency of the wave in kHz.

Volume attenuation is taken into account within dBSea, which is used for sound propagation modelling.

6.4. Sound Propagation Software

Numerical models can be used to simulate and predict underwater sound propagation in sea water. These models involve a computer-based simulation that uses mathematical equations to describe the sound propagation as it travels through the sea. In this regard, environmental conditions such as temperature, salinity, sediment and bathymetry must be taken into account. Different numerical models exist to treat different environmental and source specific conditions, and the choice of numerical model should always be based on the project specific environmental parameters.

NIRAS uses the software tool dBSea, which incorporates three numerical algorithms for predicting sound propagation in complex underwater environments: dBSeaRay, dBSeaPE, and dBSeaNM.

dBSeaRay is a ray-tracing algorithm that simulates the paths of individual sound rays as they travel through the sea, taking into account the effects of sea properties, such as temperature, salinity, and bathymetry, on sound propagation. This allows users to predict sound propagation in a wide range of ocean environments. Inherent limitations for this algorithm limit its use in shallow waters for very low frequencies below a few hundred Hz.

dBSeaPE is a parabolic equation algorithm that solves the parabolic wave equation to simulate sound propagation in the ocean. It is particularly useful for modelling sound propagation over long distances or in areas with complex bathymetry. It however lacks computational efficiency at higher frequencies and is primarily suited for low frequencies.

dBSeaNM uses the normal modes method to predict sound propagation in the ocean. This algorithm takes into account the effects of vertical variations in ocean properties, such as sound speed and density, on sound propagation. It is particularly useful for predicting sound propagation in regions with significant vertical mixing or internal waves, and is most suitable for low frequencies, up to several hundred Hz.

Depending on the local environment and source characteristics, a mix of two numerical models may provide the best result, whereby one algorithm handles the low frequencies, and another handles the high frequencies.

Typically, dBSeaNM or dBSeaPE is used for low frequencies and dBSeaPE or dBSeaRay for high frequencies with a split frequency between the two algorithms, based on $f = \frac{8 \cdot c}{d}$ [Hz], where c is the speed of sound in water [m/s] and d is the average bathymetry depth [m]. For very high frequencies, dBSeaRay is typically preferred.

Output from dBSea is primarily numerical, where each modelled sound propagation radial (direction from source) is represented by the maximum-over-depth *(MOD)* sound level at each modelled range step. *MOD*, in this regard, is found by taking the maximum sound level for each range step over all modelled depths. It therefore does not represent the sound level at a specific depth, but is a more conservative measure for the highest possible exposure at every range. An example of this concept is shown in Figure 6.20, showing the sound level (x-axis) in dB over depth (y-axis), for a specific distance and direction. On the left side, the MOD is located at 1 m depth below sea-surface and is 114.2 dB, while on the right side, in another direction from the source, MOD is located at 28 m depth and is 114.6 dB. The sound levels at all other depths are ignored in the result output.

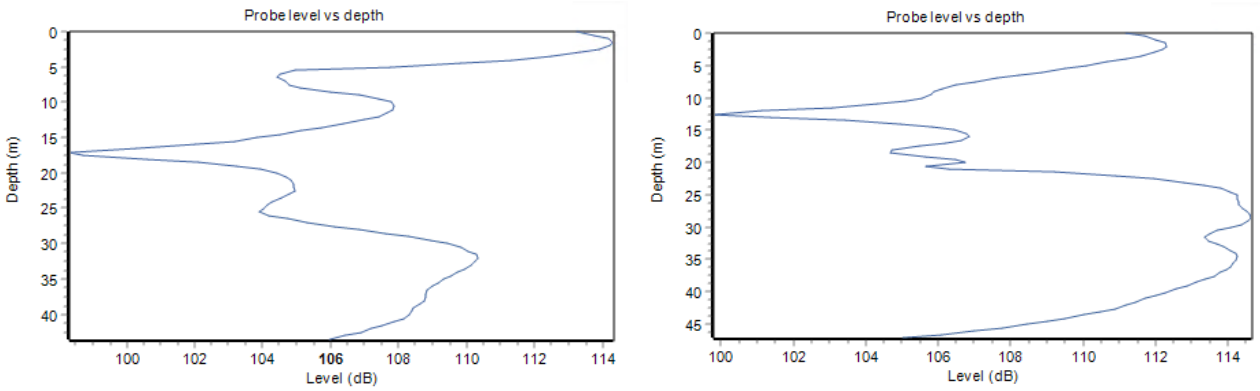

Figure 6.20: Concept of MOD, where the maximum sound level at any depth is extracted for each distance and radial interval. Example shows an MOD value of 114.2 dB (left side) at 1 m depth, and MOD value of 114.6 dB (right side) at 28 m depth.

Prognosis specific parameters for the dBSea setup is specific to the source types included, and is therefore described separately for the different source types in the prognosis.

6.4.1. Settings

The software tool dBSea was used for sound propagation modelling, with the configuration listed in Table 6.11.

Table 6.11: Sound propagation modelling tool settings for dBSea.

Parameter	Value
Software version	2.3.4
Grid (range x depth) resolution	25 m x 0.5 m
Number of radials/transects	Position 1: 90 (4°) Position 2, 3: 45 (8°)
Frerquency range modelled	12.5 Hz – 32 kHz (1/3 octave bands)
Low frequency solver	dBSeaNM
High frequency solver	dBSeaRay
Solver split frequency	200/250 Hz

Post-processing of the raw sound propagation results into impact ranges was done in NIRAS proprietary software tool NIRAS SILENCE, which implements Equation 5, page 14 for batch processing of different installation scenarios and threshold values.

6.5. Unmitigated pile driving results

Unmitigated pile driving results were calculated in dBSea. Using NIRAS SILENCE, curve fits were calculated for the direction with the strongest sound propagation for each position. The curve fit interpolates and extrapolates calculated values to obtain best possible fit in the range 1 m – 500 km. It should be noted, that extrapolation does not factor in any bathymetry beyond the model range including the occurrence of land masses. Extrapolation beyond the model range is therefore extremely conservative. Any land mass in the path would effectively stop sound propagation in that direction. Extrapolated values for unmitigated scenarios are therefore only useful in examining the general trend of sound propagation and should not be considered plausible as they do not take the actual environment beyond the model range of 20 km into consideration. Caution is warranted if extrapolated values are used to calculate impact ranges.

6.5.1. 14 m monopile foundation

The unmitigated resulting curve fits, for the 14 m monopile foundation, are shown in Figure 6.21 – Figure 6.22.

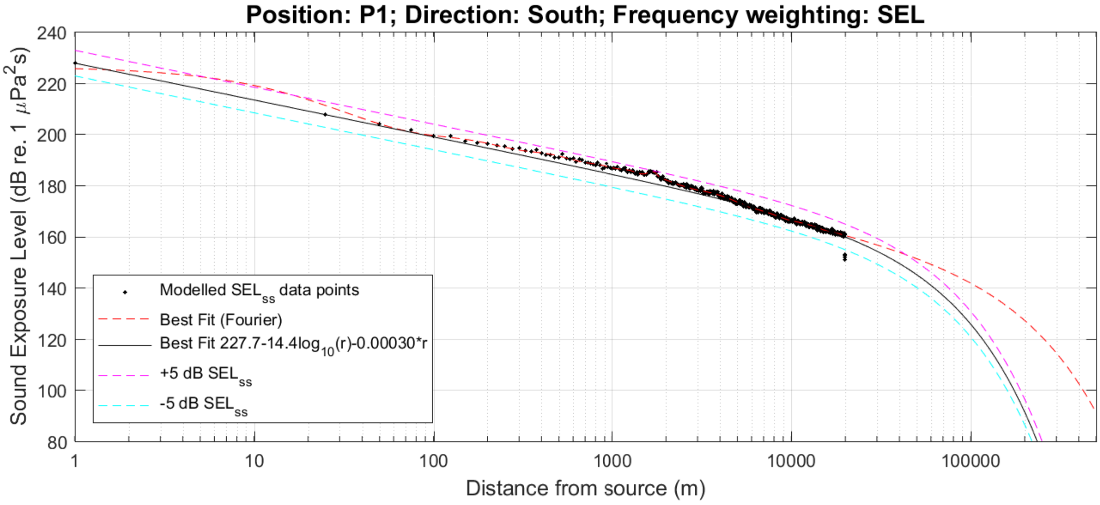

Figure 6.21: Sound propagation results for unmitigated pile driving. Best logarithmic fit and fourier (NIRAS SILENCE) curve fit are also shown. Scenario: 14 m monopile; March; Position 1.

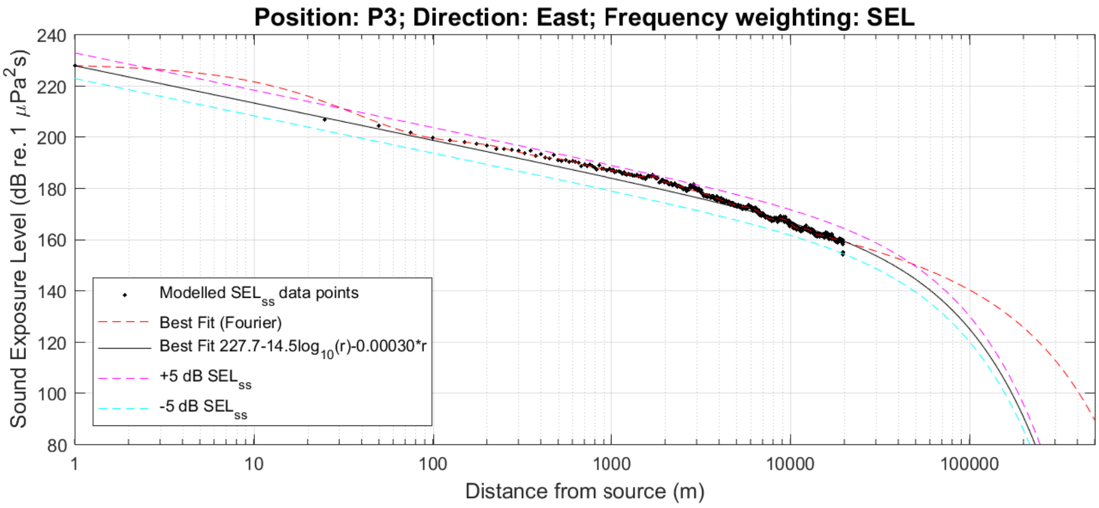

Figure 6.22: Sound propagation results for unmitigated pile driving. Best logarithmic fit and fourier (NIRAS SILENCE) curve fit are also shown. Scenario: 14 m monopile; March; Position 3.

6.5.2. Jacket foundation with 5 m pin piles

The unmitigated resulting curve fits, for the jacket foundation, are shown in Figure 6.23 – Figure 6.25.

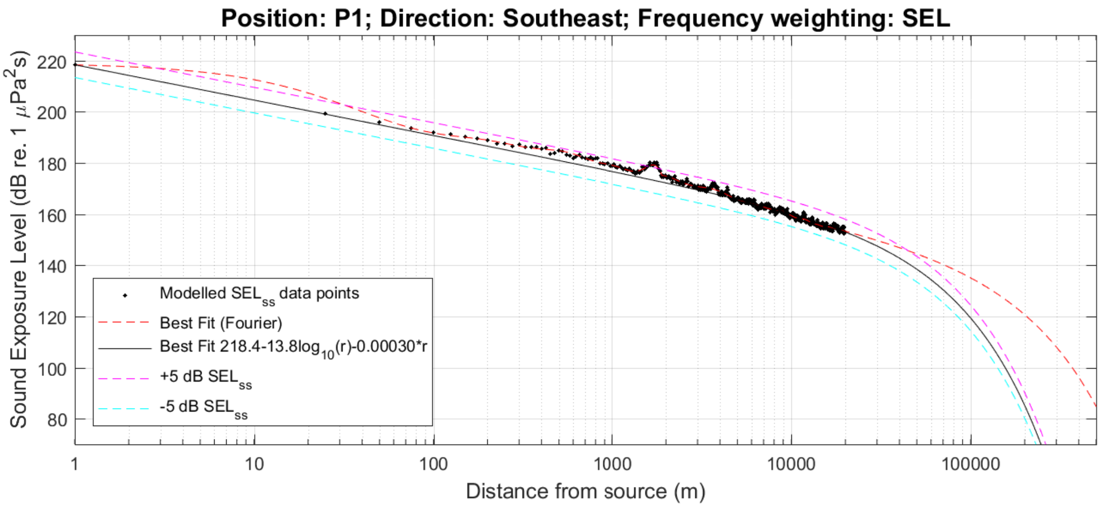

Figure 6.23: Sound propagation results for unmitigated pile driving. Best logarithmic fit and fourier (NIRAS SILENCE) curve fit are also shown. Scenario: Jacket foundation; 5 m pin pile; March; position 1.

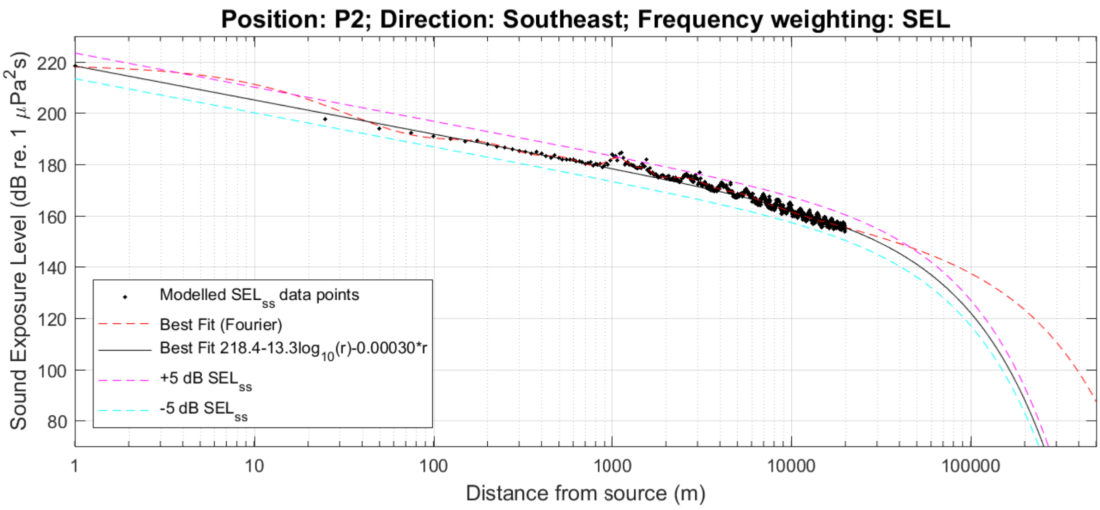

Figure 6.24: Sound propagation results for unmitigated pile driving. Best logarithmic fit and fourier (NIRAS SILENCE) curve fit are also shown. Scenario: Jacket foundation; 5 m pin pile; March; position 2.

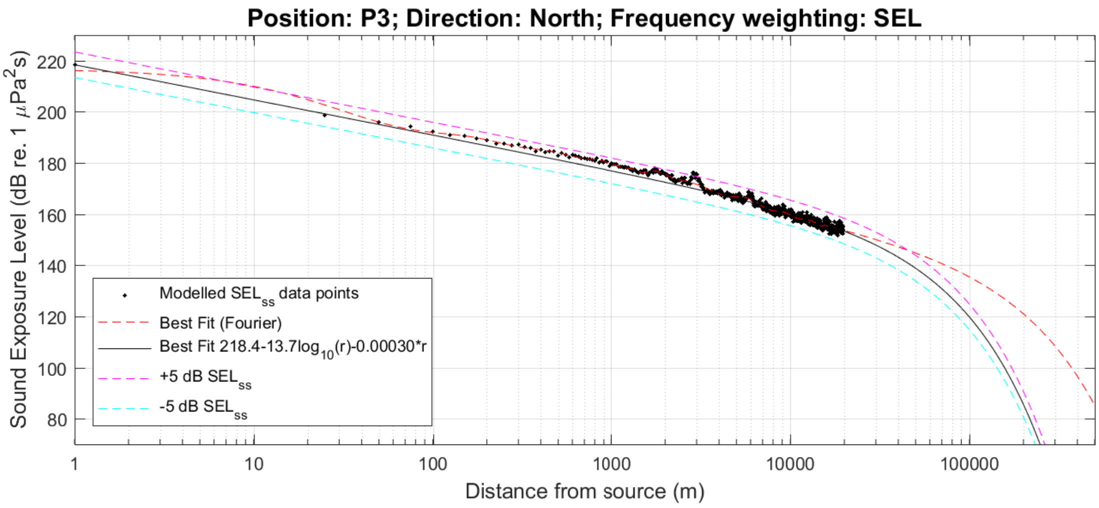

Figure 6.25: Sound propagation results for unmitigated pile driving. Best logarithmic fit and fourier (NIRAS SILENCE) curve fit are also shown. Scenario: Jacket foundation; 5 m pin pile; March; position 3.

6.5.3. Floating foundation with 8 m anchor piles

The unmitigated resulting curve fits, for the floating foundation, are shown in Figure 6.26 – Figure 6.28.

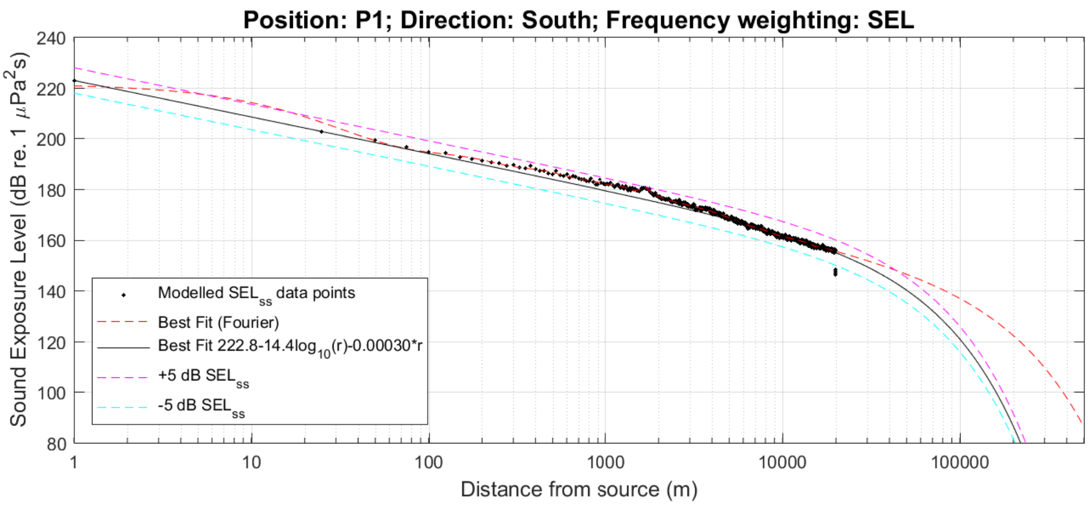

Figure 6.26: Sound propagation results for unmitigated pile driving. Best logarithmic fit and fourier (NIRAS SILENCE) curve fit are also shown. Scenario: Floating foundation; 8 m anchor pile; March; Position 1.

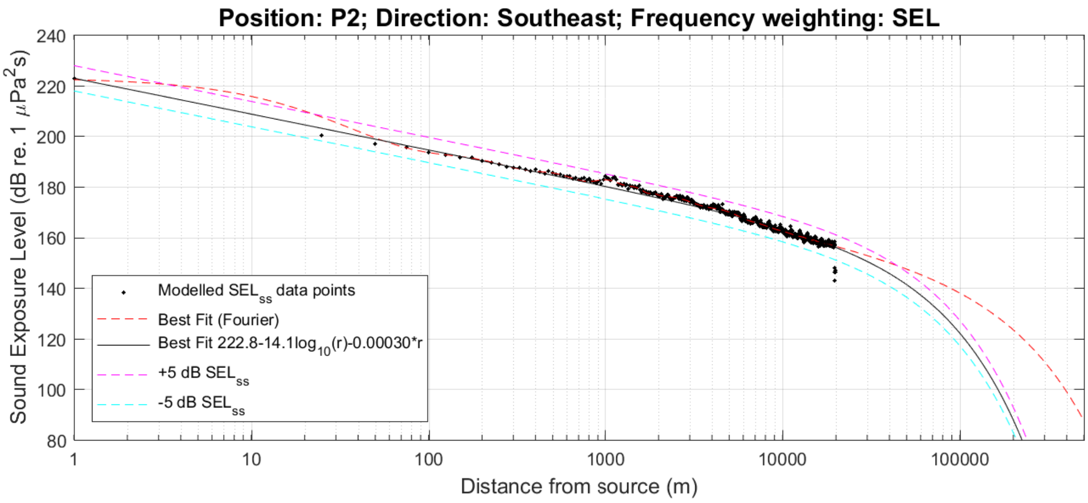

Figure 6.27: Sound propagation results for unmitigated pile driving. Best logarithmic fit and fourier (NIRAS SILENCE) curve fit are also shown. Scenario: Floating foundation; 8 m anchor pile; March; Position 2.

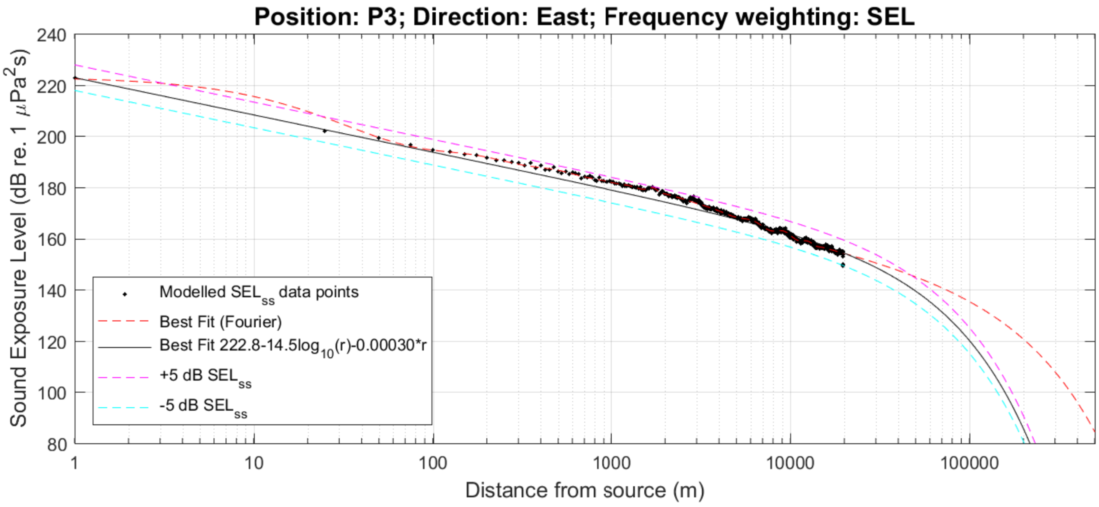

Figure 6.28: Sound propagation results for unmitigated pile driving. Best logarithmic fit and fourier (NIRAS SILENCE) curve fit are also shown. Scenario: Floating foundation; 8 m anchor pile; March; Position 3.

6.6. Mitigation

This section provides a brief description of different noise mitigation measures, both existing systems, and systems currently in development. The systems can be either on-pile systems (actively reducing the source level) or near-pile which reduces the noise emission after it has entered the water column and sediment.

6.6.1. Existing mitigation measures

This section provides a brief description of different existing and proven noise mitigation measures.

6.6.1.1. Reduced hammer blow energy

While not necessarily a mitigation system in itself, reducing the hammer energy applied to each pile strike would consequently result in lower emitted underwater noise levels per pile strike. It might however also lead to slower installation speed and a need for additional pile strikes, or in the worst case failure to reach target depth. An increased number of pile strikes, could also lead to increased PTS and TTS distances, as these are affected by not only the source level, but also the number of pile strikes and the time interval between pile strikes.

6.6.1.2. Big Bubble curtains (BBC, DBBC)

A frequently applied technique uses either a single big bubble curtain (BBC), or double (DBBC). Bubble curtains consist of a series of perforated pipes or hoses that release a continuous stream of air bubbles into the water column, thereby creating a barrier made of air, which effectively traps the acoustic energy inside the barrier. While bubble curtains are effective at reducing underwater noise, they have some limitations. The effectiveness of the curtain depends on the depth of the water, the size of the bubbles, and the distance between the noise source and the curtain. Additionally, the installation and operation of the curtains can be expensive, and the use of air compressors to generate the bubbles requires a lot of energy. The DBBC is shown in Figure 6.29.

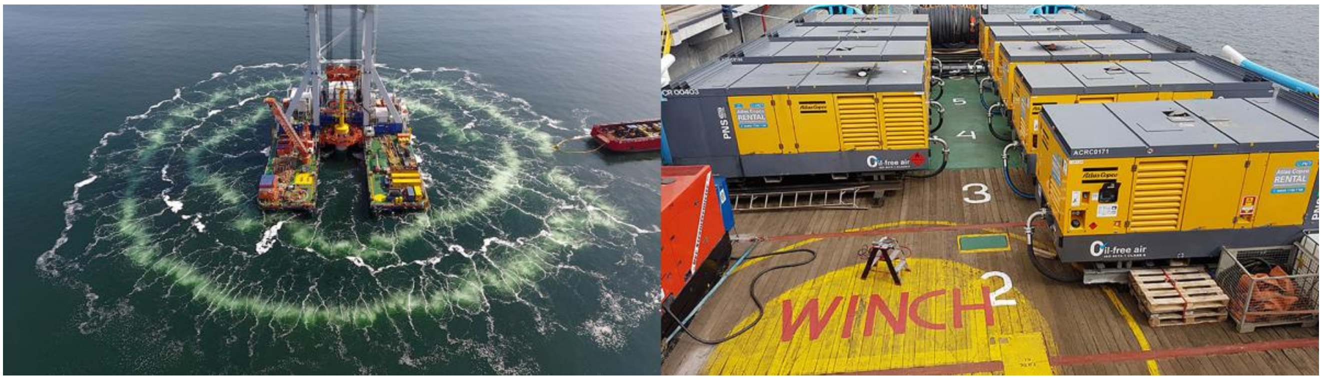

Figure 6.29: Illustration of a DBBC mitigation system (Left: in effect; Right: compressors for creating the air pressure) (Source: hydrotechnik-luebeck.de).

The curtains are typically positioned at 50 – 200 m radius around the pile. Due to the change in impedance in the water-air-water bubble interface, a significant part of the emitted noise is reflected backwards and kept near the pile, just like the water surface prevents underwater sound from being transmitted into the air. Noise energy going through the bubble curtain is greatly attenuated (Tsouvalas, 2020). The success depends on three parameters: size of holes in the hosepipe (determines bubble sizes), spacing of holes (determines density of bubble curtain) and the amount of air used (air pressure). The best configuration was found to be with relatively small holes, a small spacing and using a substantial air pressure (Diederichs, et al., 2014).

The sound moves through the sediment and is then partially reintroduced to the water column further from the pile. The distances to which sound reintroduced to the water column is of significant amplitude depends on the seabed characteristics at and near the pile site. The further from the pile the bubble curtain(s) are located, the more of the reintroduced sound can be captured. It is however in most cases considered impossible to avoid reintroduced sound from the sediment solely by use of bubble curtains given the typical bubble curtain radius of up to 200 m. The upper limit to the effectiveness of bubble curtains is therefore often dependent on the sediment.

6.6.1.3. Pile sleeves

A pile sleeve is an on-pile mitigation system forming a physical wall around the pile. One such system is the Noise Mitigation Screen from IHC (IHC-NMS) where a double walled steel sleeve with an air-filled cavity is positioned over the pile (Figure 6.30). This system utilises the impedance difference in the water-steel-air-steel-water interfaces to reduce the sound transmission. This system has been used for example at the German wind park Riffgat.

Figure 6.30: Illustration of IHC-NMS system (source: iqip.com)

Often, a pile sleeve is applied in combination with a bubble curtain solution to increase the overall mitigation effect. The pile sleeve however has an important limitation when it comes to future installations, as the weight of the system is significant. With increasing pile sizes, the pile sleeve also increases in size, and thereby weight. It is uncertain whether this system is applicable for large future monopiles. For jacket foundations, the applicability is also uncertain, as the pin piles are often installed into a template, thus preventing a seal towards the seabed.

Cofferdams are a special type of pile sleeve. They also surround the pile, however in comparison to the IHC-NMS, the water in between the pile and the sleeve is extracted, so that the interface from pile to water becomes air-steel-water. An inherent challenge with this solution is that it can be difficult to keep the water out of the cofferdam, as local sediment conditions can prevent a perfect water-tight seal with the seabed.

6.6.1.4. Hydro Sound Dampers

Hydro Sound Damper (HSD) systems are in many ways similar to the bubble curtain, however instead of using hoses with air, the curtain consists of fixed position air-filled balloons or foam-balls. The size, spacing and density of the foam balls or air-filled balloons then dictate the achievable noise mitigation. The HSD system, makes it possible to "tune" the system to work optimally at specific frequencies, thus allowing for project specific optimal solutions.

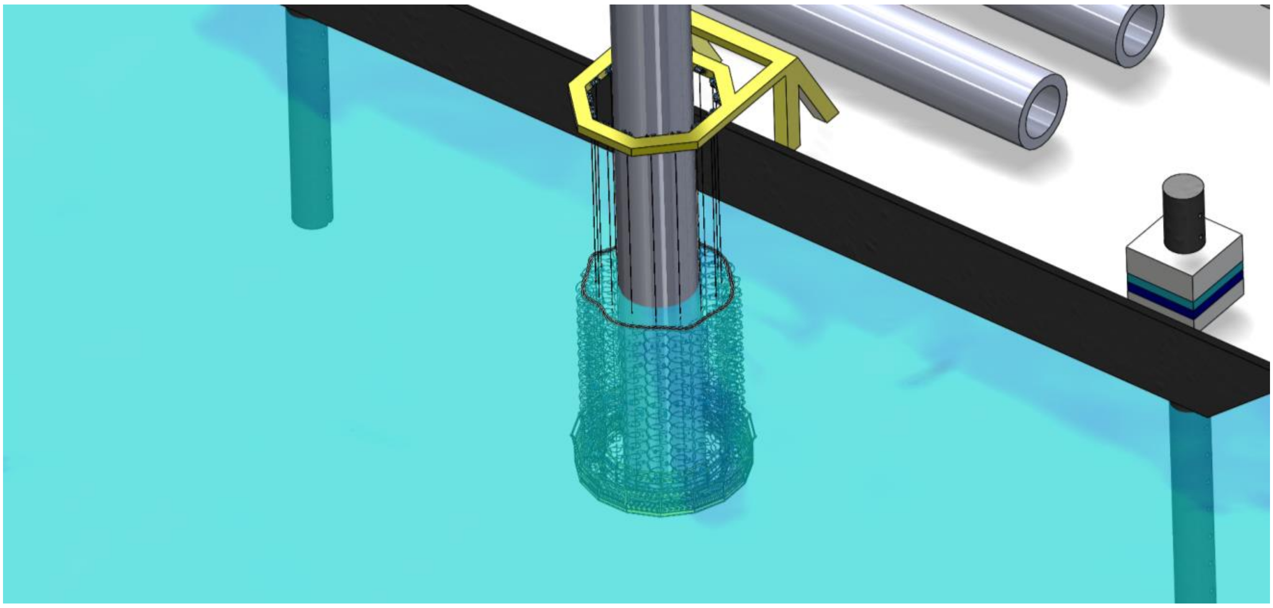

Figure 6.31: Illustration of the HSD system deployed around a monopile. (source: (Offnoise Solutions, 2023)).

6.6.2. Effectiveness of mitigation measures

For commercially available and proven mitigation systems, a summary of achieved mitigation levels throughout completed installations is given in (Bellmann, et al., 2020), and shown in Figure 6.32, for different configurations of bubble curtains, and in Figure 6.33 for HSD, IHC-NMS and combinations of different types of mitigation systems. It should be noted from Figure 6.32, that the mitigation efficiency of any bubble curtain system statistically decreases with increasing depth at the installation site. There are a very low number of measurements for depths greater than 40 m, and there are therefore uncertainties regarding the mitigation effectiveness in such cases. Due to the increasing pressure with depth, larger depths will likely require more, or larger, compressors to ensure the same bubble curtain effectiveness.

No.	**Noise Abatement System resp. combination of Noise Abatement Systems** (applied air volume for the (D)BBC; water depth)	**Insertion loss ΔSEL [dB]** (min. / average / max.)	**Number of piles**
1	Single Big Bubble Curtain – BBC (> 0.3 m^3/(min·m), water depth < 25 m)	$11 \leq 14 \leq 15$	> 150
2	Double Big Bubble Curtain – DBBC (> 0.3 m^3/(min·m), water depth < 25 m)	$14 \leq 17 \leq 18$	> 150
3	Single Big Bubble Curtain – BBC (> 0.3 m^3/(min·m), water depth ~ 30 m)	$8 \leq 11 \leq 14$	< 20
4	Single Big Bubble Curtain – BBC (> 0.3 m^3/(min·m), water depth ~ 40 m)	$7 \leq 9 \leq 11$	30
5	Double Big Bubble Curtain – DBBC (> 0.3 m^3/(min·m), water depth ~ 40 m)	$8 \leq 11 \leq 13$	8
6	Double Big Bubble Curtain – DBBC (> 0.4 m^3/(min·m), water depth ~ 40 m)	$12 \leq 15 \leq 18$	3
7	Double Big Bubble Curtain - DBBC (> 0.5 m^3/(min·m), water depth > 40 m)	~ 15 – 16	1

Figure 6.32: Achieved unweighted broadband mitigation for different configurations of bubble curtain systems. Note: unoptimized configurations yielded significantly lower mitigation effect. (Bellmann, et al., 2020)

NIRAS

No.	Noise Abatement System resp. combination of Noise Abatement Systems (applied air volume for the (D)BBC; water depth)	Insertion loss ΔSEL [dB] (minimum / average / maximum)	Number of foundations
1	IHC-NMS (different designs) (water depth up to 40 m)	$13 \leq 15 \leq 17$ dB IHC-NMS8000 $15 \leq 16 \leq 17$ dB	> 450 > 65
2	HSD (water depth up to 40 m)	$10 \leq 11 \leq 12$ dB	> 340
3	optimized double BBC*[1] (> 0,5 m^3/(min m), water depth ~ 40 m)	15 – 16	1
4	combination IHC-NMS + optimized BBC (> 0,3 m^3/(min m), water depth < 25 m)	$17 \leq 19 \leq 23$	> 100
5	combination IHC-NMS + optimized BBC (> 0,4 m^3/(min m), water depth ~ 40 m)	17 – 18	> 10
6	combination IHC-NMS + optimized DBBC (> 0,5 m^3/(min m), water depth ~ 40 m)	$19 \leq 21 \leq 22$	> 65
7	combination HSD + optimized BBC (> 0,4 m^3/(min m), water depth ~ 30 m)	$15 \leq 16 \leq 20$	> 30
8	combination HSD + optimized DBBC (> 0,5 m^3/(min m), water depth ~ 40 m)	18 – 19	> 30
9	GABC skirt-piles*[2] (water depth bis ~ 40 m)	~ 2 – 3	< 20
10	GABC main-piles*[3] (water depth bis ~ 30 m)	< 7	< 10
11	„noise-optimized“ pile-driving procedure (additional additive, primary noise mitigation measure; chapter 5.2.2)	~ 2 - 3 dB per halving of the blow energy	

Figure 6.33: Achieved source mitigation effects at completed projects using different noise mitigation systems, (Bellmann, et al., 2020).

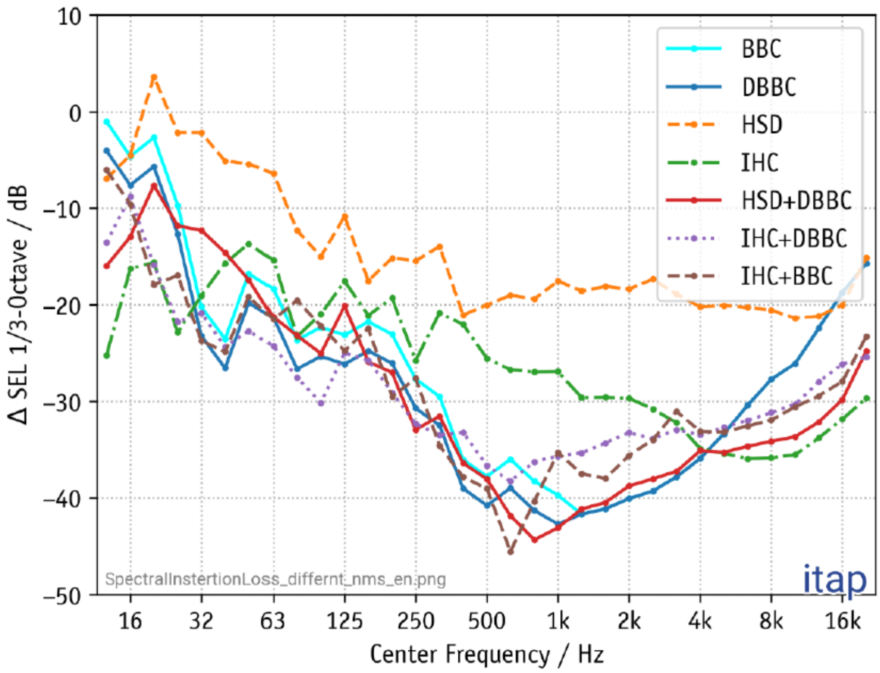

Figure 6.34: Frequency dependent noise reduction for noise abatement systems, (Bellmann, et al., 2020).

In Figure 6.34, the noise reduction with the different mitigation systems, are instead given in 1/3 octave bands, thus showing the achieved mitigation per frequency band, however normalized and not reflecting the overall mitigation efficiencies provided in Figure 6.32 and Figure 6.33. The mitigation effect is provided as the noise level relative to installation without any active mitigation measures, so the more negative the value, the better the mitigation effect.

It should be noted from Figure 6.34, that the representation method in (Bellmann, et al., 2020) does not represent the effect of a single fixed system used in different projects, but rather the average of a number of different systems, across different pile installations, across different project areas and environmental conditions. It is not clear from the report, when and where each mitigation system effect was measured, and it is therefore not possible to determine the direct contributors of any variation in effect.

As the measurement results originate from German OWFs, it is however worth noting the measurement procedure for installations including mitigation measures, where one pile is measured without any mitigation active, one pile is measured with each individual mitigation system (such as BBC or IHC-NMS) and the rest of the piles are measured with all mitigation systems active (such as IHC-NMS+DBBC). This is done to acquire information on the mitigation efficiency of the mitigation measures used, so that both further development of mitigation measures can take place, and to allow for more accurate future sound propagation modelling.

It is also worth emphasizing that the mitigation effect presented is the average of achieved mitigation over a number of years, and given the continuous development of mitigation system technology, it is considered likely that performance would typically improve over time. Utilizing the reported average mitigation effect is therefore considered conservative. It should furthermore be expected, that entirely new and more effective mitigation systems and installation methods emerge in the coming years, however until such methods exist, it is not considered feasible to include in a prognosis.

In summary, prediction of achievable mitigation effect for any system, based on past installations, must be considered cautiously, and it should be expected that variations will occur between projects. The previously achieved mitigation effects can however be used more broadly to identify which type(s) of mitigation systems are likely to be useful for the current project, based on typical frequency specific mitigation effects.

If the purpose is to limit broadband noise output, a system with a high broadband mitigation effect could be a good choice. However if the purpose is to reduce the impact on a specific group of marine mammal or fish, the frequency specific mitigation effect should be considered. As an example, DBBC is very effective at reducing the broadband noise level, however for species such as porpoise (VHF) and dolphin (HF), which both have high frequency hearing above 10 kHz, a combination of HSD with DBBC could provide better protection, as indicated by the HSD+DBBC curve in Figure 6.34, for frequencies above 4 kHz. It is therefore recommended to always carry out detailed site and pile specific underwater sound emission modelling with incorporation of mitigation, based on the project specific mitigation purpose. It must also be emphasized, that any mitigation effect included in the prognosis is based on historical data, and not a suppliers guaranteed noise mitigation effect of a specific system. Such guarantee must be procured when final pile design is available, based on the actual installation scenario.

The average broadband reduction values within each system type, as presented in Figure 6.33, with a smoothed 1/3 octave efficiency spectrum based on Figure 6.34, were used for application of mitigation measures.

6.6.3. Uncertainties in determining mitigation effectiveness

An uncertainty in the source model is the mitigation system effectiveness. While a large review (Bellmann, et al., 2020) contains data on mitigation technique effectiveness, it is reported in a statistical way, not documenting individually measured effectiveness, but averages. It is therefore not possible, from the review, to pinpoint and thereby model, the effectiveness of a specific solution individually. Using the average 1/3 octave band values is considered the best available method, however the uncertainty connected with this approach must be recognized.

Another limitation is the ambient noise level during the measurements. From (Bellmann, et al., 2020), it is noted that especially for the higher frequencies, the measured levels with active mitigation are often indistinguishable from the ambient noise. The actual effectiveness of the mitigation system can therefore not be determined with sufficient accuracy. Provided that the analysis in (Bellmann, et al., 2020) is conservative with regards to high frequency mitigation effect, it is more likely than not, that the implementation of the reported values will lead to a conservative estimate for species sensitive to high frequencies.

From (Bellmann, et al., 2020), it is also noted, that the reported mitigation effectiveness is a result of measurements acquired over a large time span, and with different iterations and variations of the same technology; this development is expected to continue. For prognosis in early stage development, where mitigation effectiveness is based on historical averages, it is likely that future innovation will allow for better mitigation than is currently available.

A source of uncertainty pertains to the local environmental conditions. For bubble curtains, strong currents have the potential to "blow the bubbles away" and disturb the intended air flow and thereby the acoustic barrier effect. Seabed characteristics can also affect sound emission from the pile, in the sense that harder sediments can lead to increased sound transmission through the sediment, thereby potentially bypassing the mitigation system.

6.6.4. Noise mitigation measures currently under development

There is a continuous ongoing development of new noise mitigation measures, as well as improvements of existing technologies. This section provides a brief overview of some systems that have the potential for efficient mitigation of underwater noise in future projects. Some of the systems might already be in use, however until a significant number of installations have been completed using these technologies, they are, for the purpose of this report, considered under development.

6.6.4.1. New hammer technologies

New hammer technologies are under development, most notably the Menck Noise Reduction Unit (MNRU) and the IQIP PULSE system. Both hammer systems aim to reduce the peak amplitude of the hammer blow, by prolonging the impact pulse. There are currently no full scale measurement results available, and the potential mitigation effect is yet to be proven.

Another such system is the BLUE piling system from IQIP, where an enclosed water mass is used to push the pile into the sediment over a prolonged duration, compared to the impact of a standard hammer. The technology is not yet proven in large scale, and it remains to be seen what levels of noise reduction can be achieved.

6.6.4.2. Enhanced big bubble curtain

A further development of the single BBC, the enhanced big bubble curtain (eBBC), is a version with significantly increased airflow and larger nozzles. No official documentation of the improvement over a standard BBC is available, however several dBs increase in mitigation effect are expected. It should be noted, that due to the increased air flow, an eBBC will require more compressors than a BBC of equal diameter.

6.6.4.3. Vibro-jetting (SIMPLE)

The company GBM works is currently developing a vibro-jetting system for installing monopiles. It consists of a number of water hoses mounted inside the monopile, and supplied with high pressure water supply from above. The water hoses end in jet nozzles, located at the pile tip. When the pile has been situated, the water supply is turned on, whereby the water will liquify the soil near the pile wall. This is coupled with a vibratory hammer, which ensures continuous downward motion of the pile. By liquifying the soil, the pile should theoretically progress downwards as long as the water jets are on, and the soil can be liquified. It is uncertain how this system would work in an environment with harder sediments, and full scale offshore tests are still to be carried out. It is therefore uncertain what the mitigation effectiveness of this system will be.

6.7. Source Model With Mitigation Measures

In agreement with Ran Vindpark AB, it was chosen to include mitigation measures in the source model with mitigation effectiveness equivalent to that listed in Figure 6.33.

6.7.1. 14 m monopile with HSD+DBBC mitigation effect

The source model parameters for the 14 m monopile foundation with HSD+DBBC equivalent mitigation effect are presented in Table 6.12. The source spectrum with and without mitigation measures is illustrated in Figure 6.35.

Table 6.12: Broadband source model parameters for impact pile driving of 14 m monopile with HSD+DBBC mitigation effect.

Parameter	Value	Reference
Unmitigated reference level @750m distance, $\mathbf{L_{E,p,750m}}$ (unweighted)	184.5 dB	Relationship between pile diameter and sound level, Figure 6.1.
Unmitigated source level @ 1m distance, $\mathbf{L_{S,E}}$ (Unweighted / PCW / VHF)	227.7 dB (-) 206.0 dB (PCW) 182.3 dB (VHF)	Back calculated using NIRAS empirical model, section 6.2.7.
Mitigation effectiveness, $\Delta \boldsymbol{SEL_{xx}}$ (Unweighted / PCW / VHF)	19.7 dB (-) 25.0 dB (PCW) 22.4 dB (VHF)	Graphical representation in Figure 6.34 (Bellmann, et al., 2020)
Mitigated source level (HSD+DBBC) @ 1m distance, $\mathbf{L_{S,E}}$ (Unweighted / PCW / VHF)	208.0 dB (-) 181.0 dB (PCW) 159.9 dB (VHF)	1/3-octave band source levels unmitigated and mitigated shown in Figure 6.35

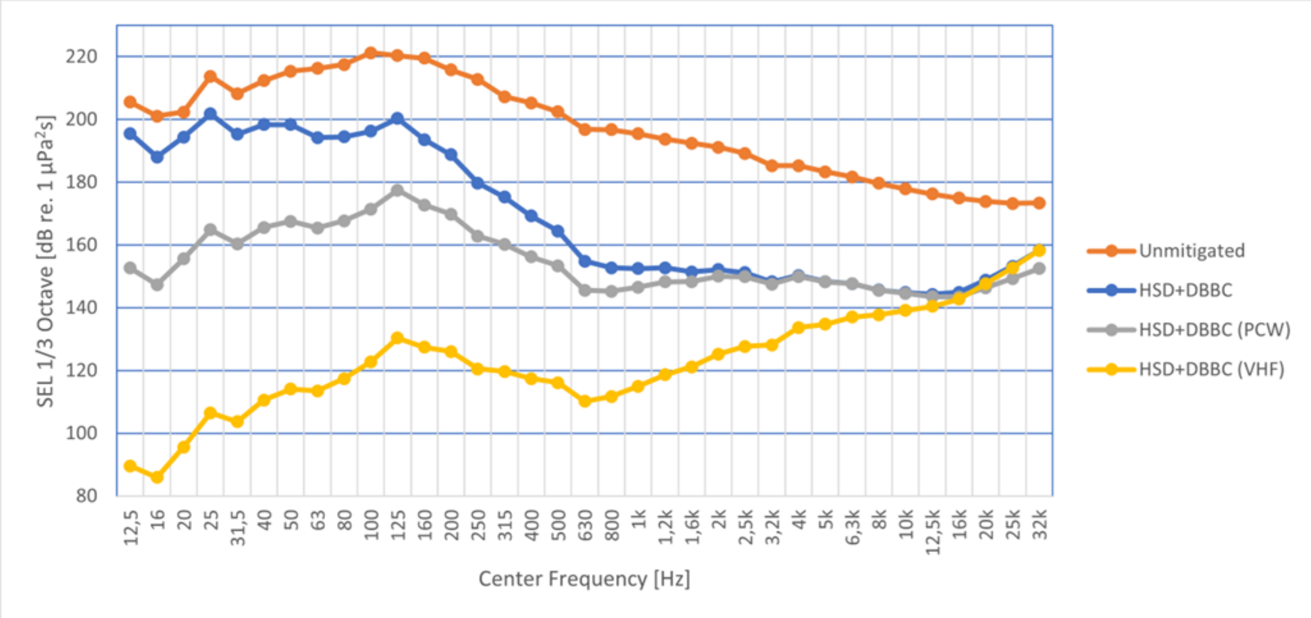

Figure 6.35: Source spectrum at 1 m distance, 14 m monopile, unmitigated and with HSD+DBBC mitigation effect.

6.7.2. 5 m pin pile with DBBC mitigation effect

The source model parameters for the 5 m pin piles in a jacket foundation with DBBC equivalent mitigation effect are presented in Table 6.13. The source spectrum with and without mitigation measures is illustrated in Figure 6.36.

Table 6.13: Broadband source model parameters for impact pile driving of 5 m pin pile with DBBC mitigation effect.

Parameter	Value	Reference
Unmitigated reference level @750m distance, $\mathbf{L_{E,p,750m}}$ (unweighted)	176.4 dB	Relationship between pile diameter and sound level, Figure 6.1.
Unmitigated source level @ 1m distance, $\mathbf{L_{S,E}}$ (Unweighted / PCW / VHF)	218.4 dB (-) 200.8 dB (PCW) 180.1 dB (VHF)	Back calculated using NIRAS empirical model, section 6.2.7.
Mitigation effectiveness, ΔSEL_{xx} (Unweighted / PCW / VHF)	22.1 dB (-) 29.6 dB (PCW) 16.4 dB (VHF)	Graphical representation in Figure 6.34 (Bellmann, et al., 2020)
Mitigated source level (DBBC) @ 1m distance, $\mathbf{L_{S,E}}$ (Unweighted / PCW / VHF)	196.2 dB (-) 171.2 dB (PCW) 163.7 dB (VHF)	1/3-octave band source levels unmitigated and mitigated shown in Figure 6.36

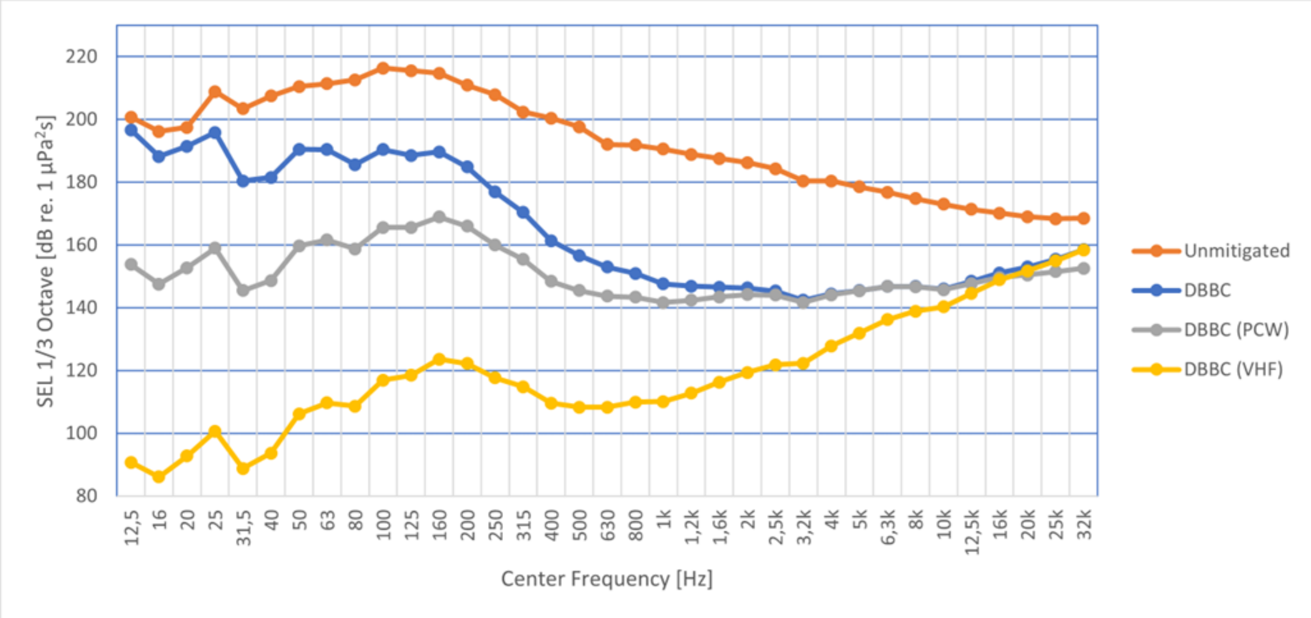

Figure 6.36: Source spectrum at 1 m distance, 5 m pin pile, unmitigated and with DBBC mitigation effect.

6.8. Mitigated pile driving results

Sound propagation modelling was carried out in dBSea and post-processing of raw sound levels into impact ranges in NIRAS SILENCE, using the threshold criteria in chapter 4. The results are presented in the following formats:

- **Numerical result tables**: showing the maximum range in any direction from the source to respective threshold criteria. Tables showing the overlap with nearby protection zones, and the total area affected are also provided.
- **Noise contour maps**: showing the direction specific impact range for certain threshold criteria, along with the total area affected.

Distance to PTS, TTS and injury threshold criteria describe the minimum distance from the source, a marine mammal, or fish, must at least be deterred to, prior to onset of pile driving, in order to avoid the respective impact. It therefore does not represent a specific measurable sound level, but rather at which distance from the pile driving activities the animals should be, to avoid the respective impact.

Distance to behavioural threshold criterion describe the range at which behavioural reactions are likely to occur when the maximum hammer energy is applied. For pile strikes where less than 100% hammer energy is utilized, the impact range will be shorter.

6.8.1. Mitigated impact ranges for fish threshold criteria

For fish, all threshold criteria are based on the frequency unweighted $L_{E,cum,24h}$ [dB re. 1 µPa^{2}s]. Impact ranges are calculated for a series of different swim speeds as well as stationary, as discussed in section 4.1.

Resulting impact ranges are provided in Table 6.14, and affected area for TTS in Table 6.15.

Table 6.14: Impact range for fish threshold criteria, with mitigation measures.

Position	Impact range for fish threshold criteria								
	Injury (r_{injury})					TTS (r_{TTS})			
	Stationary	Juvenile Cod	Adult Cod	Herring	Larvae and eggs	Stationary	Juvenile Cod	Adult Cod	Herring
14 m monopile; HSD+DBBC equivalent mitigation effect; March									
1	1.35 km	< 200 m	< 200 m	< 200 m	850 m	9.8 km	5.1 km	2.4 km	2.0 km
3	1.35 km	< 200 m	< 200 m	< 200 m	875 m	8.9 km	4.85 km	2.2 km	1.85 km
4 x 5 m pin pile (jacket foundation); DBBC equivalent mitigation effect; March									
1	500 m	< 200 m	< 200 m	< 200 m	275 m	5.5 km	< 200 m	< 200 m	< 200 m
2	450 m	< 200 m	< 200 m	< 200 m	275 m	5.8 km	< 200 m	< 200 m	< 200 m
3	500 m	< 200 m	< 200 m	< 200 m	275 m	5.6 km	< 200 m	< 200 m	< 200 m

Table 6.15: Area affected for fish TTS.

Position	Affected area (TTS) [km^2]			
	Stationary	Juvenile Cod	Adult Cod	Herring
14 m monopile; HSD+DBBC equivalent mitigation effect; March				
1	201	52	11	7
3	178	45	9	6
4 x 5 m pin pile (jacket foundation); DBBC equivalent mitigation effect; March				
1	73	< 1	< 1	< 1
2	88	< 1	< 1	< 1
3	74	< 1	< 1	< 1

Noise contour maps for fish TTS and larvae and eggs injury threshold are shown in:

- Figure 6.37 - Figure 6.38 for 14 m monopile with HSD+DBBC equivalent mitigation effect.
- Figure 6.39 - Figure 6.41 for 4x 5 m pin piles (jacket foundation) with DBBC equivalent mitigation effect.

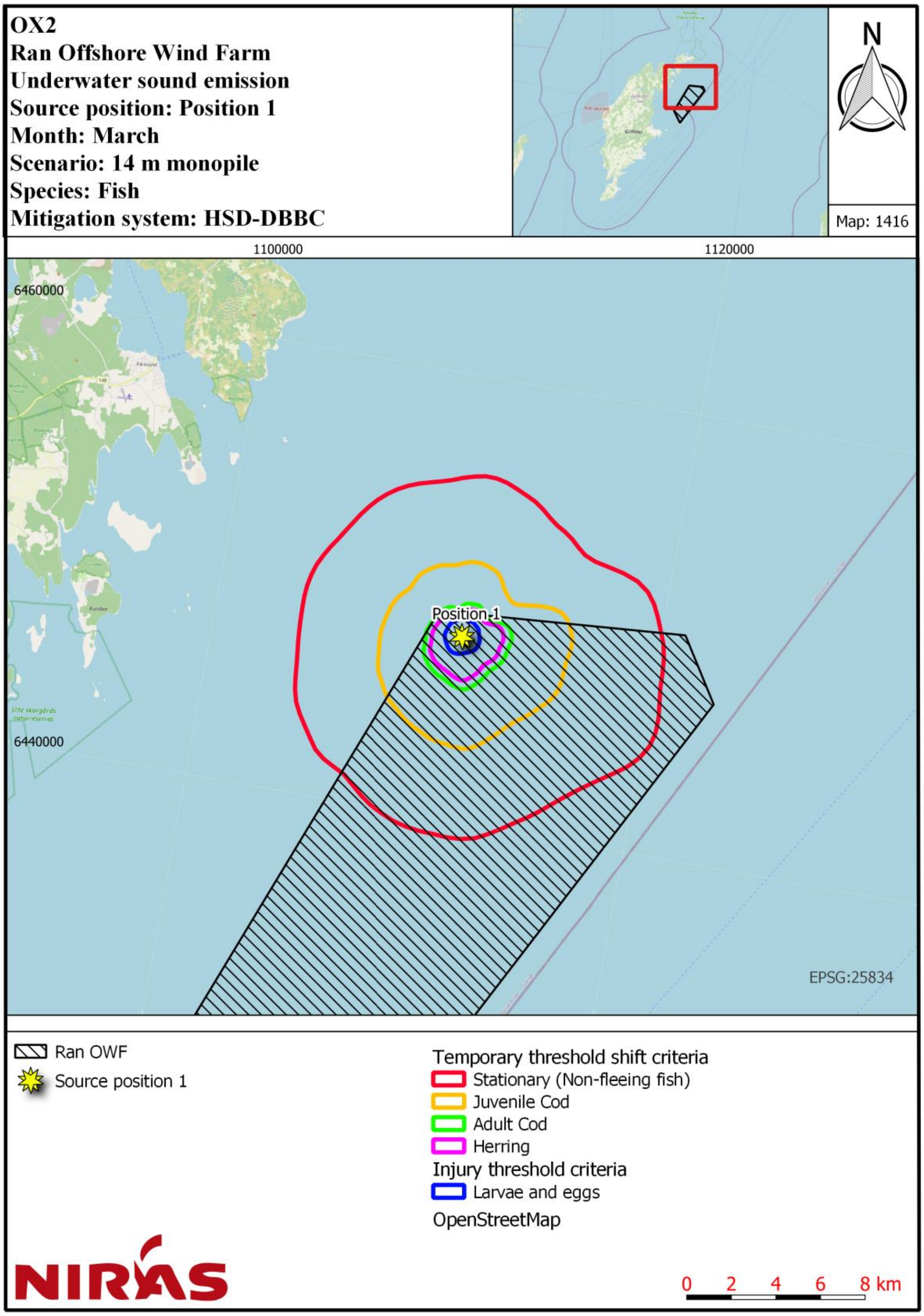

Figure 6.37: Noise contour map for fish TTS threshold and larvae & eggs injury threshold. Scenario: Monopile foundation, 14 m pile diameter; HSD+DBBC mitigation effect; Position 1.

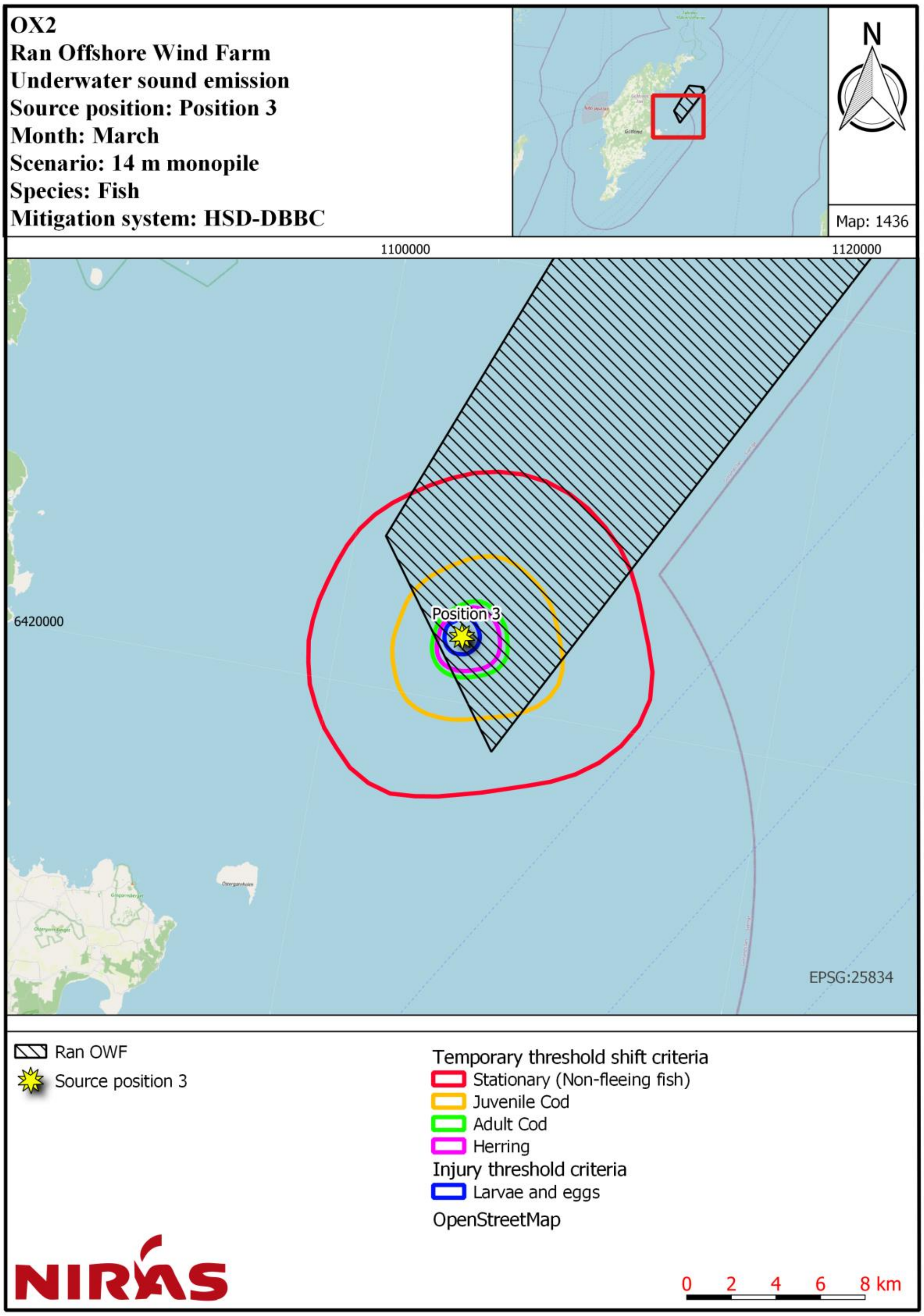

Figure 6.38: Noise contour map for fish TTS threshold and larvae & eggs injury threshold. Scenario: Monopile foundation, 14 m pile diameter; HSD+DBBC mitigation effect; Position 3.

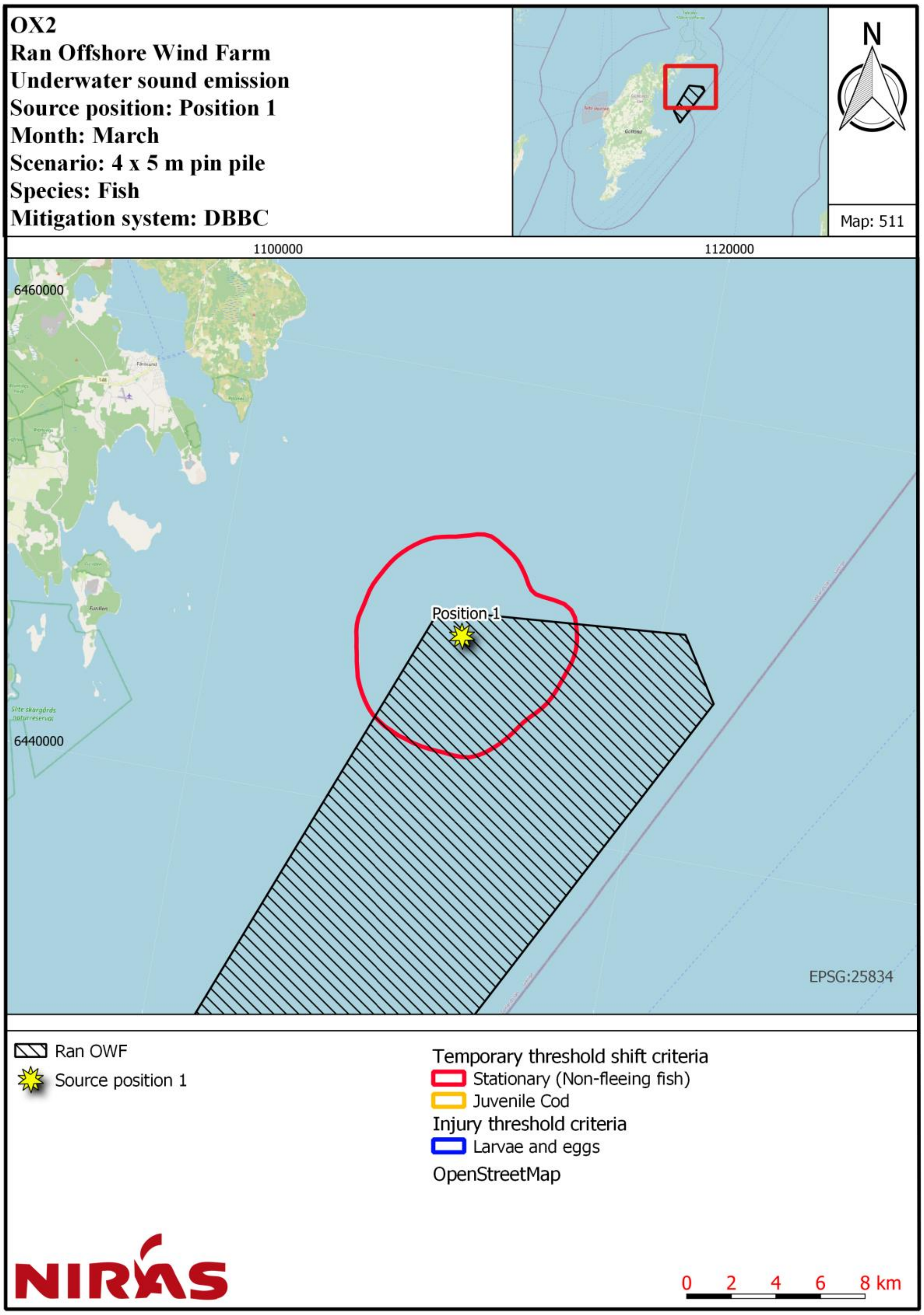

Figure 6.39: Noise contour map for fish TTS threshold and larvae & eggs injury threshold. Scenario: Jacket foundation, 5 m pile diameter; DBBC mitigation effect; Position 1.

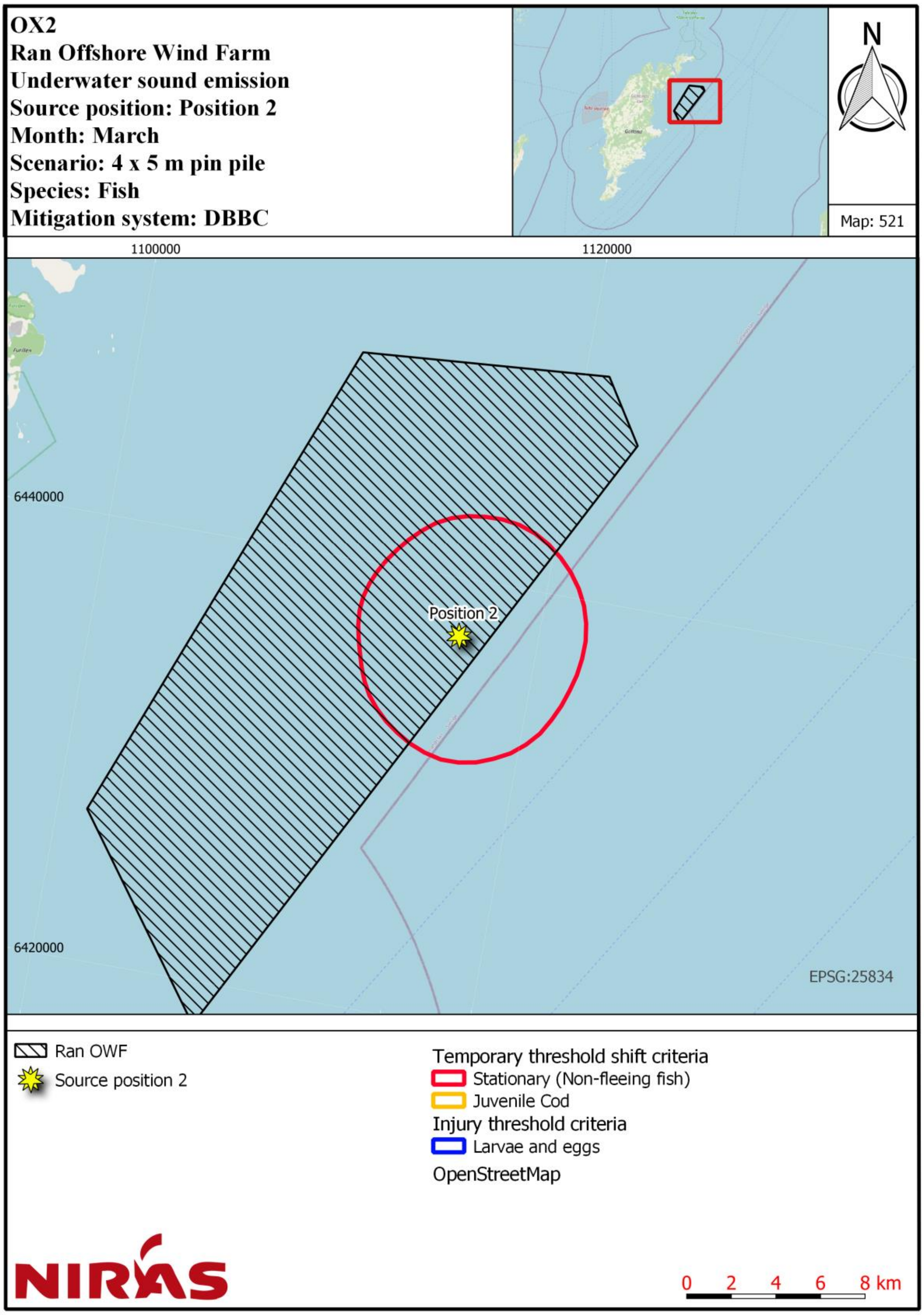

Figure 6.40: Noise contour map for fish TTS threshold and larvae & eggs injury threshold. Scenario: Jacket foundation, 5 m pile diameter; DBBC mitigation effect; Position 2.

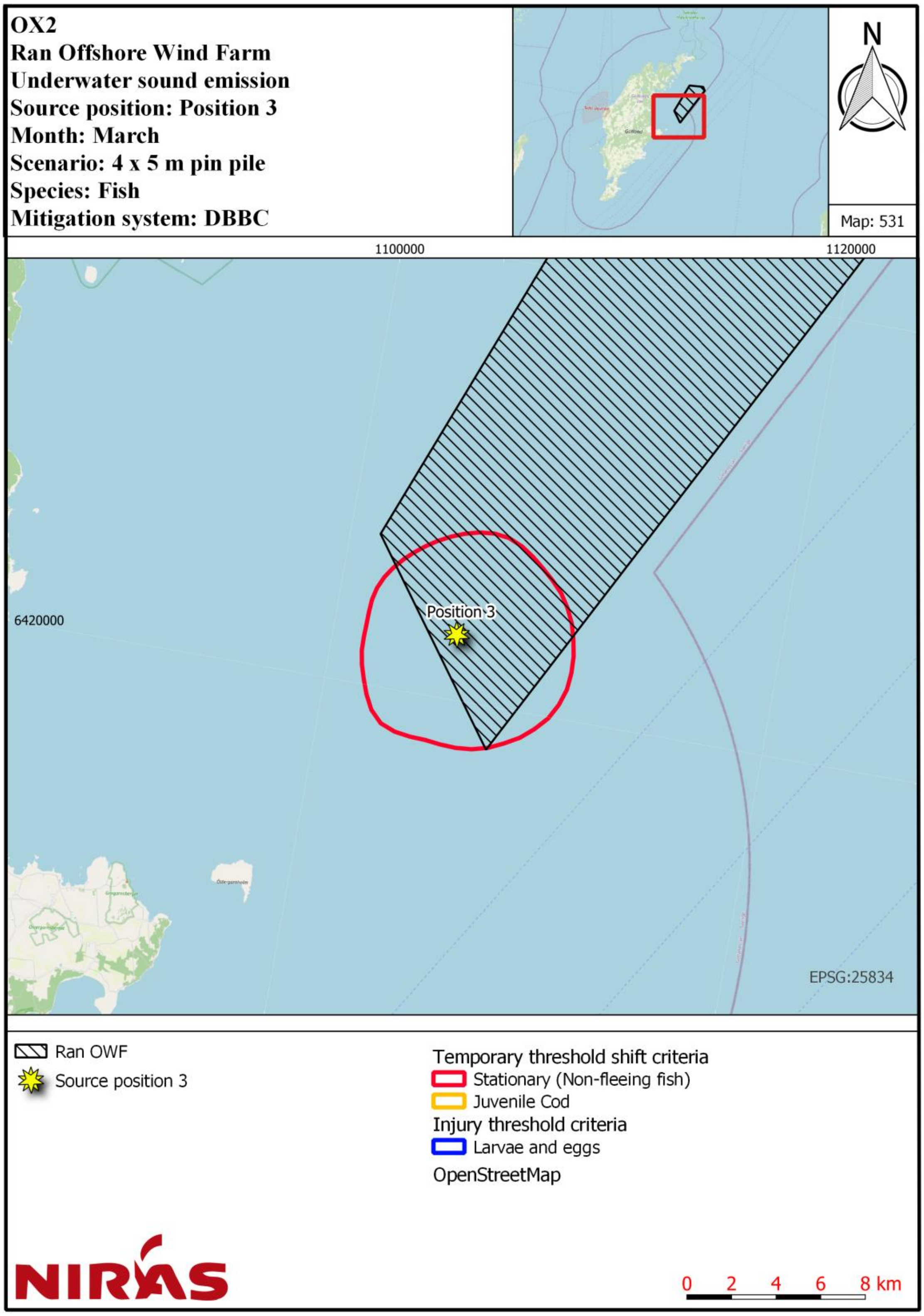

Figure 6.41: Noise contour map for fish TTS threshold and larvae & eggs injury threshold. Scenario: Jacket foundation, 5 m pile diameter; DBBC mitigation effect; Position 3.

6.8.2. Mitigated impact ranges for marine mammal threshold criteria

For marine mammals, PTS and TTS threshold criteria are based on the frequency weighted $L_{E,cum,24h,xx}$ [dB re. 1 μPa²s], where "xx" refers to the species specific weighting function. Species specific swim speed as outlined in section 4.2 is assumed.

Threshold criterion for behaviour reaction is based on the frequency weighted $L_{p,125ms,xx}$ [dB re. 1 μPa].

Resulting impact ranges are provided in Table 6.16, and affected area for harbour porpoise behaviour in Table 6.17.

Table 6.16: Impact ranges for marine mammal threshold criteria, with mitigation measures

Position	**Impact range for marine mammal threshold criteria**				
	PTS		TTS		Behaviour
	Porpoise (VHF)	Seal (PCW)	Porpoise (VHF)	Seal (PCW)	Porpoise (VHF)
14 m monopile; HSD+DBBC equivalent mitigation effect; March					
1	< 200 m	< 200 m	325 m	< 200 m	5.9 km
3	< 200 m	< 200 m	325 m	< 200 m	6.0 km
4 x 5 m pin pile (jacket foundation); DBBC equivalent mitigation effect; March					
1	< 200 m	< 200 m	700 m	< 200 m	8.3 km
2	< 200 m	< 200 m	975 m	< 200 m	9.4 km
3	< 200 m	< 200 m	700 m	< 200 m	7.6 km

Table 6.17: Area affected for harbour porpoise behaviour threshold criteria.

Position	Affected area (behaviour in harbour porpoise) [km²]
14 m monopile; HSD+DBBC equivalent mitigation effect; March	
1	99
3	103
4 x 5 m pin pile (jacket foundation); DBBC equivalent mitigation effect; March	
1	189
2	249
3	162

Noise contour maps for harbour porpoise behaviour threshold are shown in:

- Figure 6.42 - Figure 6.43 for 14 m monopile with HSD+DBBC equivalent mitigation effect.
- Figure 6.44 - Figure 6.46 for 4x 5 m pin piles (jacket foundation) with DBBC equivalent mitigation effect.

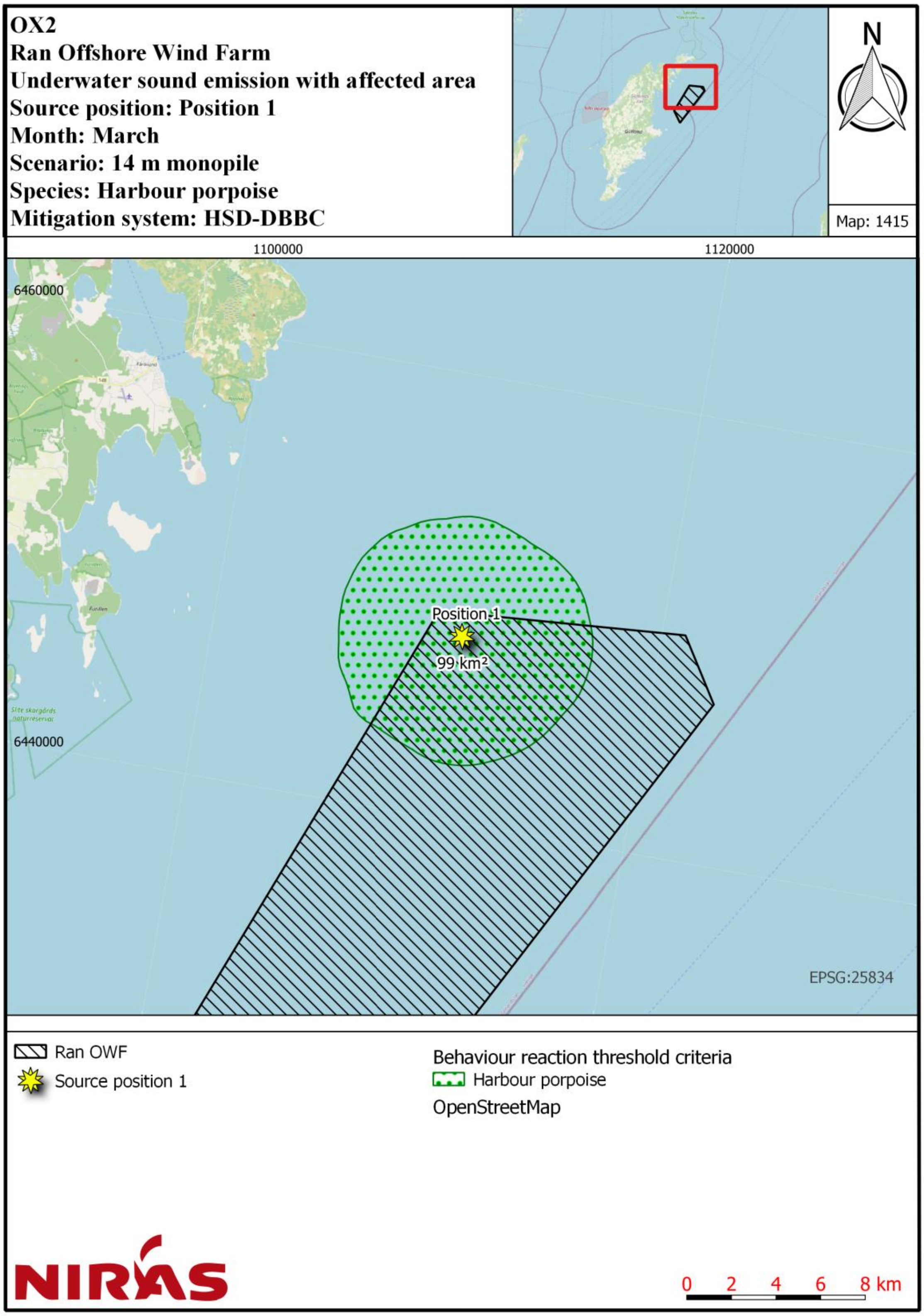

Figure 6.42: Noise contour map for harbour porpoise behaviour threshold.
Scenario: Monopile foundation, 14 m pile diameter; HSD+DBBC mitigation effect; Position 1.

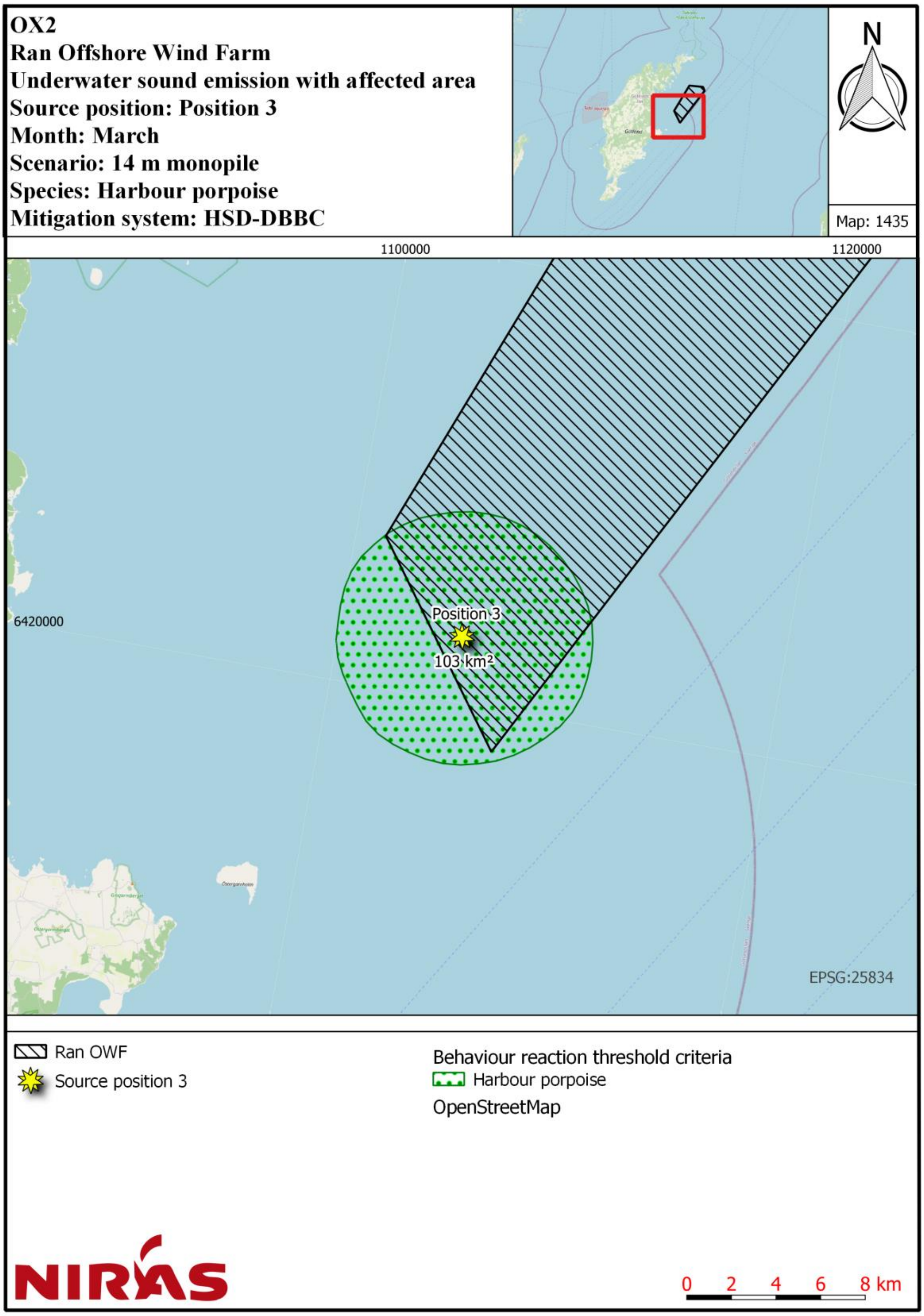

Figure 6.43: Noise contour map for harbour porpoise behaviour threshold.
Scenario: Monopile foundation, 14 m pile diameter; HSD+DBBC mitigation effect; Position 3.

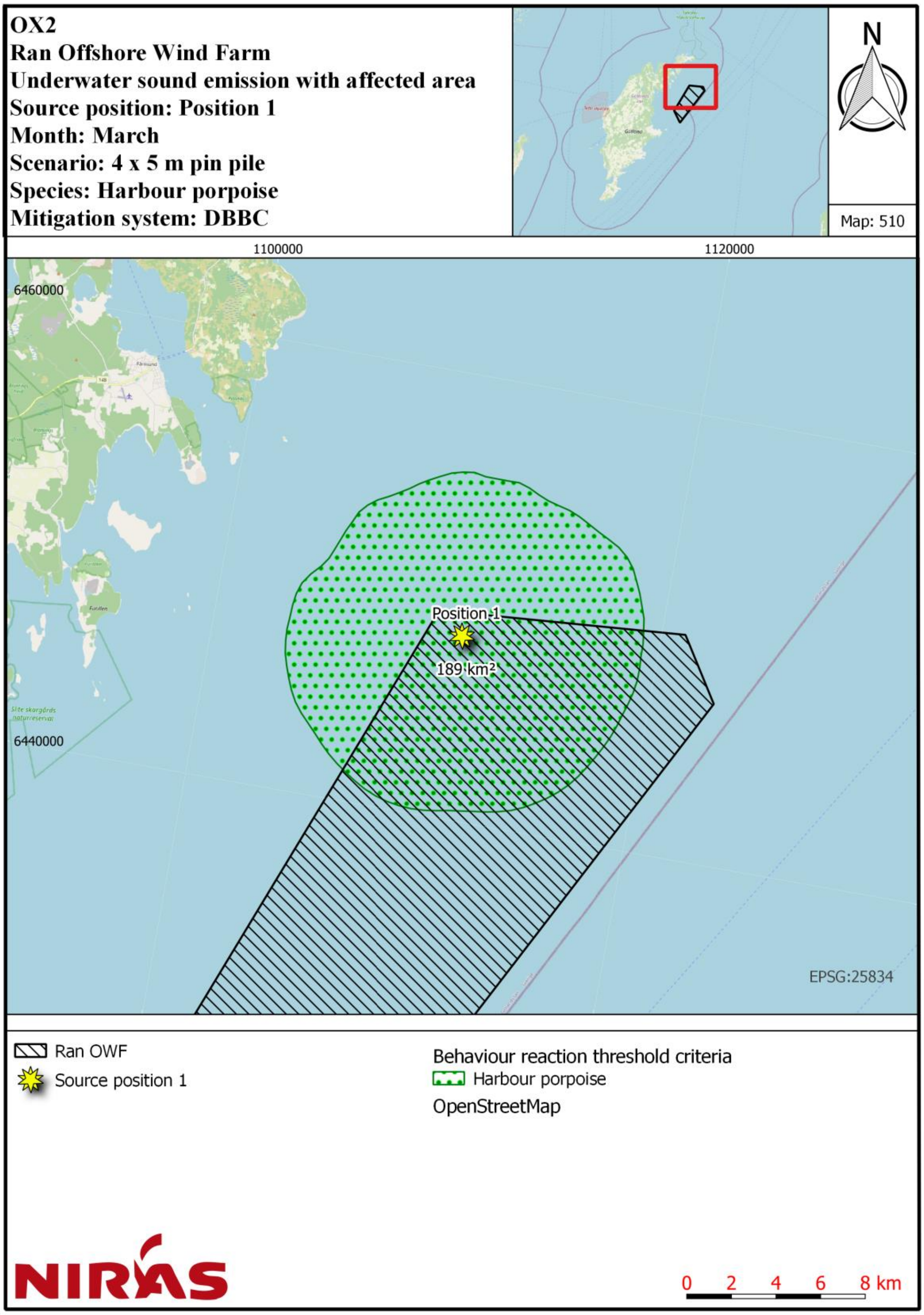

Figure 6.44: Noise contour map for harbour porpoise behaviour threshold.
Scenario: Jacket foundation, 5 m pile diameter; DBBC mitigation effect; Position 1.

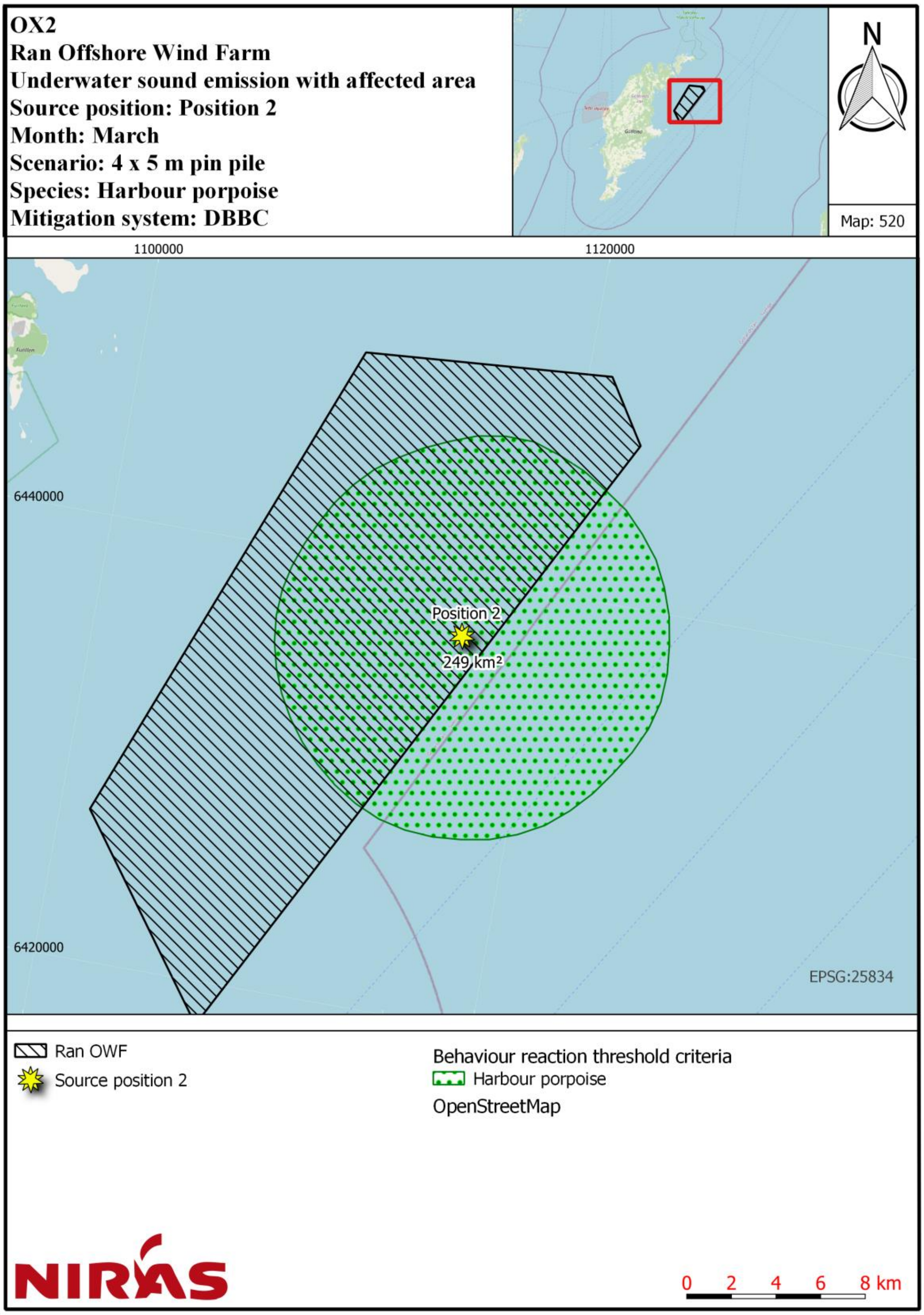

Figure 6.45: Noise contour map for harbour porpoise behaviour threshold.
Scenario: Jacket foundation, 5 m pile diameter; DBBC mitigation effect; Position 2.

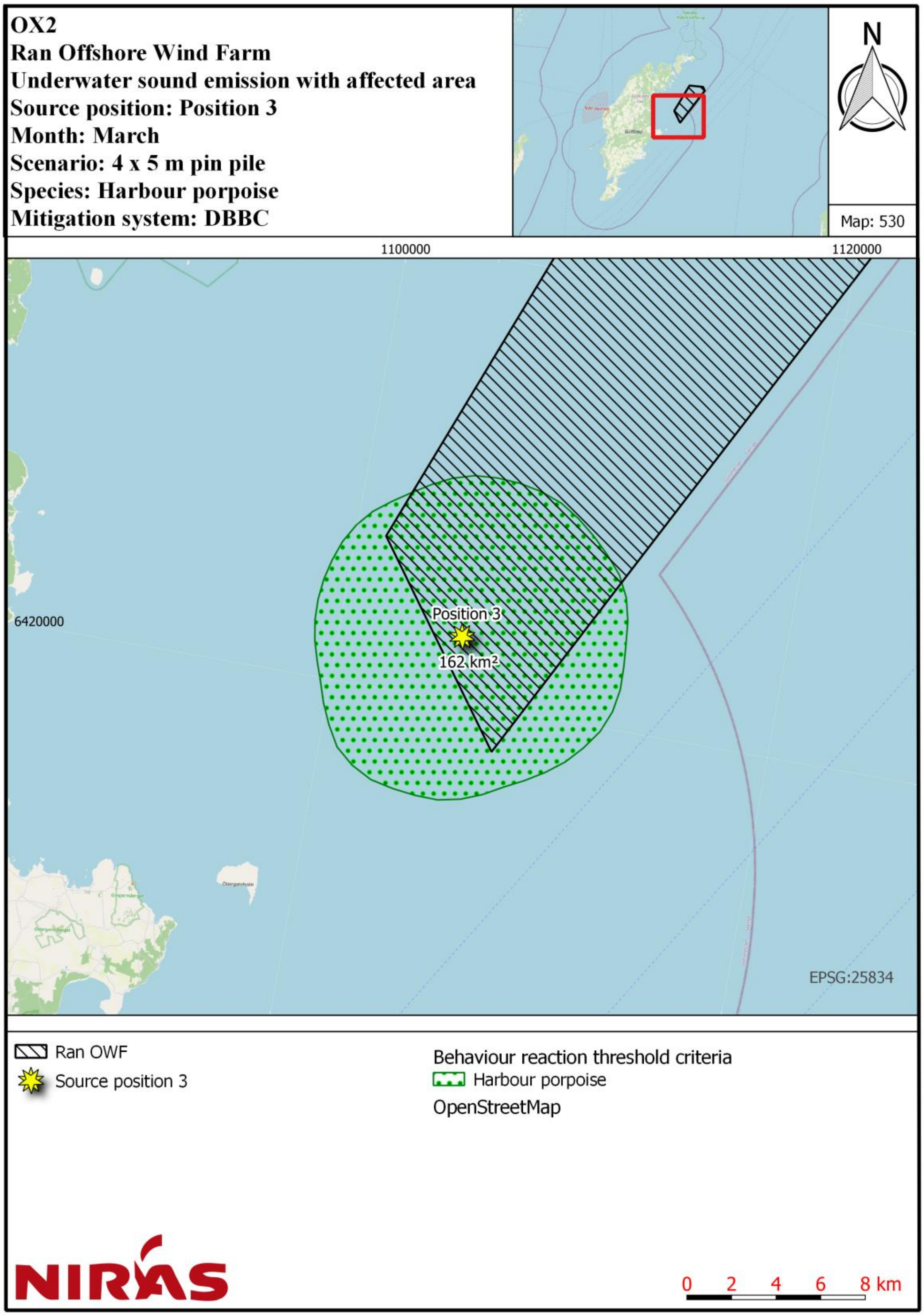

Figure 6.46: Noise contour map for harbour porpoise behaviour threshold.
Scenario: Jacket foundation, 5 m pile diameter; DBBC mitigation effect; Position 3.

7. Underwater noise evaluation for operational phase

Underwater noise from offshore wind turbines originates primarily from two sources: mechanical vibrations in the nacelle (gearbox etc.), which are transmitted through the tower and radiated into the surrounding water through the foundation; and underwater radiated noise from the service boats in the wind farm area. In a review by (Bellmann, et al., 2023), measurements of underwater noise from existing operational wind turbines are evaluated. A total of 27 operational turbines were included in the review, covering turbine sizes of 2.3 – 8.0 MW. Foundation types were primarily monopiles, but also suction jacket, jacket and tripod foundations were part of the dataset. Since the underwater noise radiated during operation will depend on the radiating structure (the foundation), its shape, material and size will matter. The turbine technologies (direct drive vs. gear box), will also have an impact on the radiated operational underwater noise. The review also covered underwater noise from service vessels.

7.1. Underwater noise as a function of turbine size

The overall trendline proposed in (Bellmann, et al., 2023), not taking foundation type or size, nor turbine technology, into account, but purely the rated power of the turbine, is shown in Figure 7.1. The trendline shows, that an increase in turbine size, does not translate into an increase in underwater noise emission. Instead, the dataset indicates a reduction in underwater noise output. The dataset includes turbines up to 8 MW rated power output, and should therefore be considered cautiously when estimating underwater noise emission from turbines larger than 8 MW.

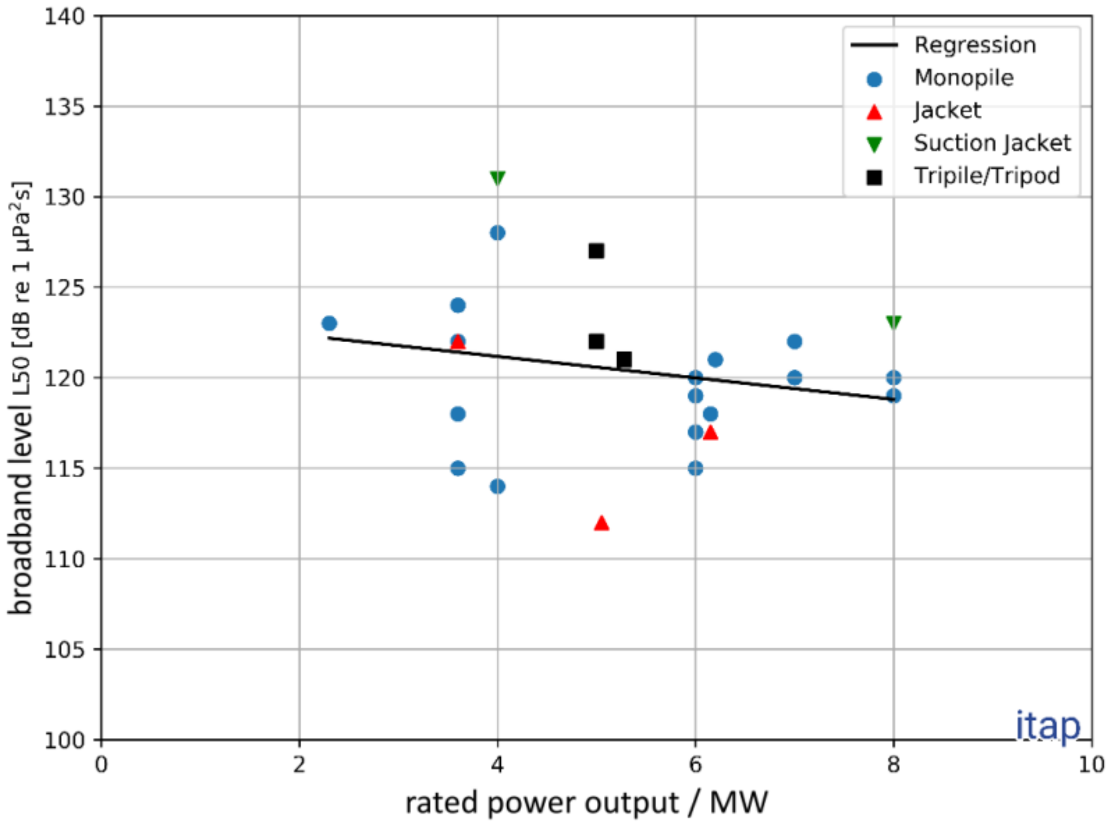

Figure 7.1: Relationship between measured broadband underwater noise and turbine size compiled from available sources. Measurements have been normalized to a distance of 100 m from the turbine foundation and wind class "High". From (Bellmann, et al., 2023)

7.2. Underwater noise as a function of water depth

The dependency on water depth is shown in Figure 7.2. The data show, that an increase in water depth, and thereby a larger pile surface in contact with the water, results in a decrease in emitted underwater noise. Whether this is due to improvements in technology for newer turbines, or other factors, is unknown.

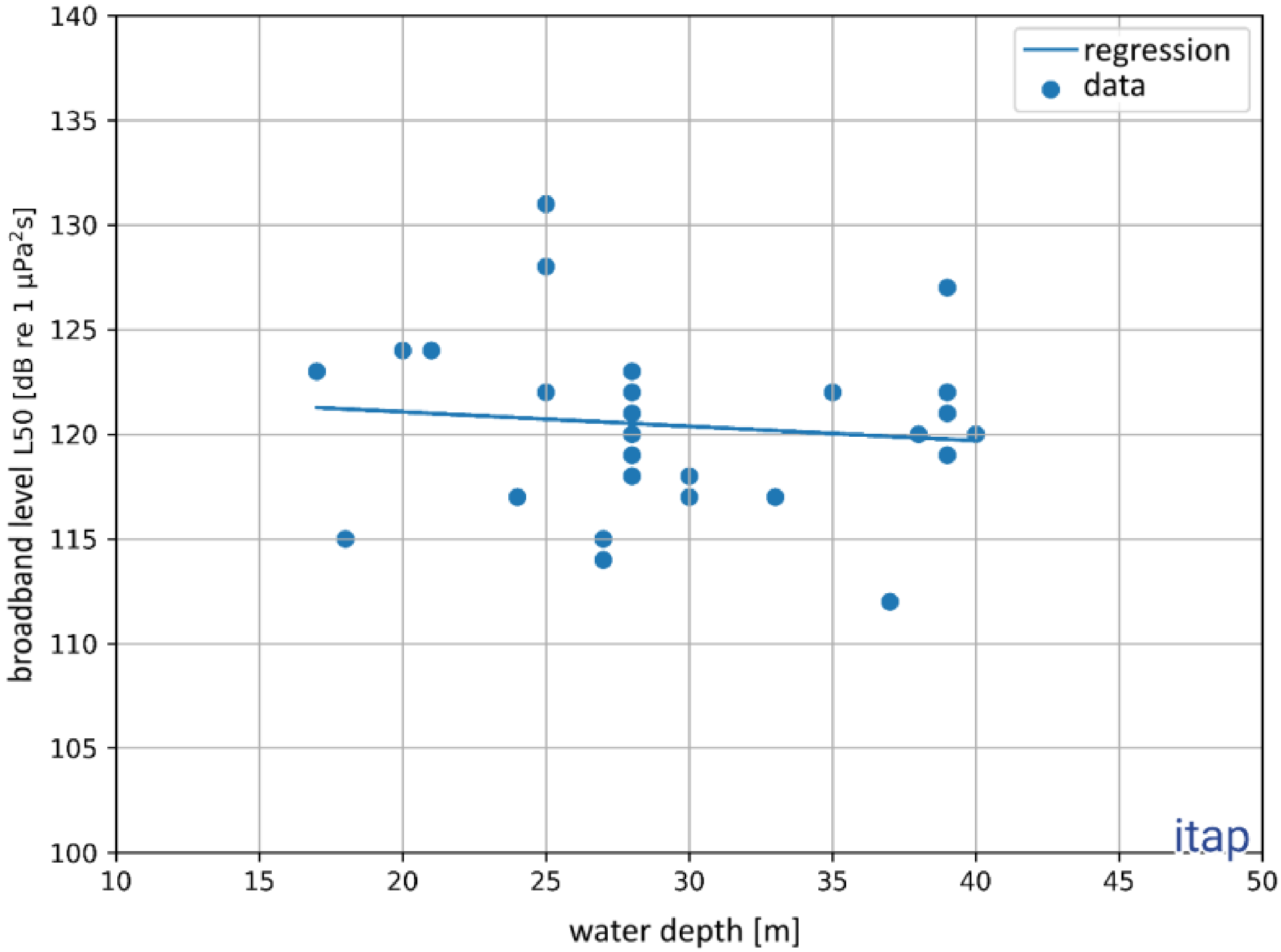

Figure 7.2: Reported underwater noise levels at 100 m distance as a function of water depth. From (Bellmann, et al., 2023)

7.3. Influence of wind speed

There is a strong dependency between wind speeds and radiated noise levels (Figure 7.3). At the lowest wind speeds, below the cut-in (the wind speed at which the turbine starts generating energy), there is no noise from the turbine. Above cut-in, there is a pronounced increase in the noise level with increasing wind speed, until the noise peaks at nominal turbine output capacity. Above this point, there is no further increase with wind speed and perhaps even a slight decrease.

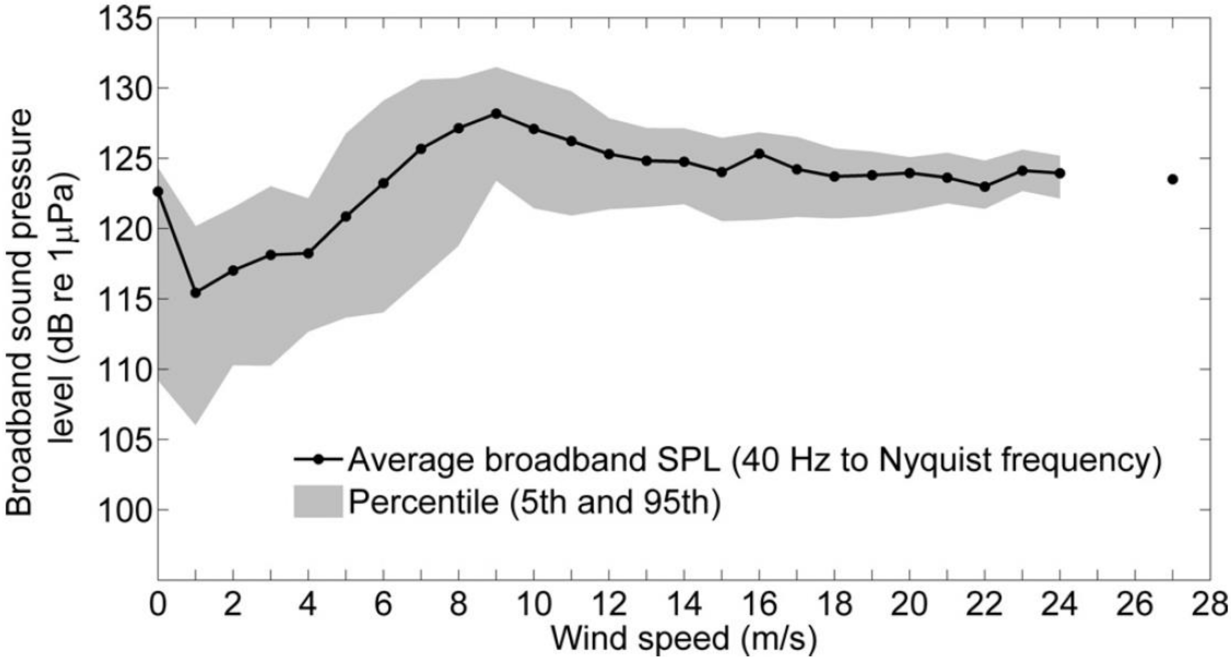

Figure 7.3: Relationship between wind speed and broadband noise level, measured about 50 m from the turbine (3.6 MW Siemens turbine at Sheringham Shoal). Maximum production of the turbine is reached at about 10 m/s, above which the production is constant. Figure from (Pangerc, et al., 2016).

7.4. Frequency content as a function of turbine size and type

The emitted underwater noise frequency content is another factor studied in (Bellmann, et al., 2023). Of the included turbine types, a significant peak within a single 1/3-octave band (not considering harmonics) was found, however not the same frequency band for all turbine types and sizes. In Figure 7.4, a comparison of 1/3-octave spectra is provided for a 3.6 MW turbine and a 6.9 MW turbine, both from Siemens.

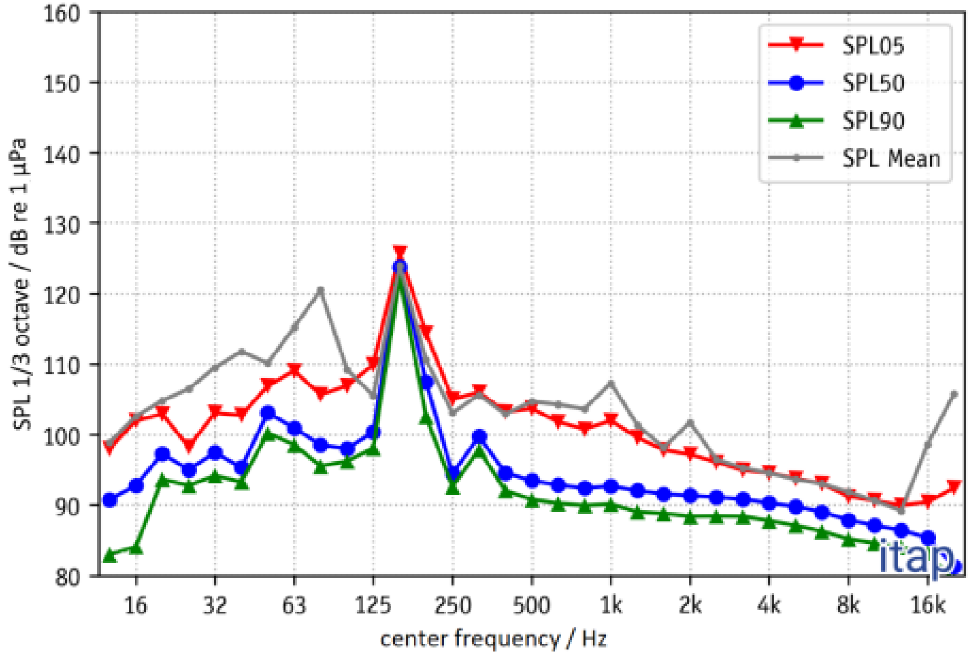

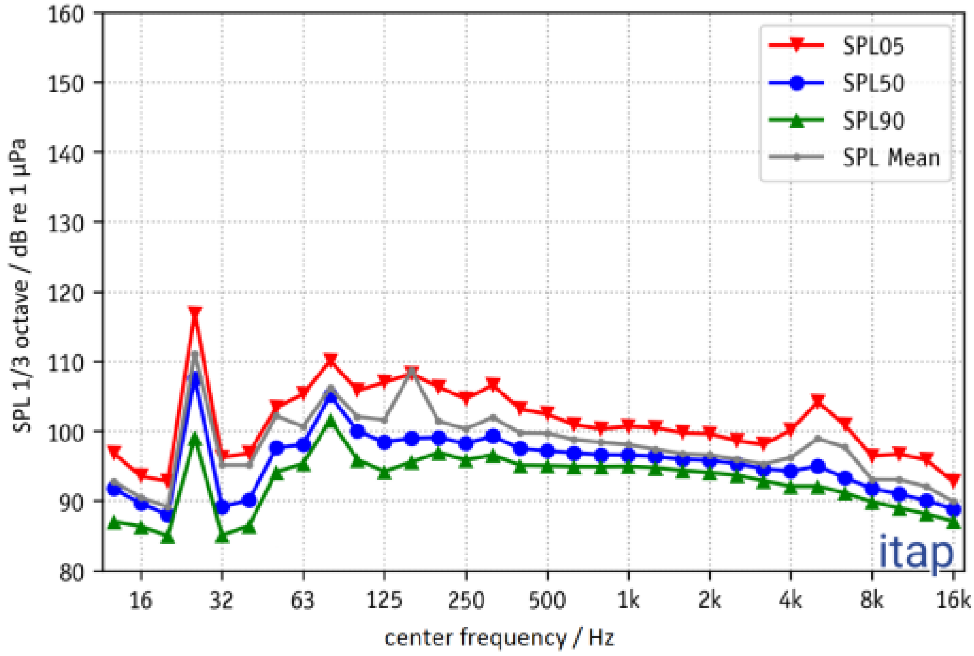

Figure 7.4: Comparison of 1/3-octave spectra of a 3.6 MW turbine with gearbox (top) and a 6.0 MW gearless turbine (bottom). From (Bellmann, et al., 2023).

The 1/3-octave spectra for the 3.6 MW turbine with gearbox is shown in the top panel in Figure 7.4, and the 1/3-octave spectra for the 6.0 MW gearless turbine is showed in the bottom panel. The gearless 6.0 MW turbine has a significantly lower frequency content with a peak in the 25 Hz 1/3-octave band, compared to 160 Hz for the 3.6 MW turbine with a gearbox. However based on the limited dataset no clear trend of the 1/3-octave band as a function of turbine size nor as a function of gearbox/direct drive can be deduced. It is therefore not possible to make a prediction of the peak 1/3-octave frequency band for any other turbine.

In the review by (Bellmann, et al., 2023), the measured underwater noise levels are also compared for the peak 1/3-octave band and the broadband level (L_{50}), see Figure 7.5. An average 6 dB difference between broadband and 1/3-octave band peak levels are noted.

	broadband Sound Pressure Level L_{50} dB re 1µPa	highest 1/3-octave level L_{50} dB re 1 µPa
Maximum	131	126
Average value	120	114
Median	120	114
Minimum	112	102

Figure 7.5: Statistical comparison of broadband SPL and peak 1/3-octave level.

7.5. Evaluation of operational turbine underwater noise

Based on the discussions in the previous sections, the underwater noise emission from the proposed 90 (20 MW) – 121 (15 MW) turbines is evaluated for both single turbines, and for the entire wind farm.

7.5.1. Operational noise from single turbines

The underwater noise level decreases approximately 3 dB per doubling of nominal capacity (see Figure 7.1). A more conservative approach would be to assume that the underwater noise level does not decrease for turbines of nominal capacity beyond the current data set (up to 8.0 MW). In order to provide a conservative estimate of the impact, the latter is assumed in the following, setting the broadband underwater noise level at 100 m of the 15 and 20 MW turbines to $SPL_{rms} = 120\ dB\ re. 1\mu Pa$. Based on the statistical distribution of energy over frequency (Figure 7.5), the peak 1/3-octave band level is expected to be approximately $SPL_{rms} = 114\ dB\ re. 1\mu Pa$.

For simplification, a standard spreading loss of $15 \cdot log_{10}(^{r_2}/_{r_1})\ [dB]$ is assumed in the following, for determining the reduction of noise level at a distance r_2, compared to a reference distance r_1, which in this case could be 100 m used in (Bellmann, et al., 2023) as the reference distance for reported sound levels.

Considering the hearing sensitivity of the relevant marine mammals (see section 3.5), the higher the frequency, the higher the auditory impact, therefore the highest 1/3-octave peak band of 160 Hz, is used as a conservative estimate in the following calculations.

Based on the 1/3-octave band spectrum in Figure 7.4 (top), species specific frequency weightings were applied, to produce broadband weighted levels at 100 m distance shown in Table 7.1, with frequency spectra shown in Figure 7.6.

Table 7.1: Species specific frequency weighted broadband levels at 100 m distance from any single operational turbine, based on frequency weighting functions discussed in section 3.5.

Species	**Weighting (xx)**	**Broadband level at 100 m distance ($SPL_{rms,xx}$)**
Seal	PCW	101 dB
Minke whale	LF	116 dB
White-beaked dolphin	HF	88 dB
Harbour porpoise	VHF	85 dB

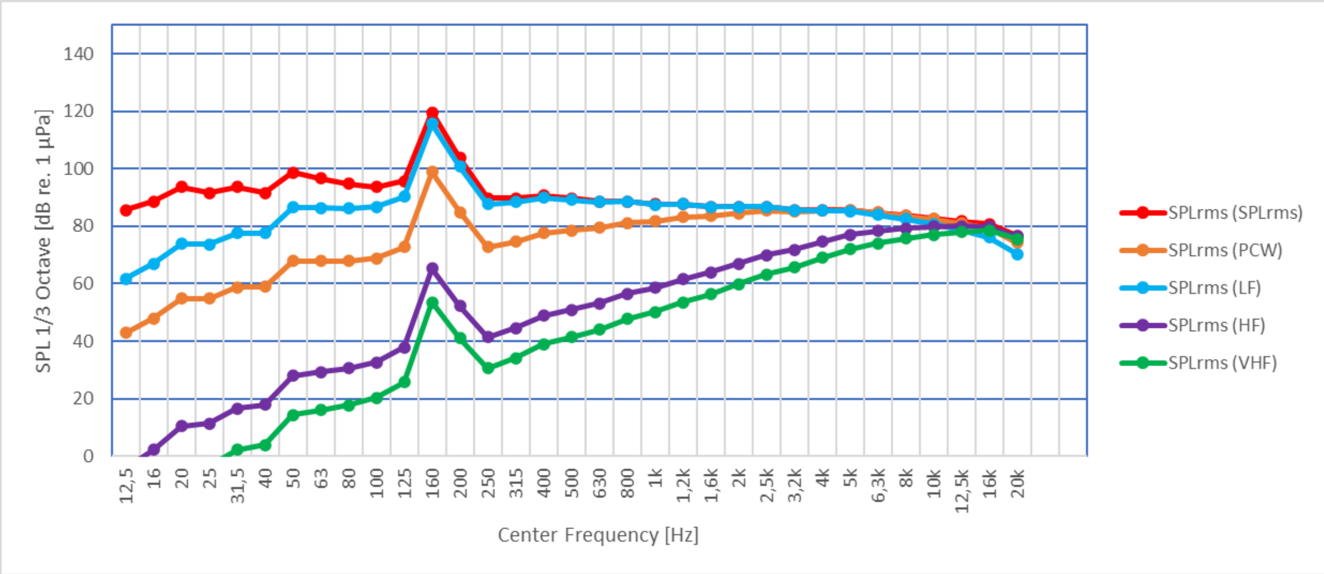

Figure 7.6: Frequency weighted 1/3-octave band levels for 160 Hz peak spectrum presented in Figure 7.4 (top).

7.5.1.1. Impact on seal from single operational turbine

For seal, no behaviour threshold is currently supported by literature, as discussed in section 4.2, and it is therefore not possible to compare the sound level at 100 m with a behavioural threshold.

Calculating the cumulative noise dose for a seal located at a constant distance of 100 m from a turbine foundation within the wind farm area, over a 24 hour period, would result in cumulative sound exposure level, $SEL_{cum,24h,PCW} = 101 + 10 \cdot log_{10}(86400) \cong 140\ dB\ re. 1\mu Pa^2 s$.

Given a threshold criteria for onset of TTS in seal for continuous noise of $SEL_{cum,24h,PCW} = 181\ dB\ re. 1\mu Pa^2 s$, the impact over a 24 hour duration is 41 dB lower than the TTS criteria. Auditory injures caused by operational noise are therefore considered unlikely to occur in seals.

A more realistic scenario than a fixed distance between seal and turbine, would be a seal foraging in the area and moving out again to rest. Without advanced behaviour modelling, it is not possible to more accurately determine the actual accumulated SEL, and thereby auditory effect. However, the simplified calculation approach above is considered very conservative.

In summary, auditory injures are considered unlikely to occur as a result of underwater noise from the wind farm in operation.

7.5.1.2. Impact on harbour porpoise from single operational turbine

For harbour porpoise, a behavioural threshold criteria of $SPL_{rms,125ms,VHF} = 103\ dB\ re\ 1\mu Pa$, is provided in (Tougaard, 2021). Noticing, that the single turbine level at 100 m (85 dB $SPL_{rms,VHF}$) is 28 dB below the behavioural threshold value, it is unlikely that the harbour porpoise will react to the noise from one operating turbine.

For harbour porpoise, the calculation of cumulative SEL, gives a received level of $SEL_{cum,24h,VHF} = 85 + 10 \cdot log_{10}(86400) \cong 134\ dB\ re. 1\mu Pa^2 s$ provided a stationary animal at 100 m distance. This is 19 dB below the threshold criteria for a harbour porpoise TTS of $SEL_{cum,24h,VHF} = 153\ dB$.

As for seal, stationary behaviour is considered unlikely and a very conservative approach in assessing the impact, and auditory injures are therefore considered unlikely to occur for harbour porpoise, as a result of a single operational wind turbine.

7.5.1.3. Impact on fish from single operational turbine

Most fish detect sound from the infrasonic frequency range (<20 Hz) up to a few hundred Hz (e.g. Salmon, dab, and cod) whereas other fish species with gas-filled structures in connection with the inner ear (e.g. herring) detect sounds up to a few kHz. The main frequency hearing range for fish is therefore overlapping with the frequencies, produces by operational wind turbines (below a few hundred Hz). There are no studies defining fish behavioural response threshold for continuous noise sources, and the scientific data addressing TTS from such noise sources is very limited. The only studies providing a TTS threshold value for fish is from experiments with goldfish. Goldfish is a freshwater hearing specialist with the most sensitive hearing in any fish species. All of the species locally occurring in the project area have a less sensitive hearing, compared to the goldfish (Popper, et al., 2014), and using threshold for goldfish will lead to an overestimation of the impact.

Empirical data for several of the fish species without a connection between the inner ear and the gas-filled swim bladder showed no TTS in responses to long term continuous noise exposure (Popper, et al., 2014). In a study by Wysocki et al. (2007), rainbow trout exposed to increased continuous noise (up to $SPL_{rms} = 150\ dB\ re.1\mu Pa$) for nine months in an aquaculture facility, showed no hearing loss nor any negative health effect.

Unweighted underwater noise levels from a single operational turbine was assessed to be $SPL_{rms} = 120\ dB\ re.1\mu Pa$ at 100 m distance from the turbine. This would increase at distances closer to the turbine. From the generalised assumption of 15 dB/decade propagation loss, an underwater noise level of $SPL_{rms} = 150\ dB\ re.1\mu Pa$ would however only occur in the absolute vicinity of the foundation within a few meters from the individual turbine. It is therefore assessed unlikely that TTS would occur as a result of underwater noise from a single operational turbine.

7.5.2. Operational noise from entire wind farm

Since an operational wind farm consists of more than just a single operational turbine, it is also important to address in the cumulative noise from nearby turbines when evaluating the impact.

In (Bellmann, et al., 2023), an example of an 87 turbine wind farm in the German North Sea is provided. The cumulated underwater noise level from all 87 turbines in operation is estimated to be $SPL_{rms} = 130\ dB\ re\ 1\mu Pa$ inside the wind farm area.

Utilizing the same approach as for a single turbine (section 7.5.1), frequency weighted broadband levels were calculated in Table 7.2, as general levels within the wind farm.

Table 7.2: Species specific frequency weighted broadband levels within the wind farm, (generalised approach), based on frequency weighting functions discussed in section 3.5.

Species	**Weighting (xx)**	**Broadband level inside the wind farm ($SPL_{rms,xx}$)**
Seal	PCW	111 dB
Minke whale	LF	126 dB
White-beaked dolphin	HF	98 dB
Harbour porpoise	VHF	95 dB

7.5.2.1. Impact on seal from entire operational wind farm

Calculating the cumulative noise dose for a seal inside the wind farm over a 24 hour period, would result in cumulative sound exposure level, $SEL_{cum,24h,PCW} = 111 + 10 \cdot log_{10}(86400) \cong 150\ dB\ re. 1\mu Pa^2 s$.

This is 31 dB below the threshold for TTS onset ($SEL_{cum,24h,PW} = 181\ dB\ re. 1\mu Pa^2 s$), and it is therefore considered unlikely that any auditory injuries would occur resulting from the operational wind farm.

7.5.2.2. Impact on harbour porpoise from entire operational wind farm

For a harbour porpoise located inside the OWF, the cumulative noise dose is estimated to $SEL_{cum,24h,VHF} = 95 + 10 \cdot log_{10}(86400) \cong 144\ dB\ re. 1\mu Pa^2 s$. This is 9 dB below the threshold criteria for a harbour porpoise TTS of $SEL_{cum,24h,VHF} = 153\ dB$, remaining within the wind farm area for 24 hours. Even though the margin between TTS threshold criterion and cumulative noise dose is significantly smaller than for seals, it is still considered unlikely that any auditory injuries will occur. Not just because it is below the TTS criterion over 24 hours, but because any given harbour porpoise is unlikely to stay within the wind farm area for such a long duration.

7.5.2.3. Impact on fish from entire operational wind farm

For the entire operational wind farm, the general underwater noise level was estimated to be $SPL_{rms} = 130\ dB\ re. 1\ \mu Pa$ on average, however possibly higher at close range (< 100 m) to individual turbines. From the generalised assumption of 15 dB/decade propagation loss, an underwater noise level of $SPL_{rms} = 150\ dB\ re. 1\mu Pa$ would occur up to 5 m from the individual turbine.

It is therefore assessed as unlikely that TTS in fish would occur as a result of underwater noise from an entire operational offshore wind farm.

7.6. Noise from service boats

In addition to the noise from the turbines in operation, service boats and vessels within offshore wind farms are likely to be a source of underwater noise during the operational phase of the wind farm. In the example provided in (Bellmann, et al., 2023), of a wind farm with 87 turbines in operation a comparison is provided (in Figure 7.7) with modelled underwater noise from the movements of a service vessel over a 50 day time period (In Figure 7.8). From this comparison it is clear that the service vessels contribution to the overall soundscape, is insignificant.

Sound source	Average acoustical power	Sound energy radiated into the sea within 50 days
Service vessel during trips in the OWF from Figure 25; in total 4 h.	119 dB re 1 µW (≈ 0.8 W)	114 dB re 1 J (≈ 0,22 MJ)
87 OWTG	130,4 dB re 1 µW (≈ 11 W)	137 dB re 1 J (≈ 47 MJ)

Figure 7.7: Comparison between radiated sound energy of a wind farm in operation and the service vessel moving to, within and from the wind farm over a 50 day period. From (Bellmann, et al., 2023)

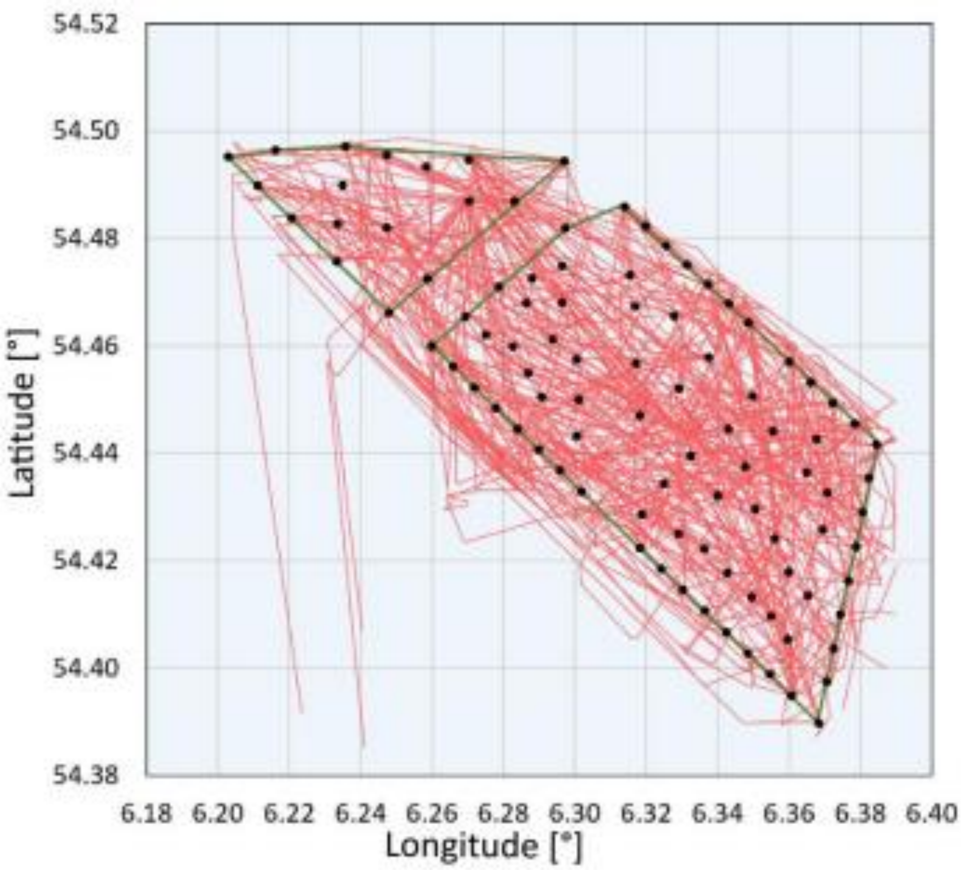

Figure 7.8: Service vessel tracks for a wind farm in the Western Zone 2 of the German EEZ in the North Sea. From (Bellmann, et al., 2023).

The Ran OWF area is located in an area with ship traffic (Figure 5.5) and the area is therefore expected already to be dominated by low-frequency ship noise. Based on data from the BIAS-project, the underwater noise level measured in the 63 and 125 Hz frequency band (indicators of ship noise) is modelled to be above 90 - 115 dB re 1uPa for both frequencies in the project area for Ran OWF (50 % of the time), see Figure 5.1 - Figure 5.4. While the radiated sound energy in Figure 7.7 and the BIAS underwater noise background level can not be compared, the difference between turbine noise and vessel noise (in Figure 7.7) clearly shows that the vessel noise is insignificant when evaluating overall noise pollution of the wind farm.

8. Bibliography

Adegbulugbe, O., Jung, S. & Kampmann, R., 2019. *Task 1 Report: Literature Review of Pile Driving System, Evaluation of Glass Fiber Reinforced Polymer (GFRP) Spirals in Corrosion Resistant Concrete Piles,* s.l.: Florida Department of Transportation.

Andersson, M. et al., 2016. *A framework for regulaing underwater noise during pile driving.* s.l.:A technical Vindval report, ISBN 978-91-620-6775-5, Swedish.

Bailey, H., Brookes, K. L. & Thompson, P. M., 2014. Assessing Environmental Impacts of Offshore Wind Farms: Lessons Learned and Recommendations for the Future. *Aquatic Biosystems,* 10(1):8(DOI:10.1186/2046-9063-10-8).

Bellmann, M. A. et al., 2020. *Underwater noise during percussive pile driving: Influencing factors on pile-driving noise and technical possibilities to comply with noise mitigation values,* Oldenburg, Germany: August, ITAP.

Bellmann, M., Müller, T., Scheiblich, K. & Betke, K., 2023. *Experience report on operational noise - Cross-project evaluation and assessment of underwater noise measurements from the operational phase of offshore wind farms, itap report no. 3926,* s.l.: funded by the German Federal Maritime and Hydrographic Agency, funding no. 10054419.

Copernicus, M. S., 2023. *Baltic Sea Physics Analysis and Forecast model, https://doi.org/10.48670/moi-00010,* s.l.: s.n.

Coppens, A., 1981. Simple equations for the speed of sound in Neptunian waters. *J. Acoust. Soc. Am. 69(3),* pp. 862-863.

Diederichs, A. et al., 2014. *Entwicklung und Erprobung des Großen Blasenschleiers zur Minderung der Hydroschallemissionen bei Offshore-Rammarbeiten. P. 240. BioConsult.* s.l.:s.n.

DS/ISO 18405, 2017. *DS/ISO 18405 - Underwater acoustics - Terminology.* s.l.:s.n.

EC Decision 2017/848, 2017. *laying down criteria and methodological standards on good environmental status of marine waters.* s.l.:s.n.

EMODnet, CLS, 2022. *EMODnet web portal (Human Activities, vessel density), Collecte Localisation Satellites (CLS).* [Online]
Available at: https://emodnet.ec.europa.eu/en/human-activities
[Accessed 14 06 2023].

EMODnet, 2021. *EMODnet-Geology portal, Seabed Substrate layer.* [Online]
Available at: https://www.emodnet-bathymetry.eu/data-products
[Accessed 2021].

EMODnet, 2022. *EMODnet bathymetry portal.* [Online]
Available at: https://portal.emodnet-bathymetry.eu/
[Accessed December 2020].

Energistyrelsen, 2023. *Guideline for underwater noise - Installation of impact or vibratory driven piles,* s.l.: March.

Erbe, C., 2011. *Underwater Acoustics: Noise and the Effects on Marine Mammals.* s.l.:jasco.

Hamilton, E., 1980. Geoacoustic modeling of the sea floor. *J. Acoust. Soc. Am., Vol. 68, No. 5*, November, pp. 1313 - 1340, doi: 10.1121/1.385100.

ICES, 2014. *ICES Continuous Underwater Noise dataset,* Copenhagen: s.n.

ICES, 2018. *ICES Continuous Underwater Noise dataset,* Copenhagen: s.n.

Jacobsen, F. & Juhl, P. M., 2013. FUGA. In: *Fundamentals of General Linear Acoustics.* s.l.:Wiley, p. 285.

Jensen, F. B., Kuperman, W. A., Porter, M. B. & Schmidt, H., 2011. *Computational Ocean Acoustics, 2nd edition.* s.l.:Springer.

Martin, B., Morris, C. & O'Neill, C., 2019. *Sound exposure level as a metric for analyzing and managing underwater.* s.l.:s.n.

NOAA, 2018. *Technical Guidance for Assessing the Effects of Anthropogenic Sound on Marine Mammal Hearing (Version 2.0), NOAA Technical Memorandum NMFS-OPR-59,* Silver Spring, MD 20910, USA: April, National Marine Fisheries Service.
Offnoise Solutions, 2023. *https://www.offnoise-solutions.com/.* [Online].
Pangerc, T. et al., 2016. *Measurement and characterisation of radiated underwater sound from a 3.6 MW monopile wind turbine.,* s.l.: Journal of the Acoustical Society of America 140:2913–2922.
Popper, A. et al., 2014. *Sound exposure guidelines for fishes and sea turtles.* s.l.:ANSI-Accredited Standards Committee S3/SC1 and registered with ANSI.
Popper, A. et al., 2014. *Sound exposure guidelines for fishes and sea turtles: A technical report prepared by ANSI-accredited standards committee S3 s−1C1 and registered with ANSI.* New York: Springer.
Russell, D. et al., 2016. *Avoidance of wind farms by harbour seals is limited to pile driving activities.* s.l.:Journal of Applied Ecology, 53, 1642-1652.
Schäfer, 2020. *Seismic stratigraphy of the Klints Bank east of Gotland (Baltic Sea): a giant drumlin sealing thermogenic hydrocarbons,* s.l.: s.n.
Sopher, D., Erlströmb, M., Bell, N. & Juhlin, C., 2016. *The structure and stratigraphy of the sedimentary succession in the Swedish sector of the Baltic Basin: New insights from vintage 2D marine seismic data.* s.l.:s.n.
Southall, B. et al., 2019. *Marine mammal noise exposure criteria: Updated Scientific Recommendations for Residual Hearing Effects.* s.l.:Aquatic Mammals, 45(2), 125-323.
Tougaard, J., 2021. *Thresholds for behavioural responses to noise in marine mammals. Background note to revision of guidelines from the Danish Energy.,* Aarhus: Aarhus University DCE – Danish Centre for Environment and Energy, 32 pp. Technical Report No. 225 http://dce2.au.dk/pub/TR225.pdf.
Tougaard, J. & Beedholm, K., 2018. *Practical implementation of auditory time and frequency weighting in marine bioacoustics.* s.l.:Department of Bioscience, Aarhus University, Denmark.
Tsouvalas, A., 2020. *Underwater Noise Emission Due to Offshore Pile.* s.l.:s.n.
Wysocki, L., Davidson, J. I. & Smith, M., 2007. *Effects of aquaculture production noise on hearing, growth, and disease resistance of rainbow trout Oncorhynchus mykiss..* s.l.:Aquaculture 272:687–697..

Appendix 1

Concurrent installation of multiple foundations

If more than one foundation were to be installed at the same time, the cumulative aspects for sound propagation must be considered. Two scenarios are considered: Simultaneous/partially overlapping and sequential installation.

Installation of two foundations simultaneously

If two foundations were to be installed at the same time, this would likely result in increased PTS and TTS impact distances (up to a factor 2 increase), as these thresholds are based on the time-dependent noise dose received by a marine mammal or fish. For certain species, this would depend on their swim speed.

The further apart the two foundations, the lower the difference in PTS/TTS relative to the single foundation scenario. However, with larger spacing, a trapping effect could potentially occur, whereby a marine mammal or fish would swim away from one foundation, only to get closer to the installation of the second foundation, thus not achieving a linear decrease in received SEL with time. In this scenario, it is difficult to predict what $L_{E,cum,24h}$, the marine mammal or fish would receive over the span of the installations. Inversely, the closer the foundations, the lower the risk of trapping, but also the longer the threshold distances for PTS and TTS would be expected.

One method for reducing the increase in impact distances for concurrent installations, would be to add a time-delay to the installation of the second foundation, such that the marine mammals are able to create distance between themselves and the pile installation(s), before both piling activities are active.

Another aspect of concurrent installations is that it can potentially result in increased behaviour distances. The interaction between wave fronts from two pile installations will however be a complex mix of positive and destructive interference patterns as the wave fronts collide. The resulting sound field would be impossible to predict but it is expected that avoidance behaviour could occur at increased distances, compared to those of a single pile installation.

Installation of two foundations sequentially

Installation of two foundations sequentially, where the second pile installation is started as soon as the former is completed, would result in more predictable effects on the underwater soundscape. In a closely spaced scenario, the marine mammals and fish that would be affected by the second pile installation, would already have had significant time to vacate the underwater noise impacted area, thereby limiting the increase in impact.

For behaviour, the impact distance would not be affected by interference patterns (which will be the case if installation of two pile installations occurs at the same time), nor would it equate the sum of impact areas for both installations, rather it would shift from one location to the next. For PTS and TTS, the impact distances would likely not increase, as the marine mammals and fish are already far from both installation sites and therefore receiving minimal additional impact from the installation of the second installation. It is however important that the second installation is not delayed significantly in time after the completion of the first, as this would allow for marine mammals and fish to return to the area.

Appendix 2

Temperature, salinity and sound speed profiles position 2 – 3

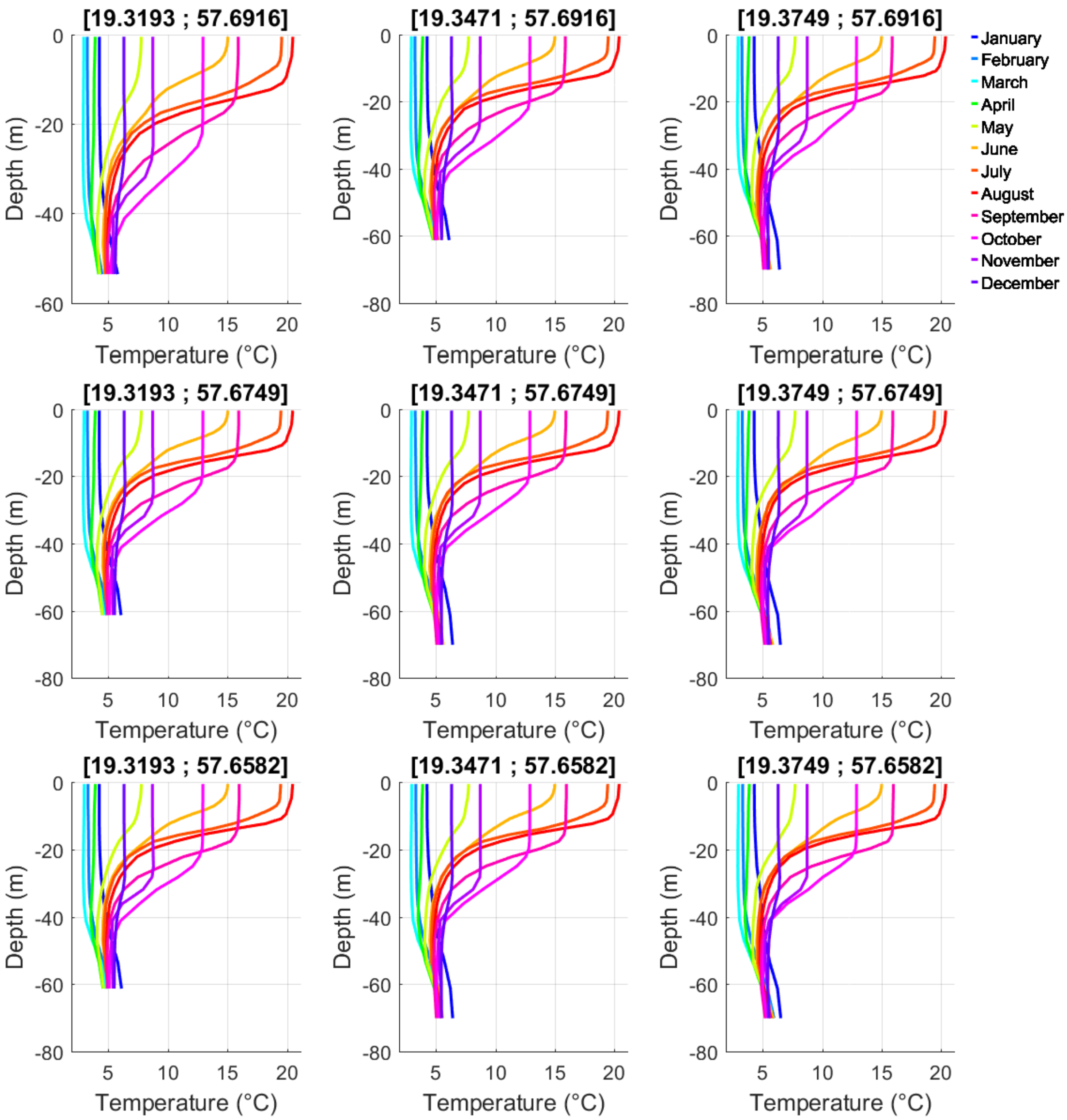

Figure 8.1: Temperature profiles for the area around source position 2 for all months. Gridded layout reflects geographical location.

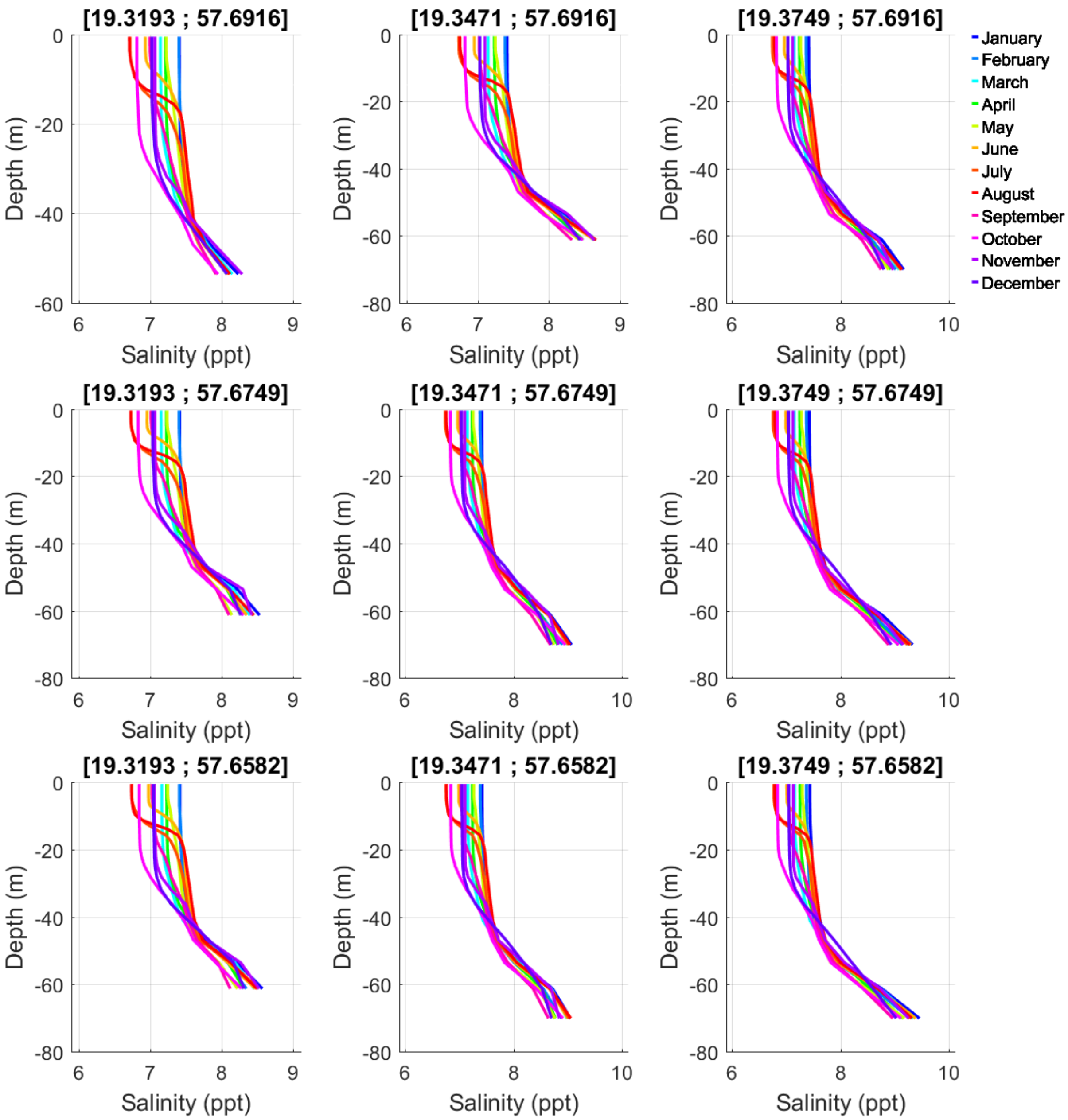

Figure 8.2: Salinity profiles for the area around source position 2 for all months. Gridded layout reflects geographical location.

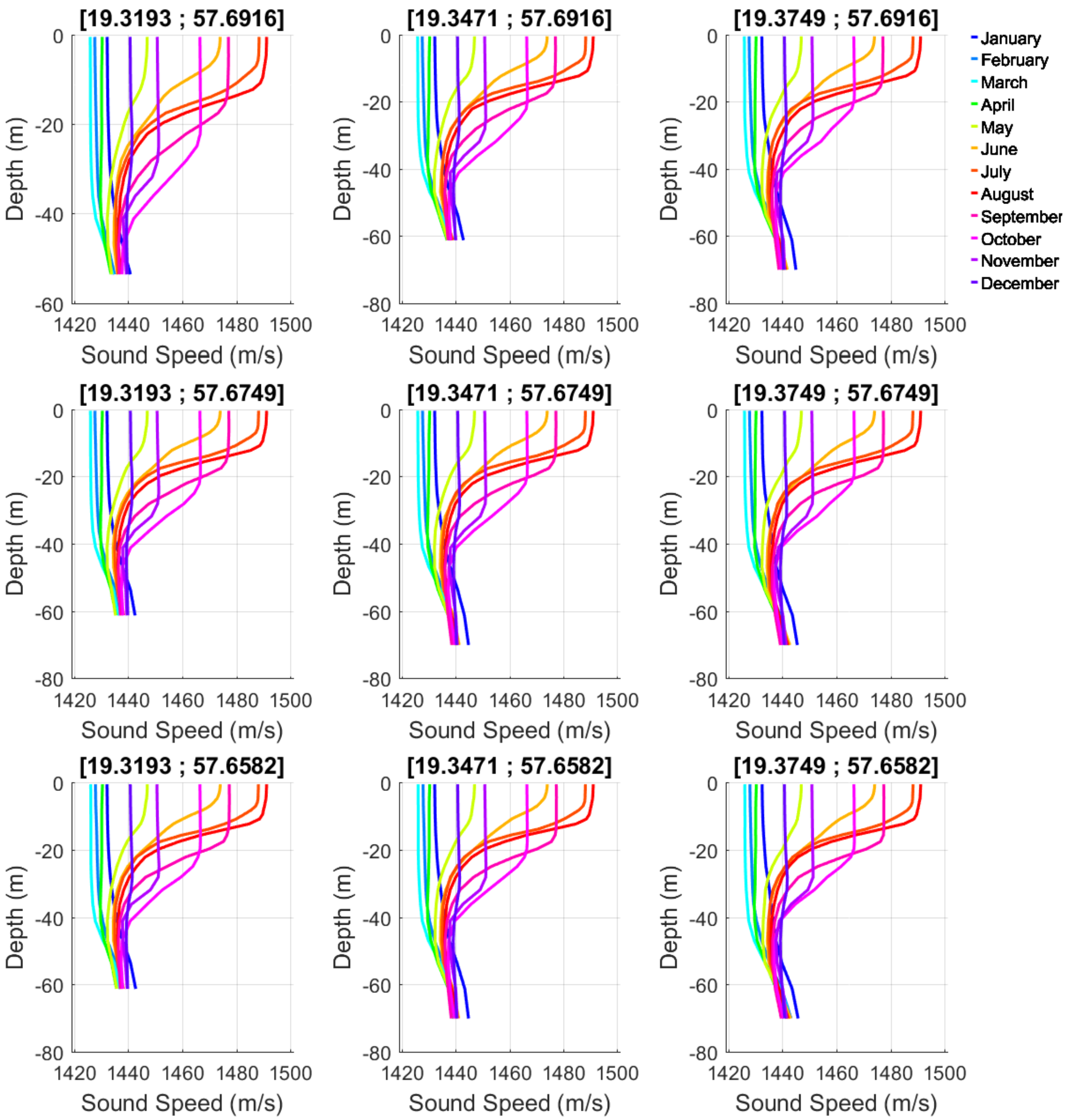

Figure 8.3: Sound speed profiles for the area around source position 2 for all months. Gridded layout reflects geographical location.

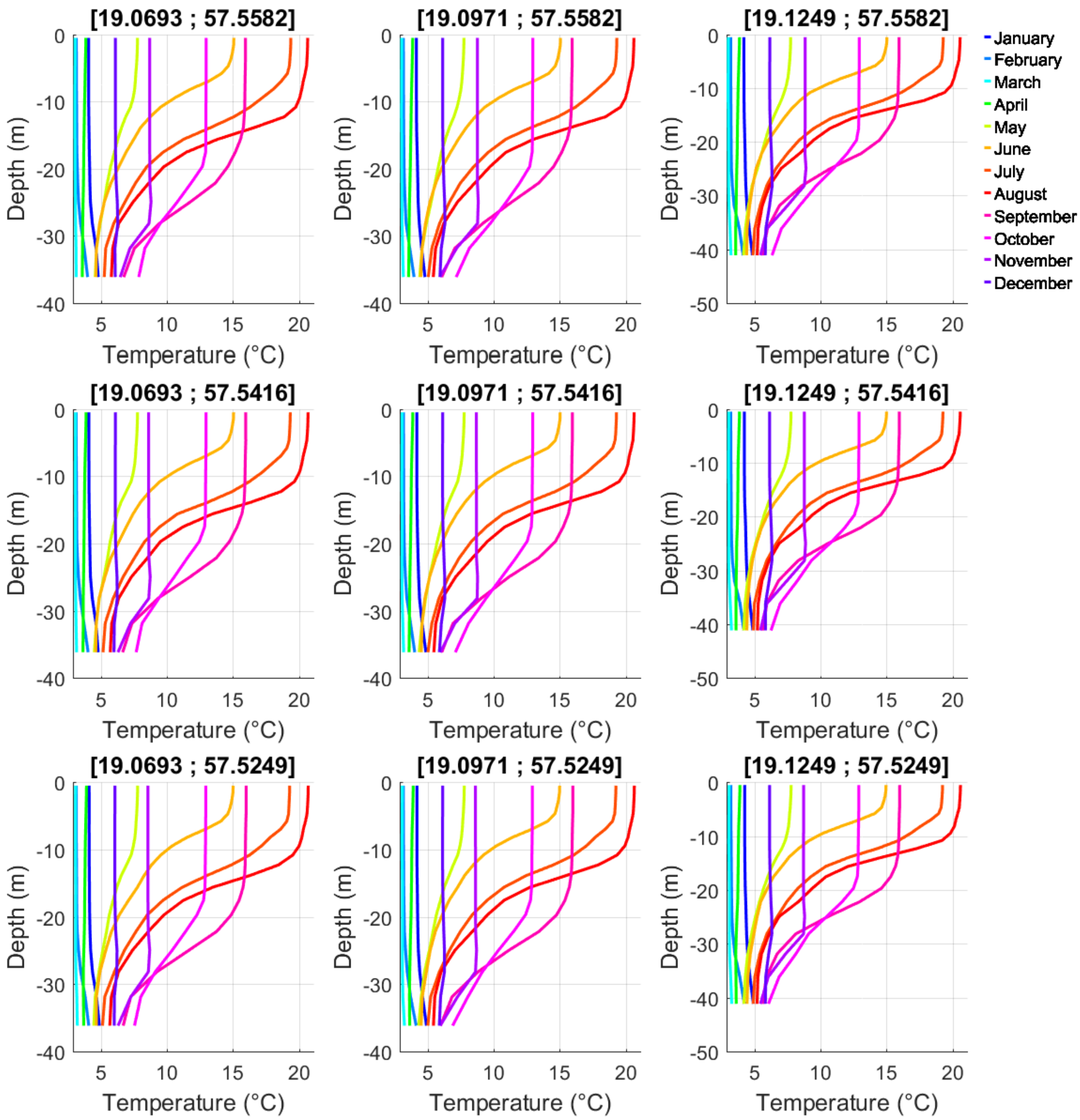

Figure 8.4: Temperature profiles for the area around source position 3 for all months. Gridded layout reflects geographical location.

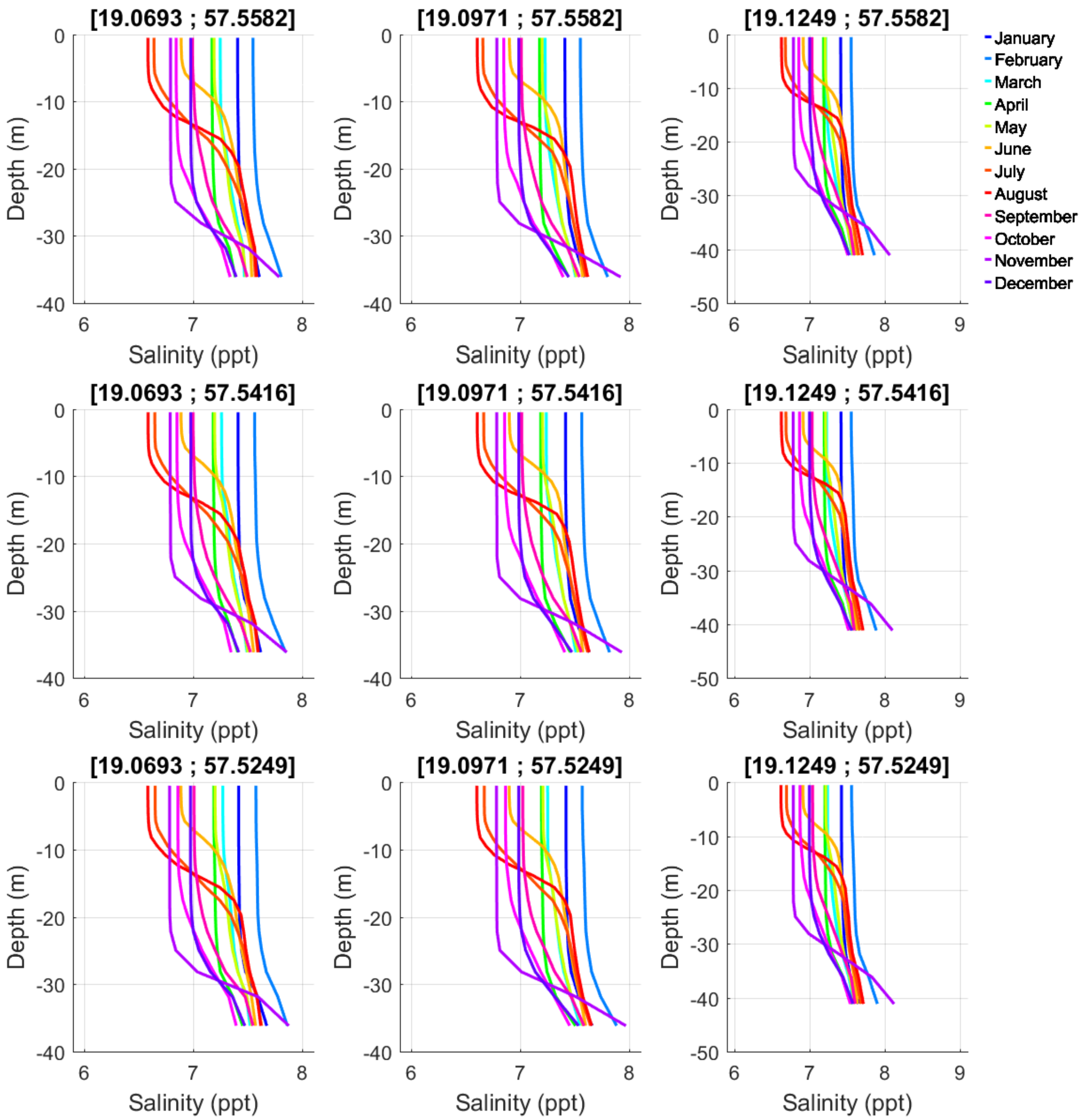

Figure 8.5: Salinity profiles for the area around source position 3 for all months. Gridded layout reflects geographical location.

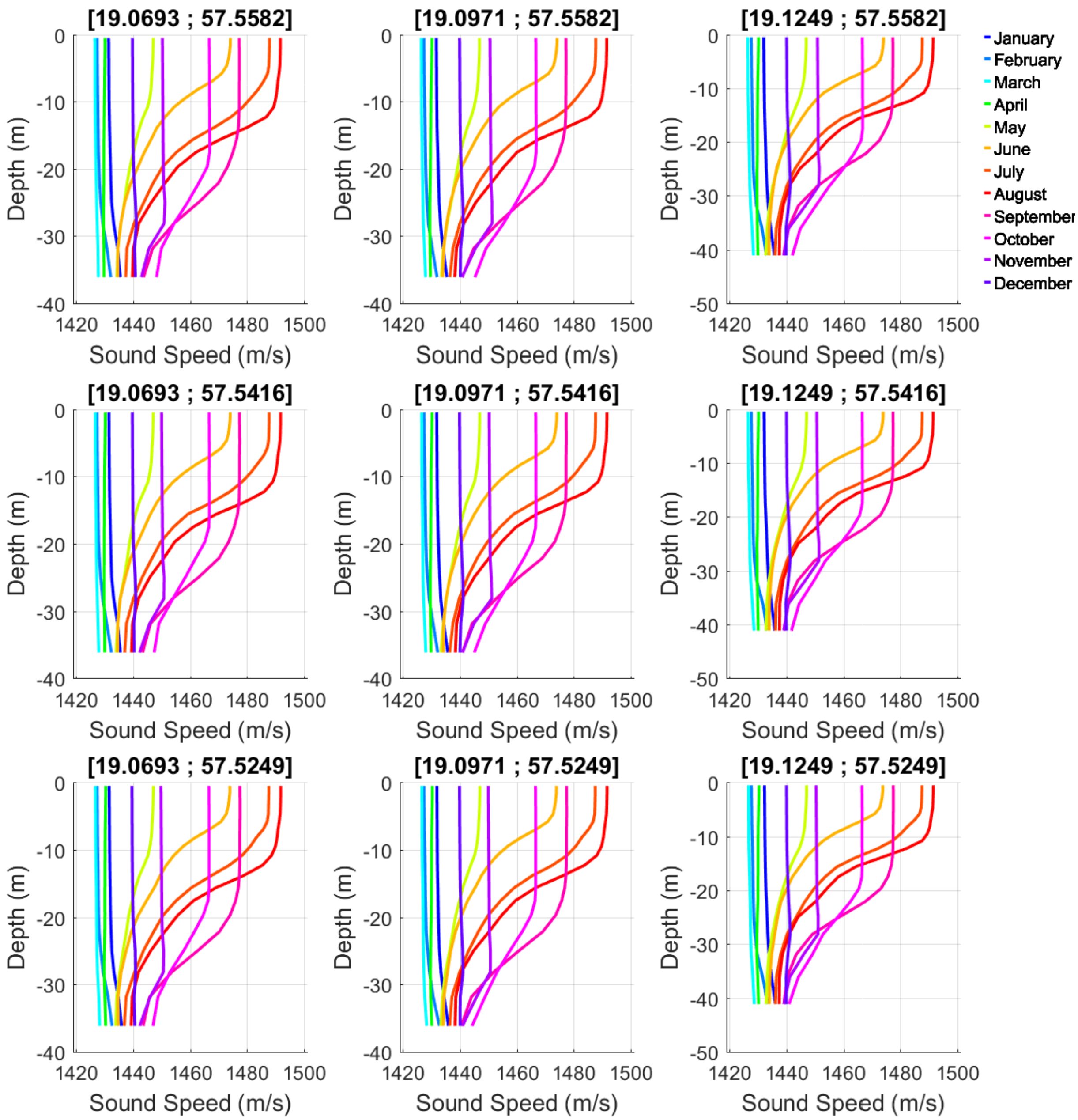

Figure 8.6: Sound speed profiles for the area around source position 3 for all months. Gridded layout reflects geographical location.